Master Thesis

submitted within the UNIGIS MSc. programme
at the Department of Geoinformatics - Z_GIS
University of Salzburg, Austria
Under the provisions of UNIGIS India framework

Land Use Land Cover Change in Ash-Sharqiyah Governorate of Egypt from 2005 to 2015

by

Ahmed Nabil Reda Abdelkhalek
GIS_104597

A thesis submitted in partial fulfilment of the requirements of
the degree of
Master of Science (Geographical Information Science & Systems) – MSc (GISc)

Advisor (s):

Dr. Shahnawaz

University of Salzburg, Austria

April 2019

Science Pledge

By my signature below, I certify that my project report is entirely the result of my own work. I have cited all sources of information and data I have used in my project report and indicated their origin.

Cairo, Egypt 11 April 2019

Place and Date	Signature

Acknowledgements:

Foremost, I am grateful to Almighty Allah for giving me the strength and knowledge to accomplish this thesis.

I would like to express my sincere gratitude to all my teachers at UNIGIS program at University Salzburg. Especially, Dr. Shahnawaz for the continuous support of my MSc study for his patience, motivation, enthusiasm and immense knowledge. His guidance helped me in all the time of research and writing of this thesis.

I also further acknowledge the reliable cooperation from The DigitalGlobe foundation and Egyptian General Surveying authority for providing me the data.

Finally, I must express my very profound gratitude to my parents and to my beloved wife and daughters for providing me with unfailing support and continuous encouragement throughout my years of study and through the process of researching and writing this thesis. This accomplishment would not have been possible without them. Thank you.

List of acronyms

GIS	Geographic Information System
LULC	Land use / Land Cover
UDWT	Undecimated Discrete Wavelet Transform
OBIA	Object Based Image Analysis
GEOBIA	GEOgraphic-Object-Based Image Analysis
DN	Digital Numbers
TOA	Top Of Atmosphere
FLAASH	Fast Line-of-sight Atmospheric Analysis of Hypercubes
NDVI	Normalized Difference Vegetation Index
NDWI	Normalized Difference Water Index
FAO	Food and Agriculture Organization of the United Nations
MAD	Multivariate Alteration Detection
SAR	Synthetic Aperture Radar
MSS	Multispectral Scanner System
VHR	Very High Resolution
ETM+	Enhanced Thematic Mapper Plus
OLI	Operational Land Imager
OCIs	Object Correlation Images
NCIs	Neighborhood Correlation Images
ESA	European Space Agency
MSI	Multi-Spectral Instrument
VNIR	Visible Near Infrared
SWIR	Short Wave Infrared Spectral Range
ER	Electromagnetic Radiation
SSI	Spectral Sciences, Inc
AFRL	Air Force Research Laboratory
AOI	Area of Interest
MOI	Material of Interest
IFOV	Instantaneous Field Of View

Abstract:

The land falls into the category of prime resources. Land use / Land cover (LULC) changes are identified as the prime issue in global environmental changes. Thus, it is necessary to initiate the land change detection process for land sustainability as well as to develop a competent land use planning. Egypt has experienced changes in LULC quickly over the past few decades. According to World Bank data for agricultural land of Egypt between 2005 and 2015 the area of agricultural land fluctuated between increases and decreases. Where the period between 2005 and 2010 there have been increases that can be explained by the economic reforms development and rehabilitate many arid lands in various Egyptian governorates. While the period between 2010 and 2015 there was a decrease that can be explained by the exceptional political events that occurred during that period like January 2011 and June 2013 revolutions. This study to detect changes of LULC in Ash-Sharqiyah governorate, Egypt using two different classification approaches (Pixel-based and Object-based) to classify LULC in the study area, by using satellite imagery of (QuickBird II, Worldview-2 and DubaiSat-2). The accuracy assessment results showed the superiority of the object-based classification that proved to be closer reality.

The results indicated many land changes in the period 2010-2015, but the biggest change in agricultural land, whether the change to built-up area by about 2130 hectares or the changes to bare land by 119 hectares. While in the period 2005-2010 the results showed the changes of many bare lands, whether to agriculture land by 398 hectares or to built-up area by about 254 hectares in the same period. As for the municipalities, the results showed that Al-Husayniyah municipality was affected by change of more than 799 hectares of agricultural land to built-up in the period 2010-2015, while built-up area increased in 10-Ramadan municipality as a result of changing bare land to built-up area by 245 hectares in the period 2005-2010.

Key Words: Remote sensing, Change detection, Pixel-based and object-based classification, Land use/ Land cover (LULC).

Table of Contents

List of Tables

List of Figures

List of Maps

List of Equations

Chapter-1: Introduction

1 Introduction

1.1 Background

A modern nation, as a modern business, must have adequate information on many complex interrelated aspects of its activities in order to make decisions. Land use is only one such aspect, but knowledge about land use and land cover has become increasingly important as the Nation plans to overcome the problems of haphazard, uncontrolled development, deteriorating environmental quality, loss of prime agricultural lands (Anderson, 1976, pp.29).

Egypt has undergone rapid changes in LULC over the past few decades. During the period between 2005 and 2015, Egypt was affected by political and economic events such as the January 2011 and June 2013 revolutions, which negatively affected loss of many agricultural lands due of insecurity, which led some citizens to build on agricultural land. While the government tried before 2011 to reclaim large areas of desert land to meet the food deficit suffered by Egypt.

Egypt has limited natural resources; agriculture is the primary resource in achieving food security, so cultivation of agricultural land is the source of living for many families like other developing countries. Agriculture is also one of the most important sectors in the Egyptian economy. It is estimated that the agricultural land base of Egypt is about 3.3 million hectares, which means that per capita portion is 0.03 hectares in 2014, one of the lowest in the world. Where the fertile arable land is limited to the valley and Delta of the Nile, which does not exceed 4 percent of Egypt's surface. Arable land faces serious challenges, most important of which is urban encroachment. It is estimated that 30 percent of the soil most suitable for agriculture is under urban land cover. This is seriously considering that Egypt suffers from a food deficit and imports more than 40 percent of its food needs according to The Food and Agriculture Organization of the United Nations (FAO). Wheat is the most important agricultural crop for the Egyptian economy. It is the largest crop in terms of the

cultivated area in Egypt. According to estimates of the Egyptian Ministry of Agriculture for 2015 Ash-Sharqiyah governorate produces about 35% of wheat production in Egypt.

For these reasons, the goal of the current study is to monitor changes of LULC in Ash-Sharqiyah province of Egypt from 2005 to 2015.

1.2 Objectives

The aim of this study is to detect changes of LULC between 2005 and 2015 in Ash-Sharqiyah governorate, Egypt. By using two different classification approaches (Pixel-based and Object-based) separately and compare between results and each other. In addressing the above, the following research questions were identified:

How much is the total area of LULC changes between 2005 and 2015 in the study area? How much is the amount of LULC changes in period from 2005 to 2010 and from 2010 to 2015 with compare them to each other? What is the amount of quantitative distribution of LULC changes according to municipalities of Ash-Sharqiyah governorate? What is the largest and smallest LULC class that have changed in Ash-Sharqiyah governorate and its affiliated municipalities? Which is the best classification approach used (object-based or pixel-based) in terms of accuracy assessment results or called closest to reality in the study area?

1.3 Justification of the Study

Several regions around the world are currently undergoing rapid, wide-ranging changes in LULC. Especially regarding urban sprawl on agricultural lands which has become a global phenomenon that afflicts all countries of the world and affecting the economy, the environment and the food security whether rich or poor countries. This phenomenon has challenged most countries in the world, especially developing ones, due to the high population growth that leads to a lack of agricultural land especially around cities. Ash-Sharqiyah is the third most populous of the governorates of Egypt. In addition, it is the largest agricultural governorate, where reporting the area of arable land about 80% of the

total area of it. It is also the largest province in the production and cultivation of wheat and cotton, one of the pillars of the Egyptian economy, yet it lacks reliable, modern, scientific monitoring techniques to effectively monitor and manage land use / cover changes brought about by urbanization.

On the other hand, all the governorates of Egypt was affected during the period between 2005 and 2015 by exceptional political and economic events. For example, the agricultural lands were negatively affected during January 2011 and June 2013 revolution as many arable lands were lost and built on them. While before 2011, the government tried to find solutions to meet the food deficit suffered in Egypt by implementing projects to reclaim new agricultural land in various governorates. All these factors led to study of monitoring and detect of changes of LULC between 2005 and 2015 in Ash-Sharkia governorate.

1.4 Study Area

1.4.1 Location

Ash-Sharqiyah governorate is located in the northern part of the country, its capital is the city of Zagazig. Where is located in the east of Damietta branch of Nile River, only three kilometers away.

Geographically, it is located between longitudes 31^{o} 10' and 32^{o} 20' E and latitudes 31^{o} 10' and 31^{o} 20' N. Ash-Sharqiyah governorate is bordered to the south by Cairo governorate, to the north by Bur Sa`id governorate and from the east the governorates of Al-Isma`iliyah and As-Suways, while are located both the Ad-Daqahliyah and Al-Qalyubiyah governorates to the west of it as shown in Map No. 1.1.

In addition to, Ash-Sharqiyah governorate is one of the six governorates of the Suez Canal region, namely Al-Isma`iliyah, As-Suways, North Sinai, South Sinai and Bur Sa`id which is an addition to the governorate comparative economic advantage through its geographical location near the Suez Canal, which connecting the Mediterranean Sea to the Red Sea and separates the continent of Asia from Africa, making it one of the most important navigation lanes.

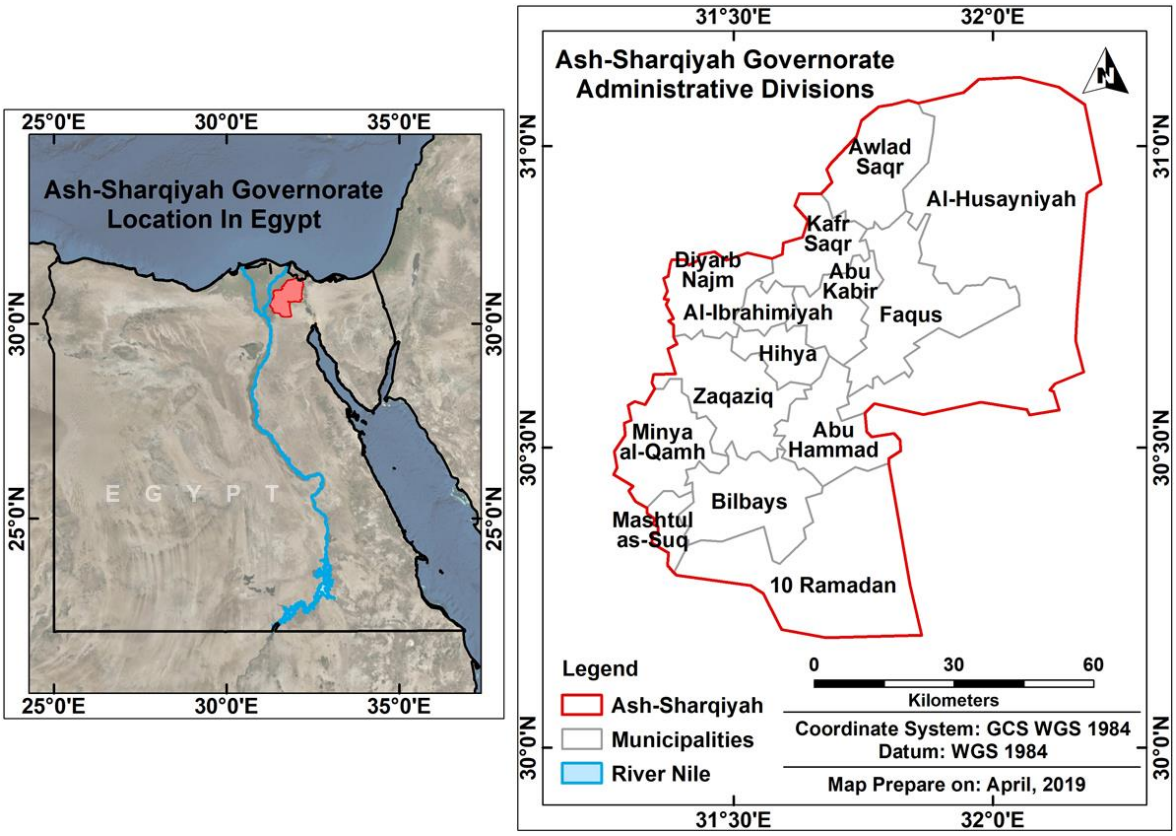

Map 1.1: Location of Ash-Sharqiyah Governorate

1.4.2 Area and Shape

Ash-Sharqia has covered an area of approximately 5000 square kilometers, which is 0.5% of the total area of Egypt. While inhabited area is estimated at about 4.700 square kilometers, representing 97% of its total area according to report of the Egyptian General Organization for Physical Planning in May 2017.

1.4.3 Land use / Land cover

Land use / Land cover of Ash-Sharqia governorate is divide into four main sections. Agriculture is the main component in land use / land cover. Wheat, cotton, rice, maize and beans are cultivated in most of the governorate area except for small areas on the eastern and southern borders of governorate. While human activities are scattered randomly throughout the governorate, but they are often beside the waterways because most of the inhabitants of the governorate are engaged in agriculture. Except for the south-east of the governorate where locate the 10th of Ramadan city which is the largest industrial city in the governorate. Bare lands is the third section of land uses where increased area of

administrative boundaries of the governorate in the last decade by annexing a lot of arid desert lands from neighboring governorates to accommodate the population increase in the governorate in addition to the future urban growth. These lands are concentrated in the east and south sides of the governorate. Finally, the water bodies like canals, which are most important element of it. That are appear in satellite images like the arteries feeding the agricultural lands. In general, the water bodies are spread in many locations of the governorate, where the Ismaili and Bahr Morris canals are the largest in the governorate.

1.4.4 Population

The population of Ash-Sharqiyah is about 6.5 million, representing about 7.5% of the total population of Egypt, while population density is 13.34 people per hectares, which is reflected in the per capita share of the total area of 0.08 hectares per capita. Where they are divided into 24% urban people and 76% rural according to the demographic structure, while the population growth rate is estimated at 2.3% per year between 2006 and 2016 and will fall to 1.37% in 2027 according to report of the Egyptian Central Agency for Public Mobilization and Statistics for 2017.

1.4.5 Climate

The climate in Ash-Sharqiyah governorate is called a desert climate same in various governorates of Egypt (Köppen climate classification BWh).

The climate is generally extremely dry all years, where is virtually no rainfall during the year except in winter which receives little rainfall in it. The driest month is May. There is 0 mm of precipitation in May. The greatest amount of precipitation occurs in January, with an average of 5 mm. The precipitation varies 5 mm between the driest month and the wettest month, where Precipitation here averages 18 mm as shown Figure No. 1.1.

In addition to rarity of rain, extreme heat during summer months is also a general climate feature although daytime temperatures are more moderated during the spring and autumn months. The average annual temperature is 21.3 °C in the study area. With an average of

27.6 °C, July is the warmest month. The lowest average temperatures in the year occur in January, when it is around 13.1 °C. The variation in temperatures throughout the year is 14.5 °C as shown in Figure No.1.2.

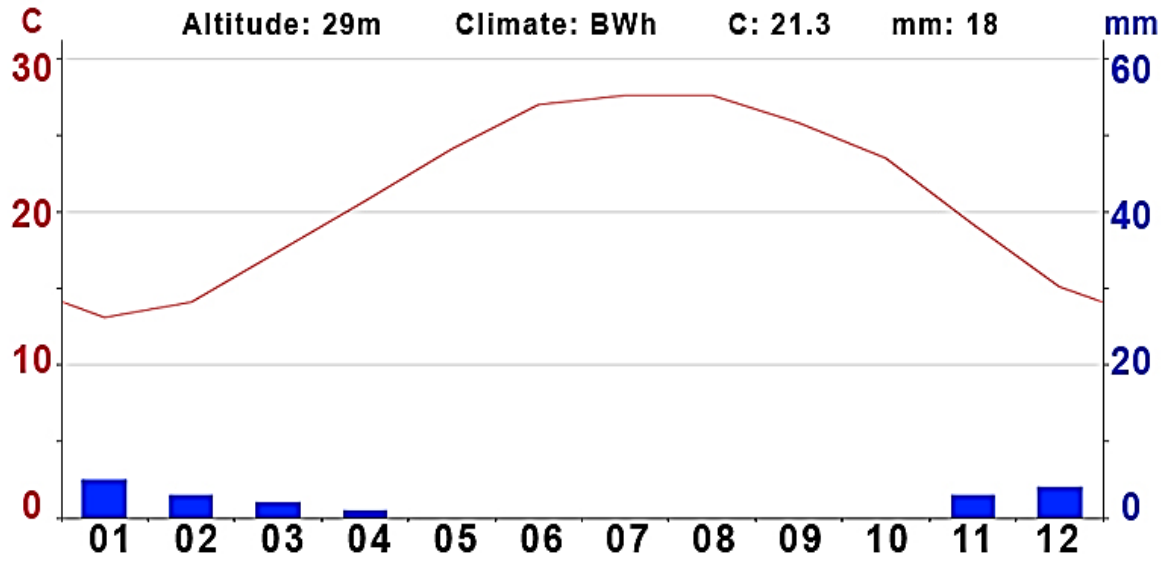

Figure 1.1: Climate / weather by month for Ash-Sharqiyah governorate

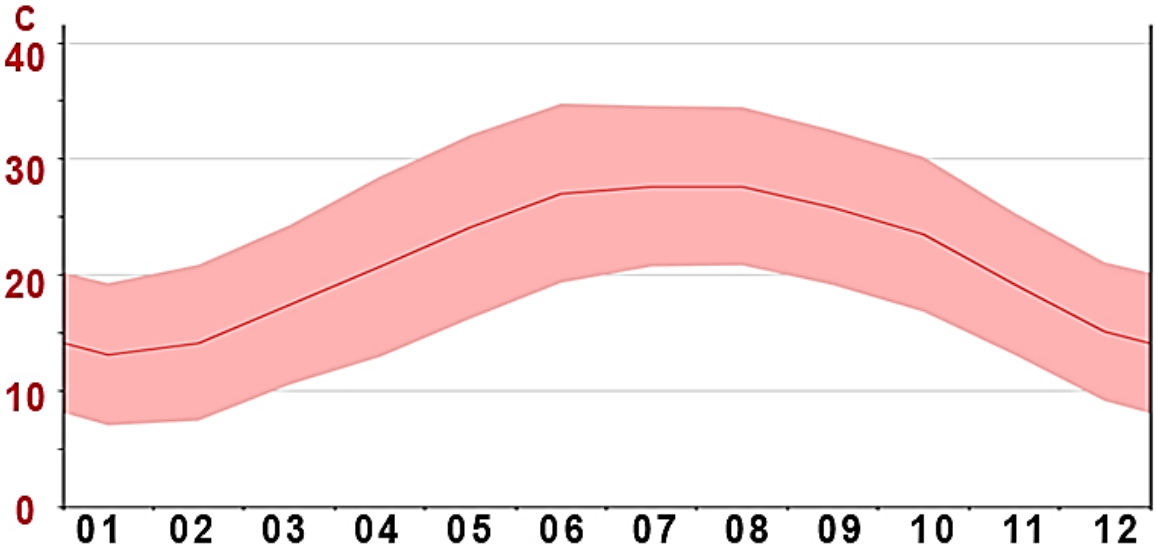

Figure 1.2: Average temperature over the months of the year

A summary of this chapter: this chapter presented the motivation for this research work. It also provided a comprehensive overview of geographic location of the study area, area, shape, population and climate / weather. Where is highlighted the importance and sensitivity the location of the study area, which requires the selection of data suitable for that information to study the detection of changes of land use / land cover.

Chapter-2: Literature Review

2.1 Introduction

Change detection of LULC has a long history of development and number of researches and investigation has been applied in many case studies of the world. Nevertheless, a matter of dissemination and losing of data records and/or paper works during last decades has a negative impact in the past. While, presently was possible to find a quite number of reports and literature that could be apply for further review and study of the investigated region.

This chapter delivers information related to detect changes of LULC, where the literature review contains four major sections that document several issues relevance to the study topic, which deals with the Change Detection, Object-Based Classification, Pixel-Based Classification in addition to urban sprawl impact on agricultural land.

2.2 Change detection

Digital Change Detection Biophysical materials and human-made features are dynamic, changing rapidly. It is believed of LULC change is a major component of global change with an impact perhaps greater than that of climate change. Significant effort has gone into the development of change detection methods using remotely sensed data. There are general five steps used to conduct digital change detection using remote sensor data. The first one is state the change detection problem e.g. define study area. The second step is defined considerations of significance when performing change detection, which contain elements of remote sensing system like spatial, spectral and temporal. In addition, elements of environmental considerations like Atmospheric condition, Soil moisture conditions and Phenological cycle characteristics. The third step depends on several points, which are all concerned with image processing such as acquire appropriate change detection data, preprocess the multiple date remotely sensed data, select appropriate change detection algorithm, apply appropriate image classification logic If necessary and perform change

detection using GIS algorithms. The fourth step is quality assurance and control program, which are mean assess statistical accuracy of individual date classifications and change detection products. Finally the fifth step is distribute results by digital products and analog (hardcopy) products (Jensen, 2015, pp.623).

There are many studies conducted on change detection field based on remote sensing techniques. I will discuss the most relevant studies in the literature that related to detect changes in Land use / Land cover.

(Lu et al., 2004, pp.2365-2401) The study aimed to summarizes and reviews change detection techniques which have been developed in recent decades. The results showed that image differencing, principal component analysis and post-classification comparison are the most common methods used for change detection. In recent years, spectral mixture analysis, artificial neural networks and integration of geographical information system and remote sensing data have become important techniques for change detection applications. Different change detection algorithms have their own merits and no single approach is optimal and applicable to all cases. In practice, different algorithms are often compared to find the best change detection results for a specific application. Research of change detection techniques is still an active topic and new techniques are needed to effectively use the increasingly diverse and complex remotely sensed data available or projected to be soon available from satellite and airborne sensors.

(Pathak, 2014, pp.875) This study focused on the mining which is one of the most dynamic processes with direct as well as indirect impact on the environment. Hence, mine area provides ideal situation for evaluating the chronological changes in land use patterns. Also digital change detection of satellite data at different time interval helps in analyzing the changes in the spatial extent of mine along with the associated activities. In this study, various algorithms Iteratively Re-weighted Multivariate Alteration Detection (MAD) on raw data where class wise comparison becomes a difficult proposition and object-based segmentation and change detection as post classification comparison were assessed. The results showed that although the process of change detection may seem straightforward

from the descriptions above, there are limitations, and most are attributable to the incomplete manifestations of change within satellite imagery. Limitations in image characteristics include spatial and temporal resolutions, spectral matching of key indicators of change, view and illumination angles, atmospheric conditions and radiometric corrections / calibration, and geographic registration. Selection of threshold value and if each of these perturbing factors is carefully considered and minimized through the change detection effort, a useful result may be revealed. Multi-source data can partially help in overcoming the first limitation while improved techniques can reduce the error associated with feature/object level comparison rather than pixel.

(Radke et al., 2005, pp.294-307) This paper presents a systematic survey of the common processing steps and core decision rules in modern change detection algorithms, including significance and hypothesis testing, predictive models, the shading model, and background modeling. In addition, to discuss important preprocessing methods, approaches to enforcing the consistency of the change mask, and principles for evaluating and comparing the performance of change detection algorithms. It is hoped that our classification of algorithms into a relatively small number of categories will provide useful guidance to the algorithm designer. The results showed that two algorithms deserve special mention. Stauffer and Grimson's background modeling algorithm, provides for multiple models of background appearance as well as object appearance and motion. The algorithm by Black et al, provides for multiple models of image change and requires no preprocessing to compensate for misregistration or illumination variation. It is expected that a combination of these approaches that uses soft assignment of each pixel to an object class and one or more change models would produce a very powerful and theoretically well-justified change detection algorithm.

(Celik, 2009, pp.820-824) In this letter, propose a novel technique for unsupervised change detection in multi-temporal satellite images. The difference image which is computed from multi-temporal images acquired on the same geographical area at two different time instances is decomposed using S-levels undecimated discrete wavelet transform (UDWT).

For each pixel in the difference image, a multiscale feature vector is extract using the sub-bands of the UDWT decomposition and the difference image itself. The final change detection map is achieved by clustering the multiscale feature vectors using k-means algorithm into two disjoint classes: changed and unchanged. Experimental results confirm the efficacy of the proposed approach on both optical and synthetic aperture radar images. The results showed that an unsupervised change detection technique is developed by conducting k-means clustering on feature vectors, which are extracted using the sub bands of the undecimated discrete wavelet transform (UDWT) decomposition of the difference image. The only tunable parameter required is the number of decomposition levels (S). The proposed algorithm is simple in computation yet effective in identifying meaningful changes regardless of the type of input images, which makes it suitable for real-time applications. Simulation results show that the proposed algorithm performs quite well on combating both the zero-mean Gaussian noise and the speckle noise, which is quite attractive for change detection in both optical and Synthetic Aperture Radar (SAR) images.

2.3 Pixel-Based Classification

Pixel-based classification is done on a per pixel level, using the spectral information for that individual pixel i.e. values of pixels within the locality are ignored. To be more precise, each pixel would represent a training example for a classification algorithm, and this training example would be in the form of an n-dimensional vector, where n was the number of spectral bands in the image data. Accordingly, the trained classification algorithm would output a class prediction for each individual pixel in an image. There are many pixel-based classification approaches, but here I will focus on Subpixel classification approach which aim to address the mixed pixel problem that arises when coarse spatial resolution images. **(Arif et al., 2015, pp.9-15)** In this paper, the proposed method performs an initial non-random allocation of classes to sub pixel and optimization procedure adapted is performed to overcome multiple and non-allocated sub pixels to simplify SRM approach and curtail processing time. Proposed method uses soft classification approaches for generating

fractional maps, which are provided as input to SRM method. Early allocation of sub pixels is achieved based on amount of attractiveness to neighborhood pixels. The result showed that the proposed super resolution mapping technique provides super resolved land cover information using the output of a soft classification process. The output of soft classifier satisfies the constraint of non-negativity and sum to unity of fractional abundance within the pixels. The overall accuracy of SRM algorithm depends on certain factors like the accuracy of soft classification process, scale factor, the window size for neighbor consideration, and optimization algorithm. Evaluation of these distinct parameters requires more research, which remains as open for future scope. The proposed super resolution mapping algorithm presented in our study is also useful for super resolution reconstruction. In this case, spatially resolved remote sensing images can be used as an input. The output of the super resolution mapping algorithm will be a desired multispectral or hyper spectral image obtained at a fine spatial resolution of land cover maps.

(Aplin and Atkinson, 2001, pp.2853-2858) In this paper, the method of transform a soft land cover classification into hard land cover classes at the Subpixel scale for subsequent per-field classification was discussed. First, image pixels were segmented using vector boundaries. Second, the pixel segments (ranked by area) were labelled with a land cover class (ranked by class typicality). Third, a hard per-field classification was generated by examining each polygon (representing a land cover parcel, or field) in its entirety (by grouping the fragments of the polygon contained within different image pixels) and assigning to it the modal land cover class. The results showed four main points; first, Hard per-pixel classification was relatively inaccurate due to the presence of mixed pixels. Second, Soft per-pixel classification overcame the problem of mixed pixels by indicating class typicality. Spatial information was limited though, since land cover was not mapped within each pixel. Thirdly, Hard per-field classification based on a hard per-pixel classified image averaged out the majority of errors present at the per-pixel stage. However, since this per- field approach did not account for mixed boundary pixels, some misclassification remained. Fourthly, Hard per-field classification based on a soft per-pixel classified image

accounted for all mixed pixels, including boundary pixels. This was achieved by mapping land cover within each pixel through pixel segmentation. Overall, this method of classification was the most accurate of those tested.

(Verhoeye and De Wulf, 2002, pp.96-104) This paper describes a new approach that formulates the Subpixel mapping concept as a linear optimization problem maximizing the spatial autocorrelation within the image. It produces a sharpened crisp land cover map, without the need of finer spatial resolution data. Which have been applied on situated in the Lake Chad basin and stretches from Nigeria across northern Cameroon to Chad, Africa. This algorithm yielded land cover maps at 500, 200, and 100 m resolution with accuracies close to 89%. Subsequent mode filtering further increased these values. When applied to a real data set, the accuracy reached 78%. While this study suggests other possibilities for improvement exist. An important topic of research may be the optimization of the geostatistical analysis. The algorithm may be altered in order to accommodate a limited exchange of fractions between neighboring pixels. Lastly, the study suggests the potential of the proposed technique.

(El-Aziz, 2013, pp.276) This Article is set to track and monitor changes through the spatial dependence of remote sensing data and GIS analysis, the suggested working method in this research is by Subpixel classification techniques. Change detection is a central task for land cover monitoring by remote sensing. It uses multi temporal image data sets in order to detect land cover changes from spectral discrepancies. It is discussed monitor of situation in the past, the current and finally the future potential status of land use changes in Eastern Qena, Egypt. Specifically, in places of estuary floods, and the most important estuary leading to Qena, and whether these changes in land are used in direction of the mouth of the stream or not, especially that when it happened before, it caused destruction of both activities, urban and agricultural land. The results showed more accurate in use Subpixel classification approach, especially when use of low-resolution satellite images, like Landsat from years of 1972 to 2013 with sensors as MSS, TM, ETM+ and OLI which gives an important dimension.

2.4 Object-Base Classification

Object-Based Image Analysis (OBIA) is a sub-discipline of GIScience devoted to partitioning remote sensing imagery into meaningful image-objects, and assessing their characteristics through spatial, spectral and temporal scale. At its most fundamental level, OBIA requires image segmentation, attribution, classification and the ability to query and link individual objects (segments) in space and time. Object-based classification is based on information from a set of similar pixels called objects or image objects. Image objects are groups of pixels that are like one another based on the spectral properties i.e., color, size, shape, and texture, as well as context from a neighborhood surrounding the pixels. In order to achieve this, OBIA incorporates knowledge from a vast array of disciplines involved in the generation and use of geographic information. It is this unique focus on remote sensing and geographic information that distinguishes OBIA from related disciplines (Hay and Castilla, 2006, pp.4-5).

(Walter, 2004, pp.225-238) In this paper, a change detection approach based on an object-based classification of remote sensing data is introduced. The approach classifies no single pixels but groups of pixels that represent already existing objects in a GIS database. The approach is based on a supervised maximum likelihood classification. The multispectral bands grouped by objects and very different measures that can be derived from multispectral bands represent the n-dimensional feature space for the classification. The training areas are derived automatically from the geographical information system (GIS) database. The results of a test on two test areas are presented. Afterwards, further measures, which can improve the result of the classification and enable the distinction between more land-use classes than with the introduced approach, are presented. The result showed that the basic idea of the approach is that image interpretation is not based only on the interpretation of single pixels but on whole object structures. Therefore, do not classify only single pixels but groups of pixels that represent already existing objects in a GIS database. Each object is described by an *n*-dimensional feature vector and classified

to the most likely class based on a supervised maximum likelihood classification. The object-based classification needs no tuning parameters like user-defined thresholds. It works fully automatically because all information for the classification is derived from automatically generated training areas. The result is not only a change detection but also a classification into the most likely land-use class. On the other hand, a change in the landscape can only be detected if it affects a large part of an object because the object-based classification uses the existing object geometry. If, for example, a forest object has a size of 5000 m2 and in that forest object a small settlement area with 200 m2 is built up, then this approach will fail. Further techniques have to be developed in order to cover this problem. Because forest areas can be classified very accurately in pixel-based classification, it could be additionally tested whether there are large areas in a forest object that are classified to another land-use class. The same approach could be used for water areas because water is also a land-use class that can be classified very accurately in pixel-based classification. More difficult is the situation for the land use classes Greenland and settlement, which have typically an inhomogeneous appearance in a pixel-based classification.

(Chen et al., 2018, pp.159-182) The main objective of this paper is to elucidate the emerging trends in GEOBIA and discuss potential opportunities for future development. The result showed emerging trends were found in multiple subfields of GEOBIA, including data sources, image segmentation, object-based feature extraction, and geo-object-based modeling frameworks. It is our view that understanding the state-of-the-art in GEOBIA will further facilitate and support the study of geographic entities and phenomena at multiple scales with effective incorporation of semantics, informing high-quality project design, and improving geo-object-based model performance and results.

(Im et al., 2008, pp.399-423) This study introduces change detection based on object / neighborhood correlation image analysis and image segmentation techniques in two study sites in Las Vegas, US. The correlation image analysis is based on the fact that pairs of brightness values from the same geographic area (e.g. an object) between bi-temporal

image datasets tend to be highly correlated when little change occurred, and uncorrelated when change occurs. Five different change detection methods were investigated to determine how new contextual features could improve change classification results, and if an object-based approach could improve change classification when compared with per-pixel analysis. The five methods examined include (1) object-based change classification incorporating object correlation images (OCIs), (2) object-based change classification incorporating neighborhood correlation images (NCIs), (3) object-based change classification without contextual features, (4) per-pixel change classification incorporating NCIs, and (5) traditional per-pixel change classification using only bi-temporal image data. Two different classification algorithms (i.e. a machine-learning decision tree and nearest neighbor) were also investigated. Comparison between the OCI and the NCI variables was evaluated. Object-based change classifications incorporating the OCIs or the NCIs produced more accurate change detection classes (Kappa approximated 90%) than other change detection results (Kappa ranged from 80 to 85%). Ultimately, future research should investigate the incorporation of multi-resolution image segmentation in object-based change detection and other change-detection application of these correlation analysis derivatives (e.g. fire-severity mapping).

2.5 Urban sprawl impact on agricultural land

Urban sprawl on agricultural lands has become a global phenomenon plaguing all countries of the world, rich or poor. This phenomenon formed a challenge to most countries of the world, especially developing ones, because of the increasing of population at high rates, consequent the depletion of resources, especially agricultural lands around cities. Perhaps urbanization is one of the most widespread anthropogenic causes of the loss of arable land **(López et al., 2001, pp.271-285)** One of the reasons, the increase of population density increasing which pressure on areas already inhabited. On the other hand, Food scarcity and continuous loss of agricultural lands are issues of global concern. Therefore, many governments adopted policies aimed at self-sufficiency in food production, for example, by

extension of cultivated areas and maximization of production of the existing agricultural land. The principal purpose is to control predominating unfavorable population to agricultural land ratio. Therefore, study urban sprawl impact assessment on agriculture land is very important.

(Shalaby et al., 2012, pp.261-273) This research is discussed urban sprawl, which one of the main problems that threaten the limited highly fertile land in the Nile Delta of Egypt by using satellite images and remote sensing techniques to study the impact of urban sprawl on agricultural land in Qalubiya Governorate, Egypt between 1992 and 2009. The results indicate that integrating visual interpretation with supervised classification led to increase in the overall accuracy by 10%. The study area has undergone a very severe land cover change because of urbanization resulting from rapid population growth. A considerable increase in urban settlements has taken place at the expense of the most fertile land in the Governorate. Integrating GIS and remote sensing provided valuable information on the nature of land cover changes, especially the area and spatial distribution of different land cover changes. The main causes of urbanization are the rapid population growth and the internal migration. This problem needs to be seriously studied, through multidimensional fields including, socioeconomic, to preserve the precious and limited agricultural land and increase food production.

(Al Tarawneh, 2014, pp.97-124) This research aims to shed light on the phenomenon of urban sprawl on agricultural land by exploring the causes, the effects, and the relationship between it and land use planning. Taking Jordan as example through the selection of Shihan municipality areas as a case study. The study showed that Shihan Municipality areas lost much of its agricultural land because of urbanization and indiscriminate. There are several conclusions that emerged from this study, including the causes that led to urban sprawl on agricultural land in the region such as the increase in population and therefore increasing the demand for housing construction to meet the needs of the population, the traditional view of agricultural work, which leads to the neglect of land and used in construction, as well as inadequate legislation and poor oversight on agricultural land. The

negative impact of urban sprawl on agricultural land has declined production of these lands by a large margin in the region after it was formed tributary significantly to the city's economy. Few green spaces have led to pollution and high temperatures were not seen before areas of the Shihan Municipality.

(Doygun, 2009, pp.471) This study aims at detecting the effects of urbanization on agricultural lands for the city of Kahramanmaraş, Turkey. In particular, the loss of olive groves for a 21-year period of 1985 to 2006 was quantified due to rapid urban sprawl. The results were showed that urban sprawl appears to be one of the most important reasons for environmental issues facing the city of Kahramanmara¸s where there is a rapid population growth due to transformation of the regional economy from agriculture to industry. The results showed that especially the olive groves surrounding the city center that play an important role in traditional agricultural activities were directly lost to urban expansion. The urban development plans ignoring the expansion of the urban area into olive groves and their fragmentation also reinforce the current land use patterns and trends. Especially the current development plans and land management policies cause an increase in land prices, thus encouraging landowners to construct multi-storey buildings and abandon agricultural activities. The destruction of the olive groves, which have remained in existence for a long time without intensive care may accelerate national dependence on supplies from abroad and contribute to the process of worldwide food crisis. In this context, national land use policies should be revised by decision makers in accordance with the achievement of sustainability and recognition that the short-term economic benefits can endanger the public and environmental health of present and future generations.

A summary of this chapter: This chapter included a brief of some literature review related to the subject of study, with a focus on the results and methodology used for both of them. It was contained in four parts, from the beginning with Change detection techniques, Pixel-based and Object-based classification Finally, impact of the urban sprawl on agricultural land**.**

Chapter-3: Materials and Methodology

3.1 Introduction

This chapter details the process by which this thesis was constructed and the research it describes executed. Descriptions of the data used are provided first in Section 3.1. Section 3.2 provides an overview of the software used in this thesis to reach the desired results. The next section discusses the scientific methodology used, includes three main stages by sequence; data acquisition, pre-processing data and finally analyze the data to reach the thesis objectives.

3.2 Data Used

The study depends on two types of data; Raster data containing satellite images from three different satellites (QuickBird II, WorldView-2, DubaiSat-2) for used in classify land used / land cover for 2005, 2010 and 2015 respectively. The second type of data is Vector data includes road network from OpenStreetMap (OSM) Foundation, will be used as an auxiliary layer in the extraction of land use / land cover using Object-based classification.

3.2.1 Satellite images

The study relies on three different types of imagery, which were acquired from QuickBird II, WorldView-2 and DubaiSat-2 satellites, as the following:

3.2.1.1 QuickBird-II Imagery

A QuickBird was a high-resolution commercial earth observation satellite, owned by DigitalGlobe Foundation, launched in 2001 and decayed in 2015. The satellite collected panchromatic (black and white) imagery at 61 Centimeter resolution and multispectral imagery at 2.44 meter. A DigitalGlobe Foundation was supported the thesis with imagery needed to support for science and learning.

The following Table No. 3.1 shows the specifications of the data used from QuickBird II satellite.

Acquisition Date	Date	Product - Child Catalog ID	
	05-May-2005	A01001038A4BE000 - 203001038A4BDF00	
	30-May-2005	A01001038A4BE500 - 203001038A4BE400	
	08-July-2005	A01001038A4BEA00 - 203001038A4BE900	
	16-July-2005	A01001038A4BC600 - 203001038A4BC500	
	30-July-2005	A01001038A4BDD00 - 203001038A4BDC00	
	01-June-2005	A01001038A4BCA00 - 203001038A4BC900	
	09- June-2005	A01001038A4BD000 - 203001038A4BCF00	
	14-June-2005	A01001038A4BDA00 - 203001038A4BD900	
	05-Aug-2005	A01001038A4BC200 - 203001038A4BC100	
	16-Aug-2005	A01001038A4BD700 - 203001038A4BD600	
Band Used	Band Number	Central Wavelength (nm)	Spatial Resolution (meter)
	1 - Blue	450-520	2.44
	2 - Green	520-600	
	3 - Red	630-690	
	4 - NIR	760-900	
Study Period	2005		
Format	GeoTIFF		
Projection	UTM		
Datum	WGS84		
Platform	QuickBird II		
Source	DigitalGlobe Foundation		

Table 3.1: Specification of QuickBird II satellite imagery

3.2.1.2 WorldView-2 Imagery

The WorldView-2 is a commercial Earth observation satellite owned by DigitalGlobe foundation. It was launched 8 October 2009, which provides a high resolution panchromatic band and eight (8) multispectral bands; four (4) standard colors (red, green, blue, and near-infrared 1) and four (4) new bands (coastal, yellow, red edge, and near-infrared 2), full-color images for enhanced spectral analysis, mapping and monitoring applications, land-use planning, disaster relief, exploration, defense and intelligence, and visualization and simulation environments. The following Table No. 3.2 shows the specifications of the data used from WorldView-2 sensor.

Acquisition Date	Date	Product - Child Catalog ID
	10-July-2010	A010010396891E00 - 2030010396892300
	27-June-2010	A010010396890F00 - 2030010396891000
	10-June-2010	A010010396892900 - 2030010396892C00
	27-Aug-2010	A010010396890900 - 2030010396890A00

	07-Aug-2010	A010010396898B00 - 2030010396898C00	
Band Used	Band Number	Central Wavelength (nm)	Spatial Resolution (meter)
	2 - Blue	450-510	2.00
	3 - Green	510-580	
	5 - Red	630-690	
	7 - NIR	770-895	
Stud Period	2010		
Format	GeoTIFF		
Projection	UTM		
Datum	WGS84		
Platform	WorldView-2		
Source	DigitalGlobe Foundation		

Table 3.2: Specification of WorldView-2 satellite imagery

3.2.1.3 DubaiSat-2 Imagery

DubaiSat-2 is the second Earth observation mini satellite of United Arab Emirates. Emirates Institute for Advanced Science and Technology (EIAST) started the DubaiSat-2 development in 2009. DubaiSat-2 is designed for a sun-synchronous orbit of 600 km. The imager provides 1 m spatial resolution imagery in Panchromatic (PAN) band and 4 m resolution in Multispectral (MS) bands and a Swath of 12.2 km as shown Table No 3.3.

Acquisition Date	Date		Tile Number
	12-July-2015		Null
	25-June-2015		
	12-Aug-2015		
	22-Aug-2015		
Band Used	Band Number	Central Wavelength (nm)	Spatial Resolution (meter)
	1 - Blue	420–520	4
	2 - Green	520–590	
	3 - Red	630–690	
	4 - NIR	770–890	
	Pan	550-900	1
Study Period	2015		
Format	GeoTIFF		
Projection	UTM		
Datum	WGS84		
Platform	DubaiSat-2		
Source	Emirates Institute for Advanced Science and Technology (EIAST)		

Table 3.3: Specification of DubaiSat-2 satellite imagery

3.2.2 Vector Data

Furthermore, additional vector data were used. A road network from OpenStreetMap was used as an auxiliary layer in order to keep the resulting segments within the constraints of the built-up area segments and it was added as a thematic layer in the segmentation process to help delineating Built-up area segments. In Object-based classification. It is a data that has been used free as open source data in shapefile format.

3.3 Software Used

Many software will be using in this study, as the follows:

- ENVI 5.1: To use in the image pre-processing works e.g. radiometric calibration, Mosaic and clip area of interest.
- ERDAS IMAGINE 2016: To use in the analysis process e.g. Pixel-Based Classification (Subpixel Classification), Accuracy Assessment for classification results and Change Detection.
- eCognition 9.4: To use in Object-Based Classification.
- ArcGIS Desktop 10.5: To use in all cartographic works.
- Microsoft Excel 2013: To show the statistics of classification results by using graphs and charts.

3.4 Methodology

3.4.1 Methodology Overview

The methodology will describe the method applied in a field of study as shown in Figure No. 3.1 to answer the research objectives specified in the previous chapter. The methodology is broken down into four consecutive stages, beginning with data acquisition, which includes satellite images and vector data of the study area. The second stage includes all pre-processing steps of data, e.g. Radiometric and Atmospheric Correction, Band Composite and Mosaic. The third phase covers all the scientific analyzes applied in this study. The methodology applies two different approaches for classification of LULC: Pixel-Based

classification and Object-Based classification. Then compare the results of the accuracy assessment of both approaches to use the most accurate approach and reflect the real reality of LULC classification more precisely in detect of change LULC during the study period. The fourth and final stage includes presenting the results of this study and comparing them in the form of tables and graphs showing the answers to the objectives of this study.

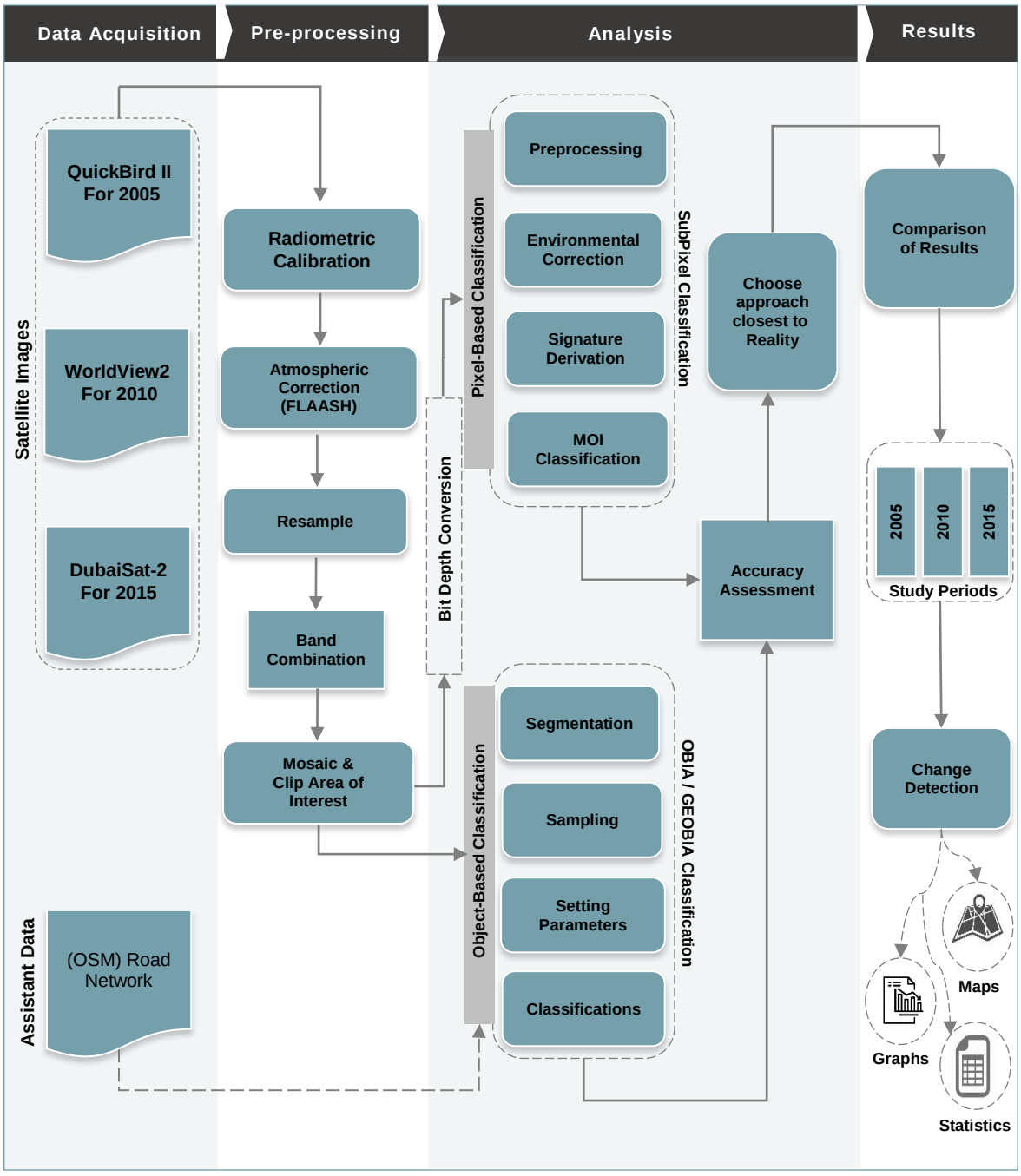

Figure 3.1: Methodology Flow Chart

3.4.2 Data Acquisition

Satellite images with very high spatial resolution were obtained from the QuickBird II and Worldview-2 satellites covering the study area for 2005 and 2010 respectively from DigitalGlobe Foundation, which aim profitability, but I was obtained it for free to encourage science and learn. Imagery for 2015 of DubaiSat-2 satellite was obtained from Emirates Institute for Advanced Science and Technology (EIAST). As well as, road network form OpenStreetMap as ancillary thematic layer in segmentation process for OBIA classification.

3.4.3 Data Pre-Processing

3.4.3.1 Radiometric Correction

Radiometric correction is concerned with improving the accuracy of surface spectral reflectance, emittance and back-scattered measurements obtained using a remote sensing system (Johannsen and Daughtry, 2009, pp.244-256).

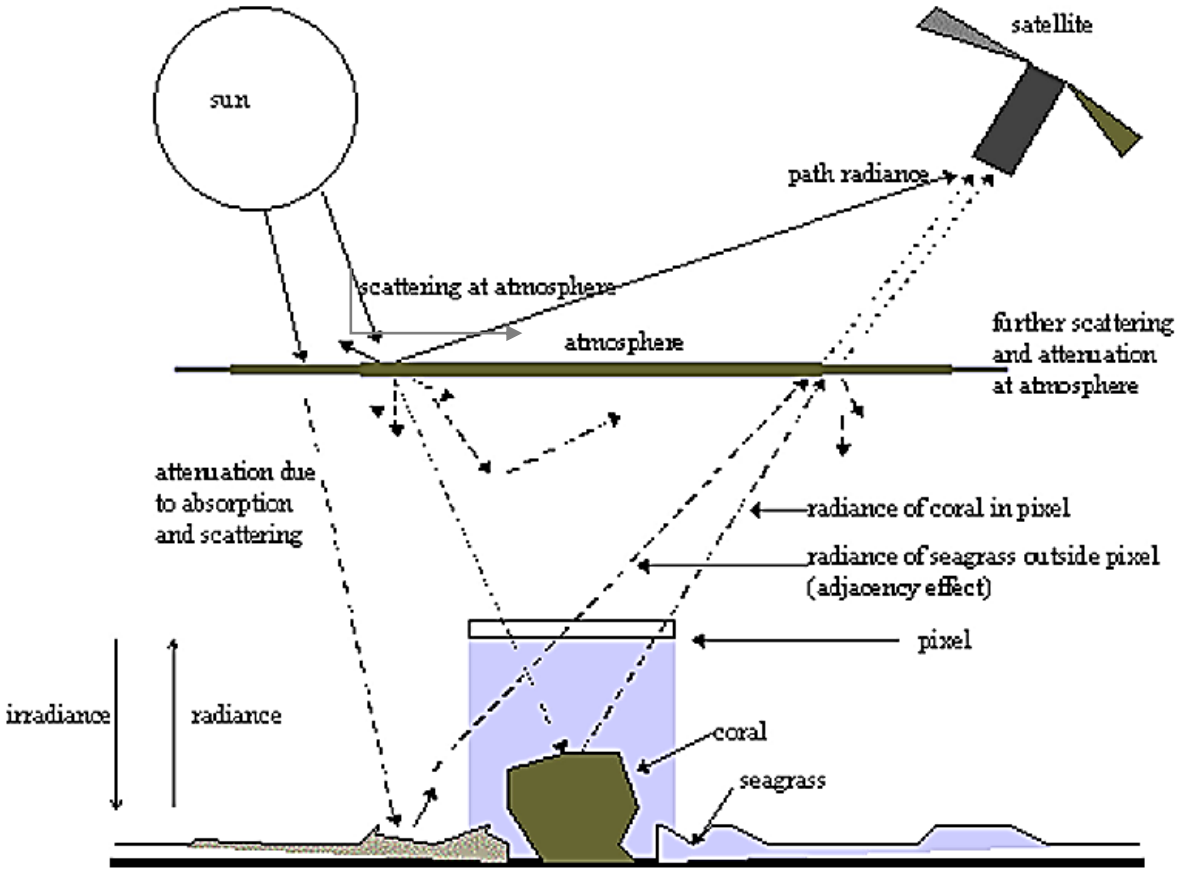

Figure 3.2: How atmospheric scattering contributes to the radiance measured at the top of the atmosphere

The spectral radiances obtained from the calibration only account for the spectral radiance measured at the satellite sensor. By the time electromagnetic radiation (ER) is recorded by a satellite or airborne sensor, it has already passed through the Earth's atmosphere twice; sun to target and target to sensor as shown in Figure No 3.2.

Where digital sensors record the intensity of electromagnetic radiation from each spot viewed on the Earth's surface as a digital number (DN) for each spectral band. These digital numbers can be converted to more meaningful real-world units like radiance, reflectance or brightness temperature. QuickBird images have much information in metadata file such as earth sun distance, solar zenith angle, exoatmospheric irradiance that used in the radiometric correction process. The radiometric correction process involves several steps, as follows:

- Radiance: Convert digital numbers (DN) value to radiance based on the scaling factors provided in the metadata file. Radiance is computed using Equation No. 3.1:

$$L_\lambda = Gain * Pixel\ value + Offset$$

Equation 3.1: Convert image pixels from digital numbers (DN) to units of absolute radiance

Where:

L_λ = Spectral Radiance at the sensor's aperture in watts / (meter ^{2}× ster × µm)

- Reflectance: Convert radiance to top-of-atmosphere (TOA) reflectance requires additional information: gains, offsets, solar irradiance, sun elevation, and acquisition time defined in the metadata file. Reflectance is computed using the following Equation No.3.2:

$$\rho_\lambda = \frac{\pi L_\lambda d^2}{ESUN_\lambda \sin\theta}$$

Equation 3.2: Convert radiance to top-of-atmosphere (TOA) reflectance

Where:

L_λ = Radiance in units of W/(m2 * sr * µm)

D = Earth-sun distance, in astronomical units.

$ESUN_\lambda$ = Solar irradiance in units of W/(m2 * µm)

θ = Sun elevation in degrees

3.4.3.2 Atmospheric Correction

Atmospheric correction of spectral imagery refers to the retrieval of surface reflectance spectra from measured radiances where it is an important step in deriving land surface properties from satellite data. A surface reflectance signal measured by passive satellite instruments is contaminate by the influence of the atmosphere: Rayleigh and Mie scattering, formation of thin cirrus clouds, and gas absorption are among the processes that prohibit one from seeing the surface behind a blurred image of radiation reflected by the atmosphere. Therefore the atmospheric correction technique was developed to eliminate the influence of these processes on a measured signal (Vermote and Kotchenova, 2008, pp.1-12).

There are many applications can eliminate the atmospheric effects caused by molecular and particulate scattering. The Fast Line-of-sight Atmospheric Analysis of Spectral Hypercubes (FLAASH) atmospheric correction algorithm/code one of these applications, which is developed by the Air Force Research Laboratory, Space Vehicles Directorate (AFRL/VS), Hanscom AFB and Spectral Sciences, Inc. (SSI) to support the analyses of visible to shortwave infrared (Vis - SWIR) hyperspectral and multispectral imaging sensors. The algorithm derives its first-principles physics-based calculations from the MODTRAN4 radiative transfer code.

The main objective of FLAASH is to eliminate atmospheric effects caused by molecular and particulate scattering and absorption from the 'radiance at detector' measurements in order to retrieve 'reflectance at surface' values (Felde et al., 2003, pp.90-92). That through applying Equation No. 3.3:

$$L = \left(\frac{A\rho}{1-\rho_e S}\right) + \left(\frac{B\rho_e}{1-\rho_e S}\right) + L_a$$

Equation 3.3: Eliminate atmospheric effects by using FLAASH

Where:

P is the pixel surface reflectance

P_e is an average surface reflectance for the pixel and a surrounding region

S is the spherical albedo of the atmosphere

L_a is the radiance back scattered by the atmosphere

A and B are coefficients that depend on atmospheric and geometric conditions but not on the surface.

3.4.3.3 Resampling

Resampling is mean changing the pixel dimensions of an image. Strictly speaking, Resampling is the process of interpolating the pixel values while transforming the raster dataset. This is used when the input and output do not line up exactly, when the pixel size changes, when the data is shifted, or a combination of these.

Where different raster datasets do not need to be stored using the same cell resolution. But when you are processing between multiple datasets, the cell resolution, like land use / land cover classification, ideally should be the same.

Very High Resolution (VHR) imagery with different spatial resolution were used in this study. Where used images from three different; QuickBird-II with spatial resolution 2.44 meter, WorldView-2 with spatial resolution 2 meter and DuabiSat-2 with spatial resolution 1 meter. There are many options or techniques of resample like Nearest, Bilinear and Cubic. But Nearest technique was used in that study, which performs a nearest neighbor assignment and is the fastest of the interpolation methods. It is used primarily for discrete data, since it will not change the values of the cells. The maximum spatial error will be one-half the cell size.

Resampling will be used to set size pixels of imagery before beginning to classify land use / land cover where set pixel size to 2.44 meter for all imagery which used in this study.

3.4.3.4 Band Composite

In order to generate the correct color composite image, one must understand the portion of the electromagnetic spectrum that each band is sensitive to. It is important to keep in mind that band combinations often vary from sensor to sensor, e.g., assigning bands 3-2-1 from either the QuickBird II satellite will create a natural color composite as is shown Table No.3.4

Band	QuickBird II		WorldView-2		DubaiSat-2	
	Band arrangement	Wavelength (nm)	Band arrangement	Wavelength (nm)	Band arrangement	Wavelength (nm)
Red	3	630-690	5	630-690	3	630-690
Green	2	520-600	3	510-580	2	520-590
Blue	1	450-520	2	450-510	1	450-520
NIR	4	760-900	7	770-895	4	770-890

Table 3.4: Bands used and their Wavelengths

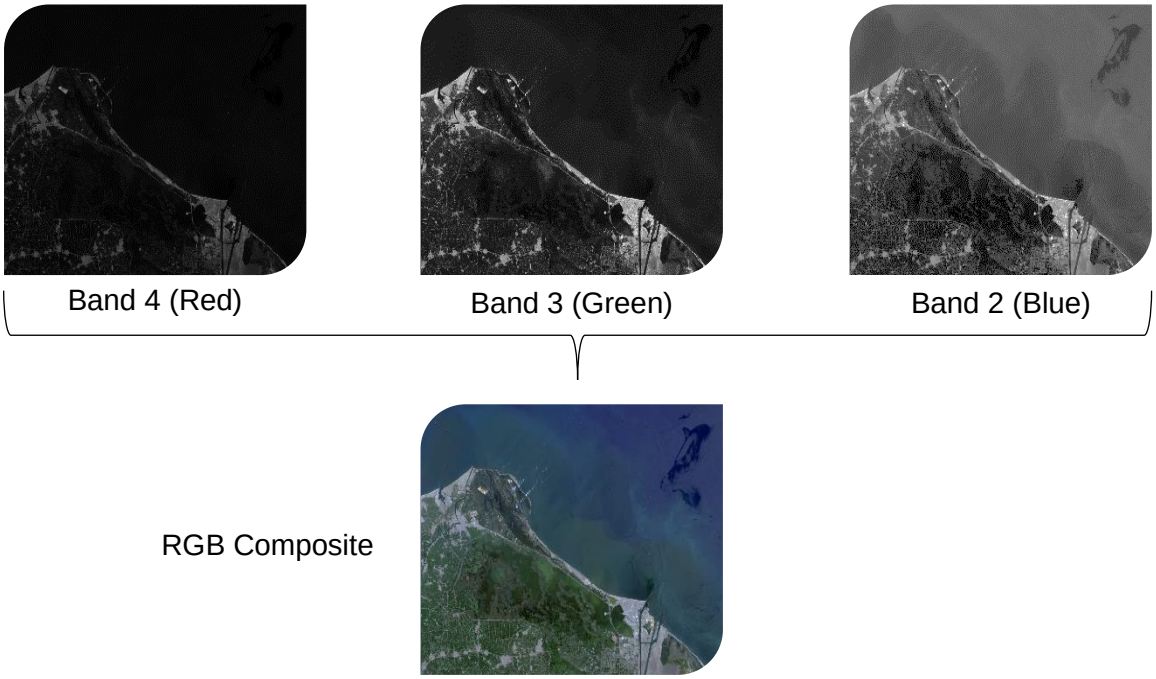

Figure 3.3: Composite three bands (Red, Green and Blue)

In order to apparent distinction between the different features, must improve the visual interpretability of the satellite images through bands composite. That is because when add single band raster to display, the default is that they will be displayed as black and white images, because the bands are collected individually. It means each single band is its own image in a particular wavelength. So, must display them in true color by combining three bands (red, green, and blue) together into composite raster as shown Figure No 3.3. Hence, can delineate land cover classes that could be easily interpret e.g. urban and agricultural land.

3.4.3.5 Mosaic and Clip Area of Interest (AOI)

Mosaicking is the process of combining multiple images into a single, seamless composite image (Jensen, 2015, pp.623). As indicated previously, the study area covered by many scenes for each of sensors which used. Therefore, it will create two mosaics dataset that contains scenes for each sensor separately. Then create a subset raster dataset by using clip area of interest (AOI) as shown in Figure No 3.4. This is aimed to remove data outside the area of interest to reducing the file size and improving the processing time for next operations of analysis.

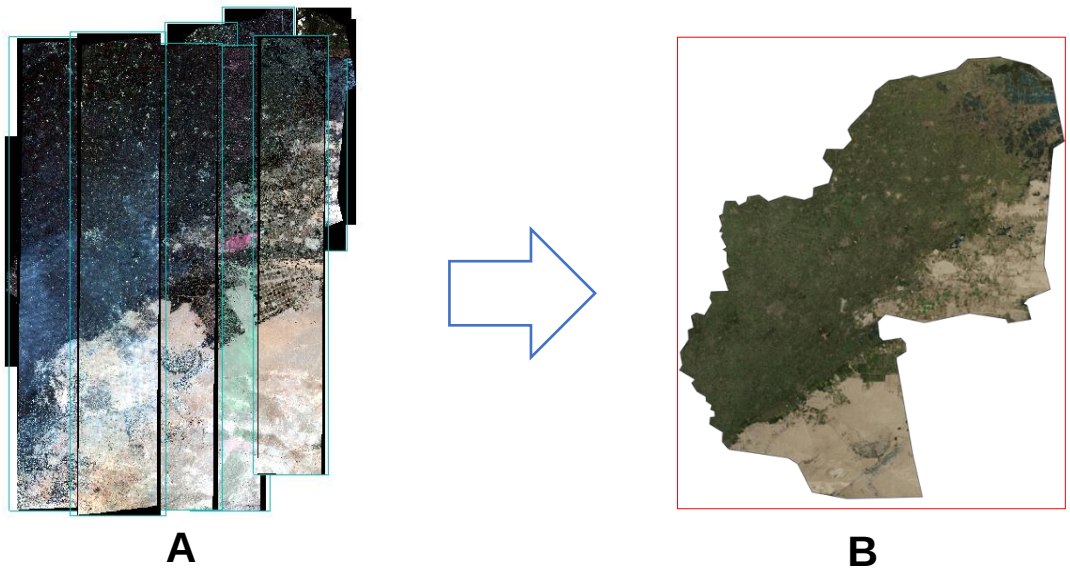

Figure 3.4: (A) Scenes before Mosaicing & (B) Scenes after Mosaicing and clip area of interest

3.4.3.6 Bit Depth conversion

Bit depth is the amount of detail in each pixel expressed in units of bits. The pixel depth, or bit depth, determines the range of values that a particular raster file can store, which is based on the formula 2^n where "n" is the pixel depth.

IMAGINE Subpixel Classifier is designed to work with raw unsigned 8-bit and 16-bit imagery. Signed data may be used, but all the image data should be positive. Negative image data values will likely produce error messages and problems with the classification results.

So, must be convert pixel depth for satellite data to correspond the range of values compatible for the Subpixel classification technique. I will choose to convert to unsigned 16 bits as shown Figure No 3.5, which means that the range of possible stored values for this type of bit depth in each image will be between 0 and 65535.

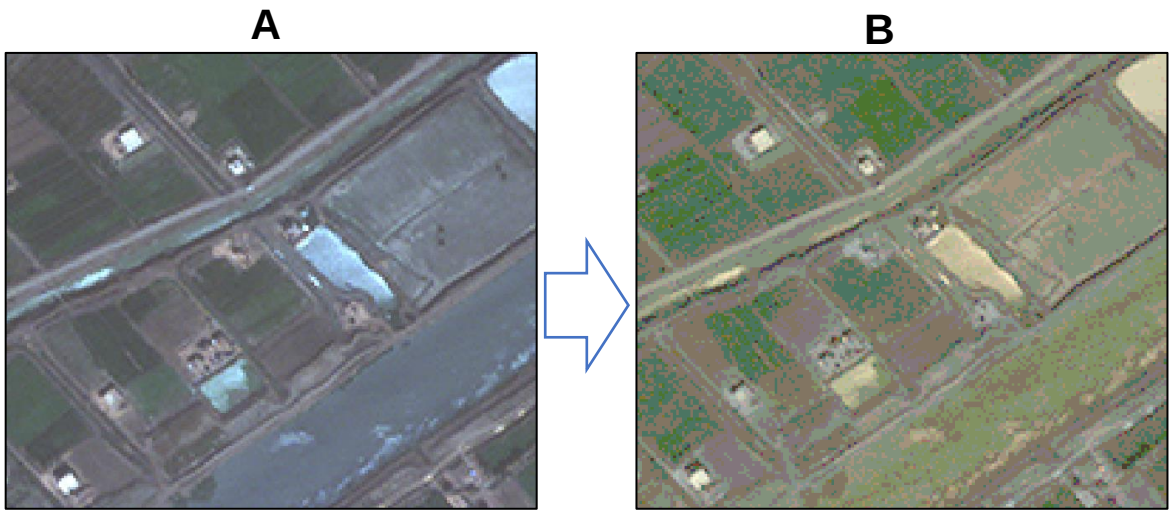

Figure 3.5: (A) Satellite image 32 Bit depth & (B) Image after convert to 16 Bit depth

3.4.4 Data Analysis

The data analysis stage includes several steps, aimed to detect of changes of LULC (LULC) between 2005 and 2015, by using two different classification approaches (Pixel-Based and Object-Based). Then assess of accuracy of the results of both approaches, to choose the closest approach for reality to use in change detection.

3.4.4.1 Pixel-Based Classification

In pixel-based classification, individual image pixels are analyzed by the spectral information that they contain (Richards and Richards, 1999, pp.). This is the traditional approach to classification since the pixel is the fundamental (spatial) unit of a satellite image, and consequently it comes naturally and is often easy to implement. There are limitations of pixel-based approaches, including the problem of mixed pixels.

One of the approaches developed to overcome this challenge is Subpixel classification, through which the proportion of different land covers within a pixel is determined. Subpixel

mapping aims to detect materials that are smaller than an image pixel, using multispectral imagery. It is also useful for detecting materials that cover larger areas but are mixed with other materials that complicate accurate classification. It is a powerful, low cost alternative to ground surveys, field sampling, and high-resolution imagery. It addresses the "mixed pixel problem" by successfully identifying a specific material when materials other than the one you are looking for are combined in a pixel. It discriminates between spectrally similar materials, such as individual plant species, specific water types, or distinctive man-made materials. This can be accomplished assuming spatial dependence, i.e. the tendency for spatially proximate observations of a given property to be more alike than more distant observations. Land cover is spatially dependent both within and between pixels on the condition that the intrinsic scale of variation is not smaller than the sampling scale imposed by the image pixels (Atkinson, 1997, pp.284).

Subpixel classifiers also known as soft classifiers, deal with the mixed pixel problem. Mixed pixels are normally found in boundaries between two or more mapping units, along gradients, such as when the occurrence of any linear or small subpixel object takes place as shown Figure No 3.6. (Sagardia, 2005, pp.75).

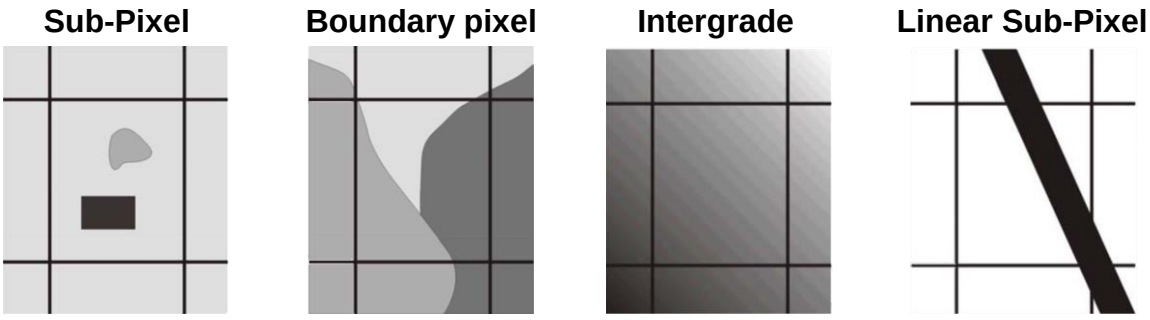

Figure 3.6: Four Cases of Mixed Pixels

There are four main sequential components to be achieve Subpixel classification of LULC as shown in Figure No.3.7.

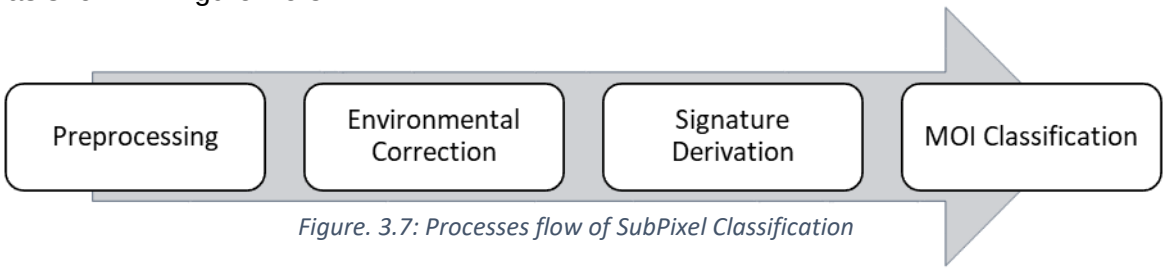

Figure. 3.7: Processes flow of SubPixel Classification

3.4.4.1.1 Preprocessing

Preprocessing is an automated process that must be performed prior to developing a signature or performing MOI Classification. This function identifies a list of potential backgrounds used during the signature extraction and MOI classification functions. To derive a subpixel signature or detection, the software must remove other materials, leaving a candidate MOI spectrum. The backgrounds identified by preprocessing are retained in a separate file for this purpose. Preprocessing need only be performed once per image. Can be used the same output each time perform classification or signature derivation.

3.4.4.1.2 Environmental Correction

The Automatic Environmental Correction feature prepares imagery for Signature Derivation and MOI Classification by automatically generating a set of environmental correction factors. These correction factors are necessary for scene-to-scene transferability of MOI signatures as well as for development of in-scene signatures. Environmental Correction compensates for unwanted spectral variations in scene pixels. These variations are caused by differences in atmospheric scattering, absorption by water vapor, and other environmental conditions. One of the benefits of this correction is that signatures derived from corrected images are scene-independent.

3.4.4.1.3 Signature Derivation

The Signature Derivation function develops a signature for a particular material of interest. A signature is more than just the material reflectance spectrum; it contains additional information required for Subpixel classification and scene to scene usage. The signature is developed using a training set, together with a source image, an environmental correction file, and the material pixel fraction in the training set. This process extracts the subpixel part of the material signature that is common to all pixels in the training set.

There are two approaches of Signature Derivation (Automatic and Manual), but I will be using Manual Signature Derivation in this thesis, which is used to generate a single

signature from a fixed set of input parameters. Also, to generate a signature from a whole-pixel training set. This approach used when confident of the Material Pixel Fraction in the training set. Accordingly, training samples are collected for each LULC class, which are previously determined as the Table No. 3.5.

Class ID	Class Name	Class Description
1	Agricultural Land	Dry land, wet land and orchards
2	Built-up Area	Settlements, industrial complexes and road network
3	Bare Land	Bare soils, degraded area and desert Lands
4	Water Bodies	River, lakes, canals and swamps

Table 3.5: Land use Land Cover Classification Schema

A total of 100 training samples were randomly distributed in the study area, with 25 samples for each LULC class as shown in Figure No 3.8.

The Manual Signature Derivation Report is exported for signatures to verify the quality and suitability of the signatures before moving on to the next step, as shown in Table No.3.6

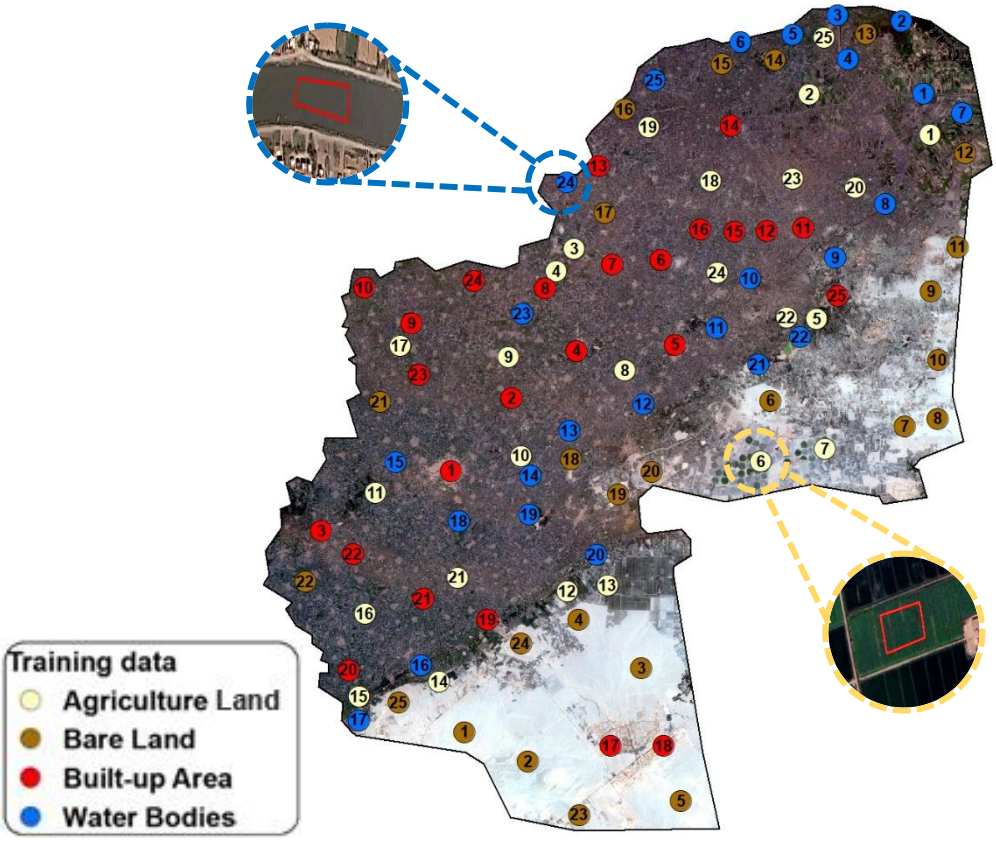

Figure 3.8: Locations of training samples for LULC classes

Specifications of Signatures	Agriculture	Built-up Area	Bare Land	Water Bodies
Number of bands	4			
Band selection	1,2,3,4			
Number of training pixels	987	990	999	919
Mean Material Pixel Fraction	0.900	0.900	0.900	0.900
Confidence	0.800	0.800	0.800	0.800
Signature Spectrum mean	70.043	51.839	118.054	28.476
Actual rau min	27.103	35.603	87.853	3.353
Actual rau max	105.603	73.853	153.853	47.853
Calc rau min	32.975	38.464	92.790	6.682
Calc rau max	99.732	70.992	148.917	44.525

Table 3.6: Signature report for Subpixel Classification method

The above table shows the signatures specifications for each of the LULC classes collected, which have been mentioned previously. The table indicates that the signatures was collected from four bands, which representing all signatures in the satellite images used in the classification (Red, Green, Blue, NIR).

The number of training pixels detected by the signature that are compared to the number of training pixels used to derive the signature. Where the table shows the number of training pixels ranging from 987 for the class of agriculture and 999 for the category of water bodies. As indicated previously, The IMAGINE Subpixel Classifier Signature Derivation function derives a signature for a material that is common to the training set.

As for values of the signature spectrum mean is the equivalent spectrum of a pixel that is exclusively inhabited by the MOI. The numbers in the spectrum should fall within the range 0:65,535 for 16-bit imagery. The mean values range between 51 for the Built-up area and around 118 for bare land, which proves the suitability of the signatures for the classification.

3.4.4.1.4 Material of Interest (MOI) Classification

Classification is the process of finding those pixels within the scene which have spectral properties that are like a given signature material of interest. This function can identify materials of interest even when they are mixed with other materials and occupy only a fraction of the pixel ground sample area. Figure No.3.9 shows the ground area covered by the instantaneous field of view (IFOV) of the sensor at the time the image is acquired. For

frame-capture sensors this can be considered the area covered by one pixel. For simplicity, consider that the land area covered by the pixel consists of two materials:

- Material of Interest (MOI)
- A background material which could be a mixture of several separate materials, but the mixture is considered one material.

Where:

- MOI has reflectance R1(λ) and covers area A_1.
- Background material (mixture) has reflectance $R_2(\lambda)$ and covers area A_2 such that $A_1 + A_2 = A$, the total area of the pixel.
- Incident irradiance on the pixel is $I_0(\lambda)$ and the upwelling radiance reflected by the pixel is $I_1(\lambda)$.

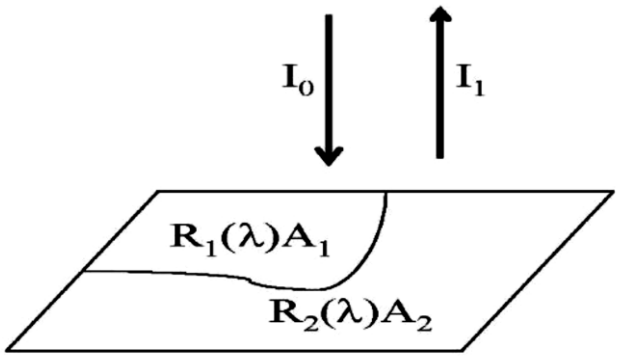

Figure 3.9: Reflectance and Radiance through Subpixel Classifier Theory

The pixel radiance is a mixture of the radiance due to the two materials, as shown Equation No.3.4

$$\mathbf{I_1(\lambda) = I_0(\lambda)\frac{(R_1(\lambda)A_1 + R_2(\lambda)A_2)}{A}}$$

Equation 3.4: Mixture of the radiance

Introducing the material pixel fraction, k, such that A_1=kA, the radiance becomes as shown in Equation No. 3.5

$$\mathbf{I_1(\lambda) = k(I_0(\lambda)R_1(\lambda)) + (1-k)(I_0(\lambda)R_2(\lambda))}$$

Equation 3.5: The radiance after introduce the material pixel fraction (k)

Following atmospheric and sensor gain/offset correction, the pixel intensity P(λ) is proportional to the upwelling radiance so that as shown Equation No.3.6

$$\mathbf{P(\lambda) = k \times S(\lambda) + (1 - k) \times B(\lambda)}$$

Equation 3.6: Atmospheric and sensor gain/offset correction

Where:

- $S(\lambda)=R_1(\lambda)$ is the MOI signature
- $B(\lambda)=R_2(\lambda)$ is the background spectrum

3.4.4.2 Object-Based Classification

Object-Based image analysis (OBIA) also called Geographic Object-Based image analysis (GEOBIA). GEOBIA or OBIA refers to a category of digital remote sensing image analysis approaches that study geographic entities, or phenomena through delineating and analyzing image-objects rather than individual pixels (Castilla and Hay, 2008, pp.91-110) , with increasing spatial resolution and availability of very high spatial resolution (VHR) imagery, object-based image analysis (OBIA) techniques were developed. This approach does not analyze individual pixels, but rather groups of pixels, referred to as image objects. Real-world objects vary in size, shape, texture, spectral signature, and spatial context, so OBIA must account for these factors (Strobl, 2000, pp.542). Different spectral, spatial or textural parameters of the image objects or (called as features), such as mean reflectance value, area, perimeter and many others are calculated. These features can then be used in the classification process. The goal of finding optimal parameters of segmentation to avoid over / under segmentation and thus finding meaningful optimal objects matching with real-World structures (Tian and Chen, 2007, pp.4625-4644).

As well as, OBIA approach is the ability to analyze an image at different hierarchical levels. These image object levels are created by segmentation process. Segmentation algorithm can be applied to pixel level to create the first image object level, or to an existing image object level to refine it (e.g. merge objects with similar spectral properties) or to create new

sub-levels or super-levels. Different image object levels are aware of each other and know their hierarchical relationships. Each image object has its neighboring image objects at the same hierarchical level, sub-objects at the lower level and multiple image objects are part of a super-object at higher hierarchical level. These hierarchical relationships can be used to describe class properties (Murcko, 2017, pp.76). The relationships are illustrated as shown in Figure No. 3.10.

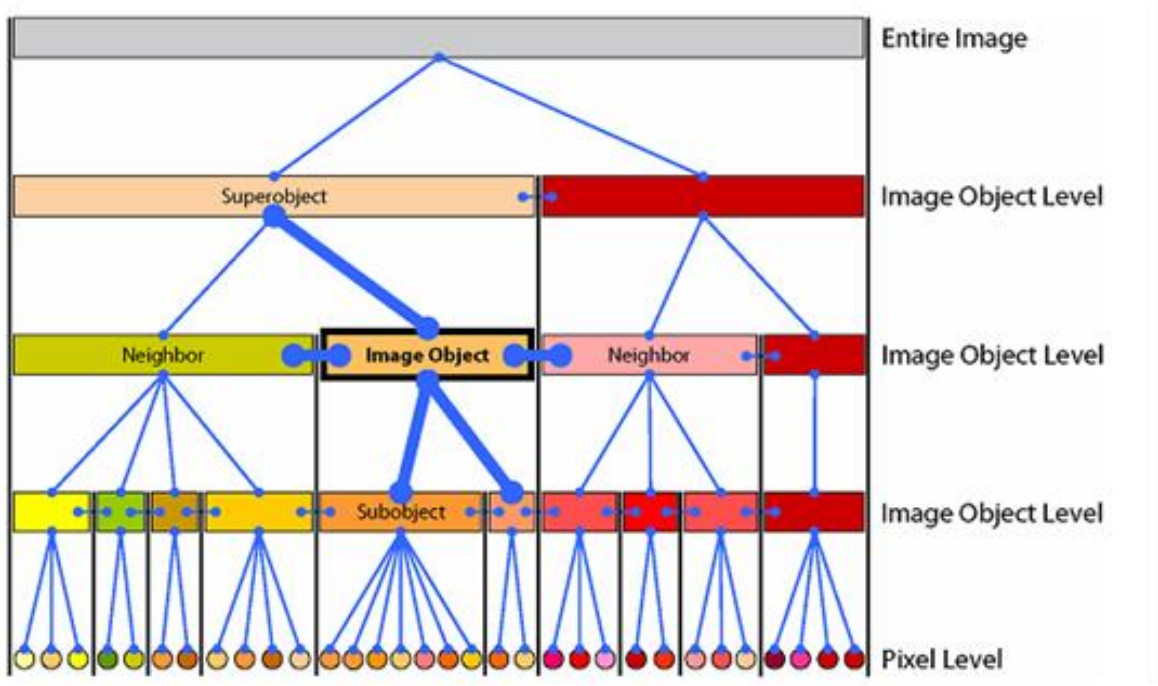

Figure 3.10: Image object hierarchy and relationships

However, humans can classify visual objects immediately and discretely, without consciously considering such things. The theoretical framework of GEOBIA / OBIA can be divided into several stages as in Figure No. 3.11, which can be summarized in two main principles as follows:

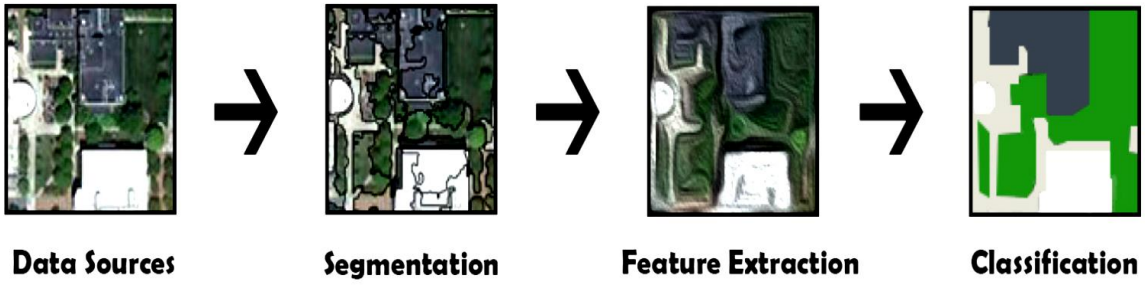

Figure 3.11: GEOBIA / OBIA Framework

3.4.4.2.1 OBIA Segmentation

Segmentation is the first and most important step in object-based image classification. The basic task of segmentation algorithms is to merge homogenous pixels into image elements to enable the differentiation between heterogeneous neighboring regions (Schiewe, 2002, pp.380-385).

There are two approaches that contain many image segmentation algorithms. The first one is the top-down approach which contains many algorithms such as Contrast Split Segmentation, Spectral Difference Segmentation, Multi-Treshold Segmentation. The second approach is the bottom-up, which contains many algorithms such as Chessboard Segmentation, Quadtree-Based Segmentation or Multiresolution Segmentation, which is probably the most popular image segmentation algorithm and will be relied upon in this study. Multiresolution segmentation algorithm is a bottom-up region-growing technique, starting at the pixel level and merging pixels into image objects. In subsequent steps, small image objects with similar spectral values are merged into larger objects (Benz et al., 2004, pp.239-258). It is based on a pairwise region merging technique. An important parameter of the algorithm is the Scale parameter. It is an abstract term that determines the maximum allowed spectral heterogeneity for the resulting image objects. The scale parameter basically determines the size of the resulting image objects. The higher the scale parameter number, the bigger in size will be the resulting objects.

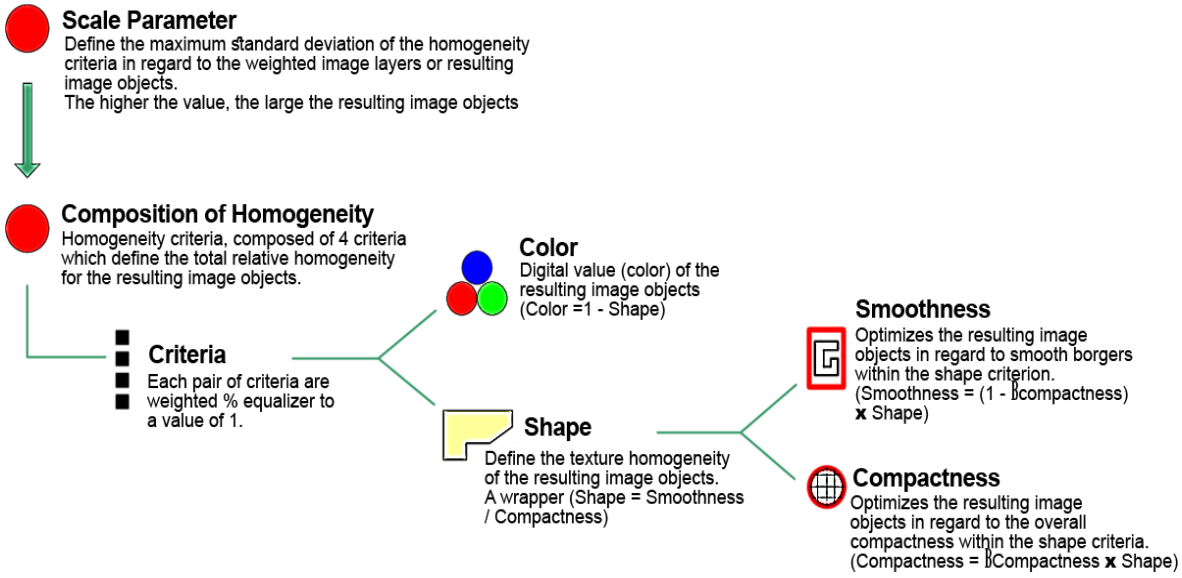

Figure 3.12: Multiresolution Segmentation Scale parameter concept

The resulting objects for heterogeneous data for a given scale parameter will be smaller than in more homogeneous data. The Scale parameter, which refers to the object homogeneity, is composed of three internal parameters, which are color, shape and compactness (Murcko, 2017, pp.76) as demonstrates the concept in Figure No 3.12.

Segmentation usually requires some supervision through the input of texture training areas, manual adjustments to segment boundaries, or the creation of additional dissolves not triggered by the chosen algorithm (Dissanska et al., 2009, pp.189-215). Though object-based classification cannot be performed without first segmenting an image, it is possible to iterate through cycles of merging, re-segmenting, and re-classifying portions of an image to improve result accuracy. Several iterations may be necessary because noise in the image data can negatively affect segmentation if it occurs on a similar spatial scale as an object's texture (Zhang and Maxwell, 2006, pp.1-5). The segmentation of sub-objects can ultimately affect the drawn accuracy of the model objects. Thus, it is preferable to over-segment the image with smaller polygons and merge upwards, stopping before the Model Object is merged with other objects. Though object-based classification cannot be performed without first segmenting an image, it is possible to iterate through cycles of merging, re-segmenting, and re-classifying portions of an image to improve result accuracy. Several iterations may be necessary because noise in the image data can negatively affect segmentation if it occurs on a similar spatial scale as an object's texture.

The goal is to produce image objects with unambiguous boundaries, uniform shapes and unique textures that represent real-world objects. First, the image was segmented using the trial and error approach and with the following parameters: Scale = 5, Shape = 0.1 and compactness = 0.7, as shown Figure No. 3.13.

Segmentation is breaking the image up into objects representing land-based features. In segmentation, grayscale texture is used to create polygons known as segments that represent homogenous regions. Multiresolution segmentation involves segmenting an image at multiple resolutions, in order to fuse homogenous lower level sub-objects into higher level model object classes. The result is a tessellation of polygons spanning the

image extent, with each texture-based polygon ideally containing adjacent pixel groupings that represent cohesive real-world objects.

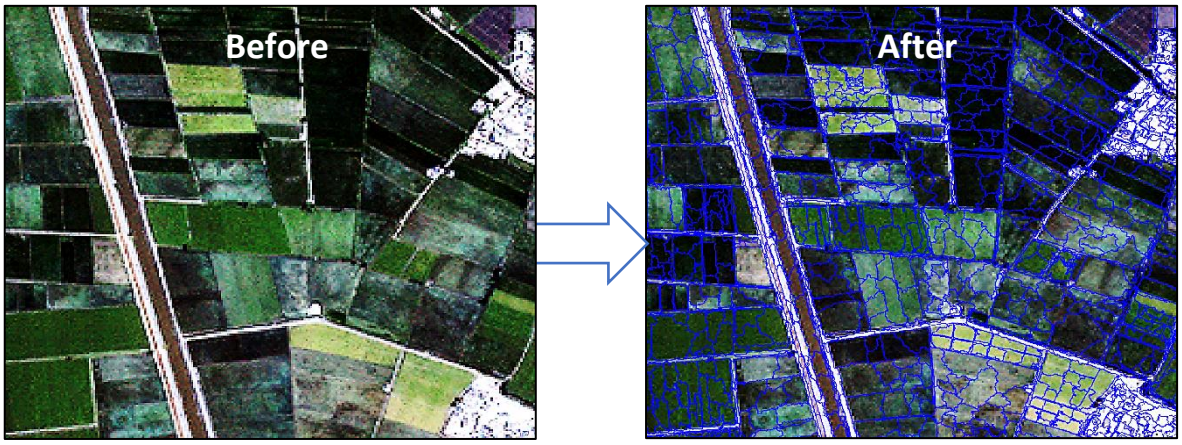

Figure 3.13: Result of Multiresolution Segmentation

In the urban part of the study area (10 Ramadan city), streets, roads and high way often represent boundaries of built-up areas of different types, and built-up areas within these boundaries tend to be of similar urban fabric. Since one of our goals was to find and extract these typical built-up areas. So, the first step of the rule set was to segment the scene into blocks encompassed by OpenStreetMap road network using Chessboard Segmentation which using vector as ancillary thematic layer and object size parameter greater than the size of the biggest object in the scene e.g.10.000, which results into segmenting the image according to the road network thematic layer as shown in Figure No.3.14.

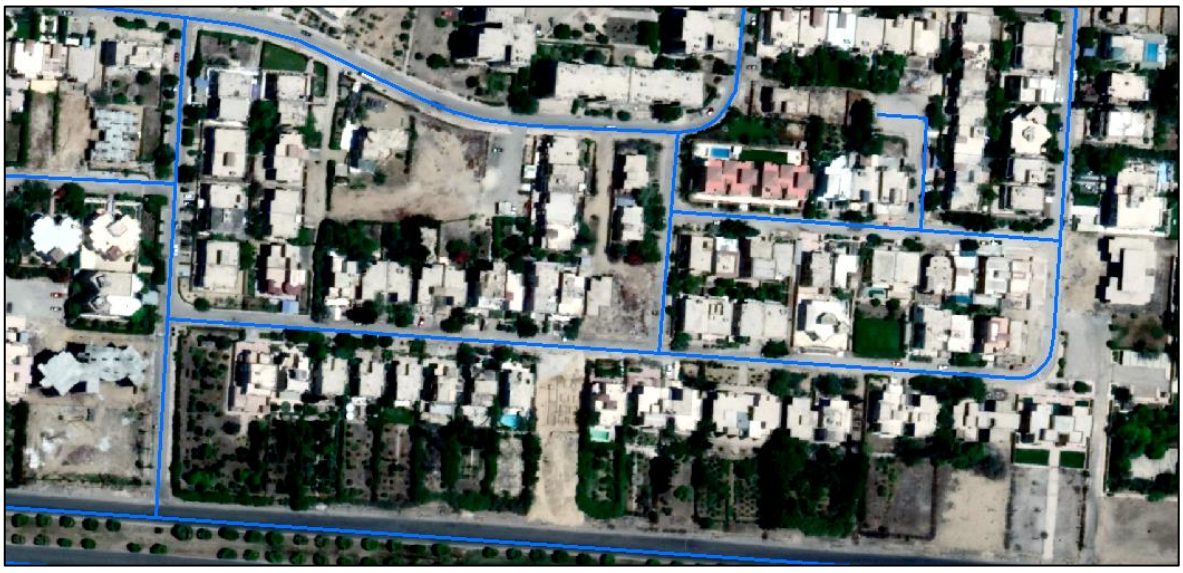

Figure 3.14: Result of first segmentation – Chessboard Segmentation using OSM road network

The second step create another subsequent segmentation was performed on the previous image object level. Then apply Multiresolution Segmentation to delineate the features class. In this way led, to keep the resulting segments within the constraints of the road network segments by using the OpenStreetMap road network as an ancillary thematic layer as shown Figure No 3.15.

Figure 3.15: Result of second segmentation – Multiresolution Segmentation for Built-up area

3.4.4.2.2 OBIA Classification

The second step in object-based image analysis is classification. Initially, four land cover were defined: Agricultural (including dry land, wet land and orchards), Built-up area (including settlements, industrial complexes and road network), Bare Land (including bare soils, degraded area and desert land) and Water bodies (including river, lakes, canals and swamps). Thus, the final classification map contains four land cover types.

In object-based image classification, we can distinguish two main approaches – supervised and rule-based. Object-based supervised classification is, similarly to pixel-based supervised classification, based on selection of training samples that are used to train the classification algorithm.

On the other hand, rule-based approach that will be relied in this study does not use any samples for the classification but is based purely on the expert knowledge of the user. The user develops a set of conditions or rules, commonly referred to as a rule set, for each target

class. The features (properties, statistics) of the image objects, such as spectral mean value, size, shape, texture, or different contextual image features are used in the rule set development. If the image object fulfills the criteria of the class, it is classified to that respective class. The advantage of this approach is that the user has full control of the classification process and he can strictly define what does and what does not belong to the class (Murcko, 2017, pp.76).

As mentioned before, a create rule sets or process trees to classify image objects into meaningful land cover classes by outputting hundreds of features (spectral, spatial, textural, and contextual information) that describe image objects created during the segmentation process (Benz, Hofmann et al., 2004, pp.239-258).

The process of establishing begins the rule sets using the trial and error approach combined with the knowledge regarding study area. In order to detect changes LULC in the study area, image objects at the analysis level were classified into several LULC classes as mention pervious. An information about classes was used in adjusting the shape of image objects in order to find the optimal shape representing segment with uniform each class. Various spectral, spatial, textural or contextual features was employed in the classification rule set establishment in order to reliably classify image objects into land cover classes. In addition, several normalized indices using different band combinations were examined to suitably extract predefined LULC classes. Among these, most used were NDVI and NDWI as demonstrated in Table No. 3.7 and Appendix.

Class	Rules
Agriculture Land	• 1 < NDVI ≥ 0.1 • NIR > 4
Built-up Area	• NDVI < 0 • Red Band > 5 • Blue Band > 7 • Area > 50 px • Texture Rang > 15.5 • Texture Variance < 168
Bare Land	• -0.2 < NDVI > -0.05 • Area > 5.000 px • Std. NIR < 0.5

Water Bodies	• NIR < 4 • 1 < NDWI > 0.2 • 0 < NDVI > -1

Table 3.7: Rules of LULC classes in rule-based classification

Part of the study area images was used to develop the hierarchical expert rule-based classification system as a pilot image. Figure No 3.16 shows the classification results of the Pilot image.

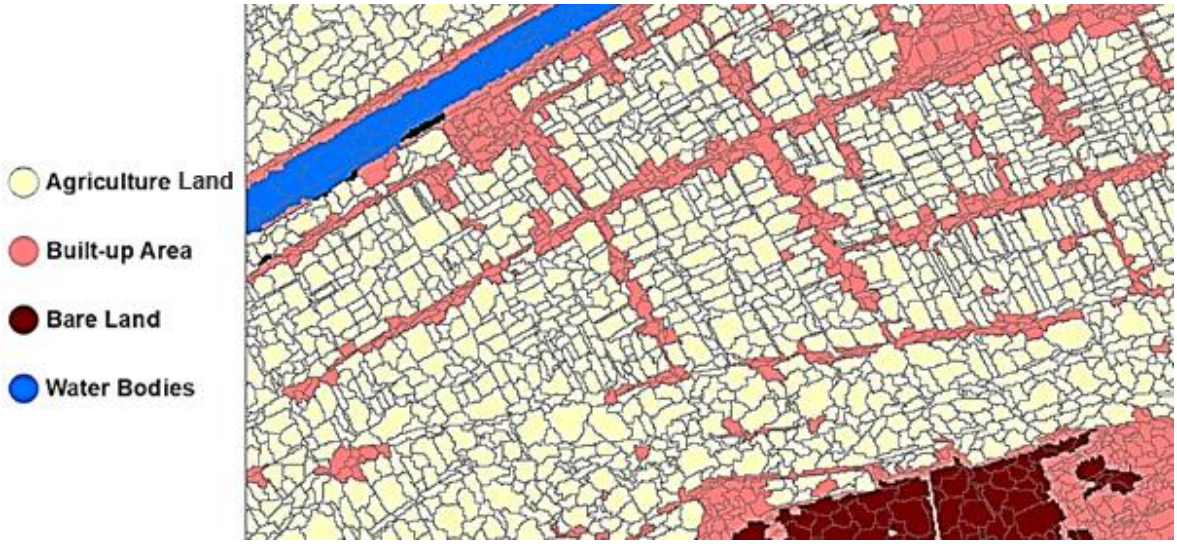

Figure 3.16: Result of the pilot image for OBIA classification rules

Undergo OBIA classification rule sets was trial and error approach as mentioned above to identify four main classes as achieve results closer to reality, as the following order:

3.4.4.2.2.1 Rule sets for Agriculture

The first step in the proposed hierarchical expert rule-based system is to extract agriculture class. Active agriculture can be identified in the near infrared spectrum due to the rise reflectance value compared to the red spectrum. Reflectivity rises sharply at 0.75 μm, the so called red-edge region (Mather and Koch, 1999, pp.306). The Normalized Difference Vegetation Index (NDVI) has been widely used in the literature to separate agriculture and others LULC classes. It is calculated by Equation No.3.7

$$NDVI = (NIR - R)/(NIR + R)$$

Equation 3.7: Normalized Difference Vegetation Index (NDVI)

Where NIR and RED are the mean values of all pixels (within the boundary of each object)

in Near Infrared band and Red band for a given object in each level of segmentation.

The values range from -1 to 1. High values of NDVI indicate presence of healthy green vegetation, whereas lower values might indicate stressed vegetation, bare soil. Based on our experience the threshold for classifying agriculture areas was set greater than or equal to 0.1 and up to 1 for NDVI in the Pilot image.

3.4.4.2.2.2 Rule sets for Bare Land

The second step in the proposed hierarchical rule-based system is to extract bare land, which is characterized by a fairly segment large size of agricultural or built-up area or even water bodies where define rule is more than 5.000 px.

Also, characterized the class by the spectral reflectance of the standard deviation of NIR where set rule by less than 0.5. As well as use the Normalized Deference Vegetation Index (NDVI) to find bare land where is set rule between -0.05 and -0.2.

3.4.4.2.2.3 Rule sets for Water Bodies

The Normalized Difference Water Index is a spectral index that has been developed to highlight the presence of open water features in remotely-sensed digital imagery. It is also used as a metric for masking out black bodies – water and shadows. The NDWI makes use of reflected near-infrared radiation and visible green light to enhance the presence of such features while suppressing soil and vegetation features. There exists another version of NDWI (Gao, 1996, pp.257-266) and is used mostly for monitoring changes in water content of leaves. In this study, however, SWIR bands are not available in the VHR datasets and the main aim was to use NDWI to classify water bodies, therefore NDWI (McFeeters, 1996, pp.1425-1432) was used. The NDWI formula is:

$$NDWI = (GREEN - NIR)/(GREEN + NIR)$$

Equation 3.8: Normalized Difference Water Index (NDWI)

Where NIR and GREEN are the mean values of all pixels (within the boundary of each object) in Near Infrared band and GREEN band for a given object in each level of segmentation. The values range from -1 to 1. High values of NDWI indicate presence of

water content, whereas lower values might indicate bright surface with no vegetation or water content. Based on our experience the threshold for classifying water bodies was set between greater than 0.2 and less than 1. As well as using Normalized Difference Vegetation Index (NDVI) to find water bodies where is set rule between 0 and 1. And set rule of reflectance near infrared (NIR) value less than 4 to find water bodies.

3.4.4.2.2.4 Rule sets for Built-up Area

The last step in the hierarchical rule-based classifier is to classify built-up area (including road network and settlements). Because of the difficulty distinguish built-up areas from other surfaces or other classes. So, set more rules to extract built-up area closest to reality. Moreover, two levels of segmentation were used as mentioned previously to find built-up area with use (OpenStreetMap) as vector road network as ancillary thematic layer and add it into built-up area class. Built-up area has low NDVI value so set rule less than 0 of NDVI values, and high reflectance in the blue and red band so set rule more than 5 and 7 respectively. As for the texture variance is small so set less than 168, but the range is big so set rule more than 15.5. Finally, the area or size factor of built-up area (e.g. building) is set in the rules to be greater than 50 px.

3.4.4.3 Accuracy Assessment

Accuracy assessment step is an important part of any classification project. Where is based on comparing the map depiction of land cover to the true land cover condition (Stehman, 2009, pp.5243-5272). Strictly speaking, it is a comparison of a classification with ground truth data to evaluate how well the classification represents the real world. The increased usage of remote sensing data and techniques has made geospatial analysis faster and more powerful, but the increased complexity also creates increased possibilities for error. In the past, accuracy assessment was not a priority in image classification studies. Because of the increased chances for error presented by digital imagery of the increased changes for error presented by digital imagery, however, accuracy assessment has become more important than ever (Congalton, 1991, pp.35-46).

Classification error occurs when a pixel (or feature) belonging to one category is assigned to another category. So, we need to evaluate the classes with independent data. Depending on the data we have or time and available resources, we can evaluate the map with several ways e.g. air photos or take map in the field and compare with the real world this is consider as the most reliable. However, it is the most costly and time-consuming approach.

Accuracy assessment was performed on 100 randomly selected points. Although point-based accuracy assessment can be considered as unstable and inferior to area-based method (Ma et al., 2017, pp.277-293). The number of required test points to generate an error matrix was calculated using the equation for a multinomial distribution provided by (Congalton and Green, 2008, pp.). Number of test points for each class was then calculated based on the proportion of the area covered by this class however, the minimum number of points for each class was set to 10, and this ensures that the smallest class has enough points for a true measure of accuracy assessment. Calculated numbers of points for each class was then randomly placed within the study area, using Stratified Random method.

There are many analysis methods to validate the accuracy of a remote sensing, but I used a KAPPA analysis (KHAT). KAPPA analysis is a discrete multivariate technique that is used in the accuracy assessment (Congalton and Mead, 1983, pp.69-74) KAPPA analysis yields a KHAT statistic (an estimation of KAPPA) that is a measure of agreement or accuracy (Rosenfield and Fitzpatrick-Lins, 1986, pp.223-227). On the other hand, Kappa statistics indicate how much better the classification is compared to one where randomly assigned a class value to each pixel. The principal advantage of computing KHAT is the ability to use their value as a basis for determining the statistical significance of any given matrix (Rahman and Saha, 2008, pp.189-201). Equation No. 3.9 computes the KHAT statistic.

$$\hat{K} = \frac{N \sum_{i=1}^{r} x_{ii} - \sum_{i=1}^{r} (x_{i+} * x_{+i})}{N^2 - \sum_{i=1}^{r} (x_{i+} * x_{+i})},$$

Equation 3.9: Kappa statistics

Where r is the number of rows in the matrix. xii is the number of observations in row I and

column i, x i+ and x +i are the marginal totals of row i and column I, respectively, N is the total number of observations (Bishop et al., 1977, pp.297-306).

3.4.4.4 Change Detection

Change detection is the process of identifying differences in the state of an object or phenomenon by observing it at different times (Singh, 1989, pp.989-1003). Biophysical materials and human-made features on the surface of the earth are inventoried using remote sensing in situ techniques. Some of the data are fairly static; they change very little over time. Conversely, some biophysical materials and human-made features are dynamic, changing rapidly. It is important that such changes be inventoried accurately so that the physical and human processes at work can be more fully under stood (Jensen, 2015, pp.623). Timely and accurate change detection of Earth's surface features is extremely important for understanding relationships and interactions between human and natural phenomena in order to promote better decision making. There are many techniques for detecting change and perhaps the most common methods used to detect changes is image differencing, principal component analysis and post-classification comparison.

In recent years, spectral mixture analysis, artificial neural networks and integration of geographical information system and remote sensing data have become important techniques for change detection applications. Different change detection algorithms have their own merits and no single approach is optimal and applicable to all cases (Lu, Mausel et al., 2004, pp.2365-2401).

A summary of this chapter: This chapter covered the detail of the data and software used the methods used in the study that has been answered which way to detect changes of LULC in the study area? Which has consisted of several stages, starting with the data acquisition which covering the study area in the specified periods. The second stage is concerned data pre-processing e.g. Radiometric Calibration and combine bands. Then classify LULC based on two approaches Pixel-Based and Object-Based, after that assess accuracy of classification to choose the best approach to applying detect changes of LULC.

Chapter-4: Processes and Results

4.1 Introduction

This chapter discusses two classification approaches of LULC to detect changes between 2005 and 2015 in ASh-Sharqiyah governorate of Egypt. Where this chapter contains four major sections that documented includes the specific steps for each classification approach (Pixel-Based Classification and Object-Based Classification), then accuracy assessment of classification results for both approaches to choose the most accurate approach to reality to apply it in detect changes for LULC.

4.2 Pixel-Based Classification

Subpixel based procedures analyses the spectral properties of every pixel within the area of interest. The spectral pattern present within the data for each pixel is used to perform the classification and the spectral pattern present within the data for each pixel is used as the numerical basis for categorization. By determining the fractional proportion of the different land cover types in a pixel based on an appropriate training data set.

The output takes the form of a single fraction plane for the material of interest, rather than number of fraction planes for number of characteristic scene materials. In order to, classify more than one material, the process is repeated for each material according to the numbers of classes previously identified (Agriculture, Built-up area, Bare land, Water bodies).

IMAGINE Subpixel Classifier reports classification results for each signature in different output classes as selected detections are reported for Material Pixel Fractions less than 20%, as this is below IMAGINE Subpixel Classifier's detection threshold, where the results are grouped into eight equal categories starting from the greater 20% To 100%.

4.2.1 Agriculture Class Results by Subpixel Classification

As indicated in Figure No. 4.1 that agriculture class is spread in Ash-Sharkia governorate during the study period between 2005 and 2015 where the agricultural lands are scattered in all directions except south and northeast.

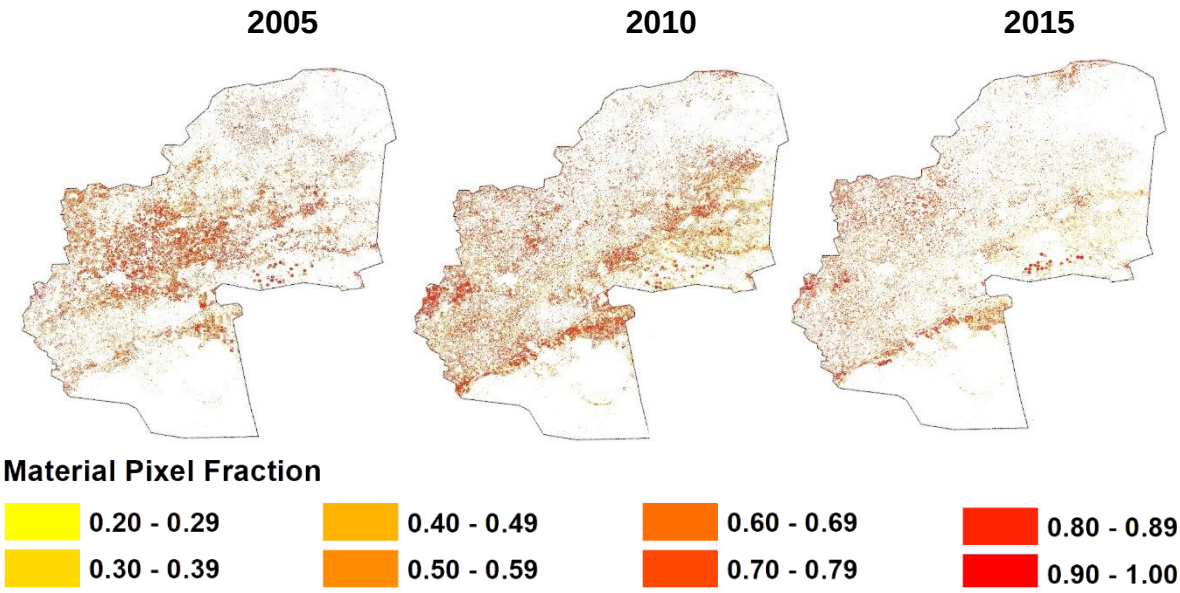

Figure 4.1: Agricultural land by Using Subpixel Classification

Through the summary of statistics, the fraction of material present in each pixel classified for agriculture land, the result shows that the eighth group (0.90 - 1.0) has most of the pixel detection which contain all the pixels that have 90% to 100% of the pixel area occupied by the Material of Interest (MOI) as shown in Table No. 4.1.

Material Pixel Fraction	2005		2010		2015	
	Detections	hectares	Detections	hectares	Detections	hectares
0.20 - 0.29	1,015,600	22,851	622,267	14,001	713,733	16,059
0.30 - 0.39	842,711	18,961	556,044	12,511	729,333	16,410
0.40 - 0.49	875,115	19,690	417,200	9,387	667,067	15,009
0.50 - 0.59	896,400	20,169	549,733	12,369	801,022	18,023
0.60 - 0.69	580,267	13,056	801,111	18,025	720,133	16,203
0.70 - 0.79	493,289	11,099	880,489	19,811	765,778	17,230
0.80 - 0.89	1,175,956	26,459	993,600	22,356	853,600	19,206
0.90 - 1.00	9,957,324	224,040	11,928,866	268,399	10,158,712	228,571
Total	16,580,213	356,325	16,749,311	376,859	15,409,379	346,711

Table 4.1: Statistics of Agricultural land by Using Subpixel Classification

Where the eighth group took the biggest share (0.90-1.00) of the detection in 2005 to nearly 10 million by 62.8% of the total. while in 2010 increased to nearly 12 million detections by 71.2% of the total. In 2015 fell to about 10 million pixels by 65.9% of the total. This of course affects the occupied area of each group, which it will be discuss later. While the seventh group (0.80-0.89) on the second largest group in terms of detections in study period. Where

in 2005 it acquired nearly 1 million detections by 7.4%. In 2010 decreased to 993,600 detections by 5.9% and the decline in 2015 to 853,600 by 5.5%.

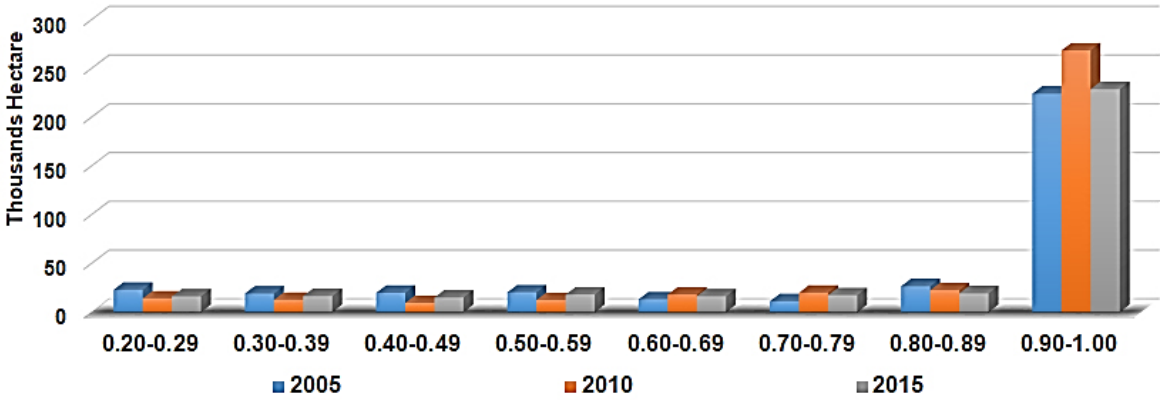

Figure 4.2: Areas Occupied of Agricultural land between 2005 and 2015 Using Subpixel Classification

The occupied areas for each group of Subpixel classification results are directly proportional to number of detections, so that whenever the number of detections increased directly proportional to the occupied area for each group.

As shown in Figure No.4.2 The eighth group (0.90-1.00) constituted most of the area occupied in the classification of agriculture land at all years of study where in 2005 it occupied an area of about 356,325 hectares, representing about 67% of the total area of the agricultural land class results. While the occupied area of the same group increased significantly in 2010 by 20,535 hectares compared to 2005, a percentage of 70% of the total area of the agricultural class, while the area decreased in 2015, reaching 346,711 about 65% of the total area of the agricultural land class of Subpixel classification results.

Whereas the rest of groups occupied small areas compared to the eighth group of the total area for agricultural class of Subpixel classification results throughout the study period.

4.2.2 Built-up Area Class Results by Subpixel Classification

Built-up area is spread in the study area but is concentrated in clusters as shown in Figure No. 4.3 perhaps the largest area in the west of the study area, and there is also a large gathering in the far north east specifically in 2015. It is also noticeable the extension of built-up areas over the study period.

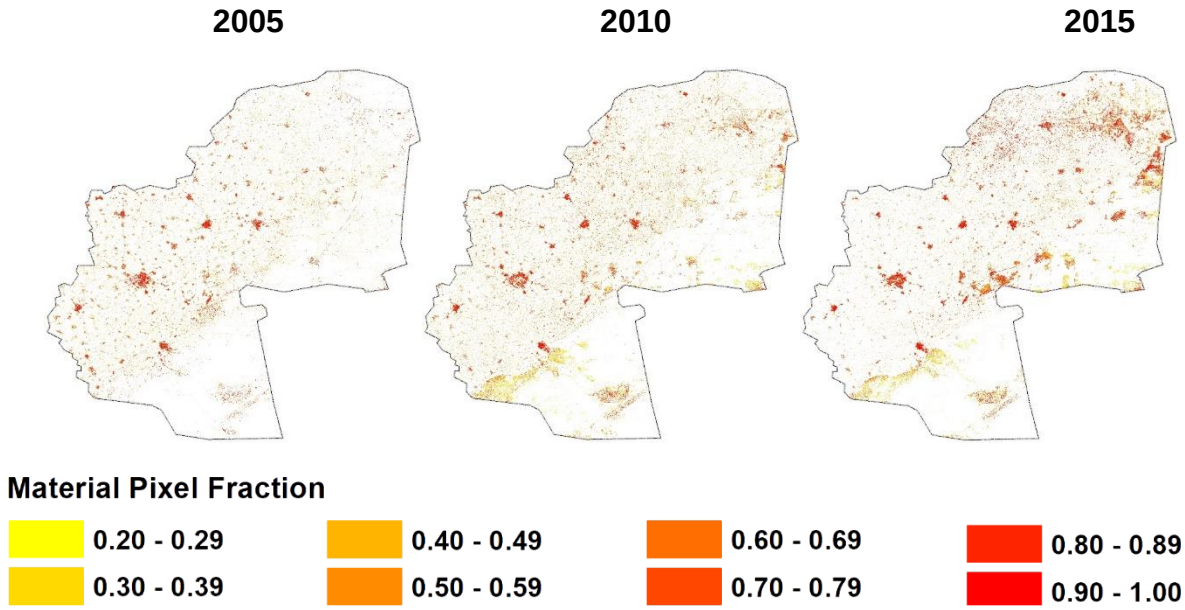

Figure 4.3: Built-up Area Using Subpixel Classification

Results statistics for built-up area indicate that the eighth group (0.90-1.00) contains most of detections through the study period as shown in Table No. 4.2. The eighth group accounted for almost 1 million detections in 2005, accounting for 32% of the total detections, while in 2010 it retained the same detections number with a decrease of 31%. In 2015, the number of detections increased to 2,758,622 by 55.8% of the total detection for the same year, which affects the area occupied for each group. While the rest of the groups acquired a small number of detections of the built-up area class compared to the eighth group.

Material Pixel Fraction	2005		2010		2015	
	Detections	hectares	Detections	hectares	Detections	hectares
0.20 - 0.29	352,044	7,921	364,578	8,203	533,600	12,006
0.30 - 0.39	339,454	7,638	355,600	8,001	356,667	8,025
0.40 - 0.49	271,644	6,112	310,267	6,981	158,222	3,560
0.50 - 0.59	267,689	6,023	316,089	7,112	178,800	4,023
0.60 - 0.69	266,089	5,987	290,800	6,543	142,444	3,205
0.70 - 0.79	242,686	5,460	233,778	5,260	357,378	8,041
0.80 - 0.89	360,889	8,120	454,489	10,226	454,667	10,230
0.90 - 1.00	1,023,333	23,025	1,092,844	24,589	2,758,622	62,069
Total	3,123,829	70,286	3,418,444	76,915	4,940,400	111,159

Table 4.2: Statistics of Built-up Area Using Subpixel Classification

While the seventh group (0.80-0.89) in 2005 accounted for the second largest number of detections by 360,889 by more than 11%. The seventh group (0.80-0.89) in 2010, where the number of detections 454,489 by more than 13%. In addition, the first group (0.20-0.29)

in 2015 the second largest detections, reaching 533,600 by nearly 10% of the total number of detections for the same year.

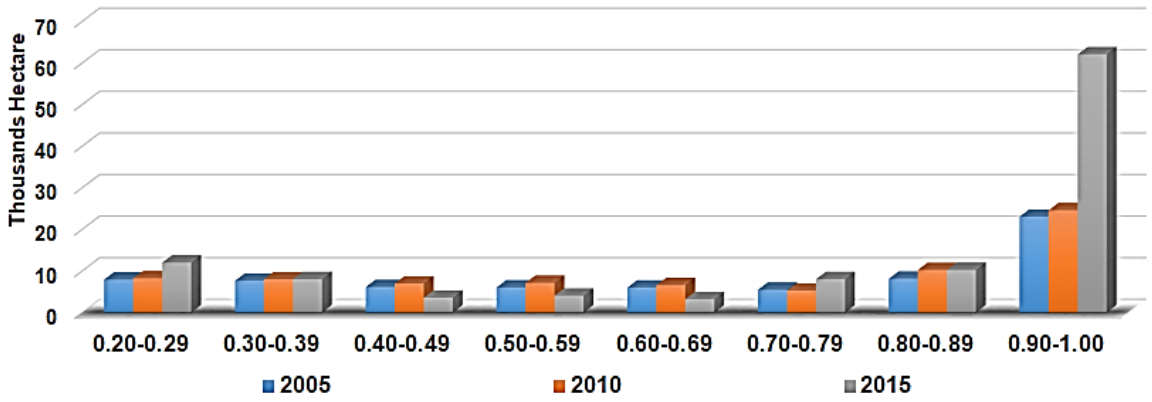

Figure 4.4: Areas Occupied of Built-up Area between 2005 and 2015 Using Subpixel Classification

As shown in Figure No.4.4 The eighth group (0.90-1.00) representing the most of the area occupied of built-up area class at all the study period where in 2005 it is about 23,025 hectares, representing 32% of total area, as it was not affected much and stabilized the same area in 2010, which amounted to 24,589 about 32%. While in 2015 increased significantly, the largest in all groups, reaching 62,069 hectares by nearly 55% of the total area for built-up area class of subpixel classification results.

While the results of the rest of the groups varied, but they were all less than the eighth group (0.90-1.00) in terms of built-up occupied areas for the subpixel classification results during the study period.

4.2.3 Bare land Class Results by Subpixel Classification

The bare land class is concentrated in the south and east of Ash-Sharqiyah Governorate as shown in Figure 4.5. It also shows that there is an inverse / negative relationship between the progress of the study period and the spread of bare lands. Where the correlation between temporal progress during the study period and the decline in bare land areas is evident.

This is evident when comparing the eastern side of the study area between 2005 and 2015, where the intensity of red color increases which indicates an increase in material pixel

fraction of bare land class. This inverse / negative relationship is natural as a result of the development and construction, which are linked to the increase in population.

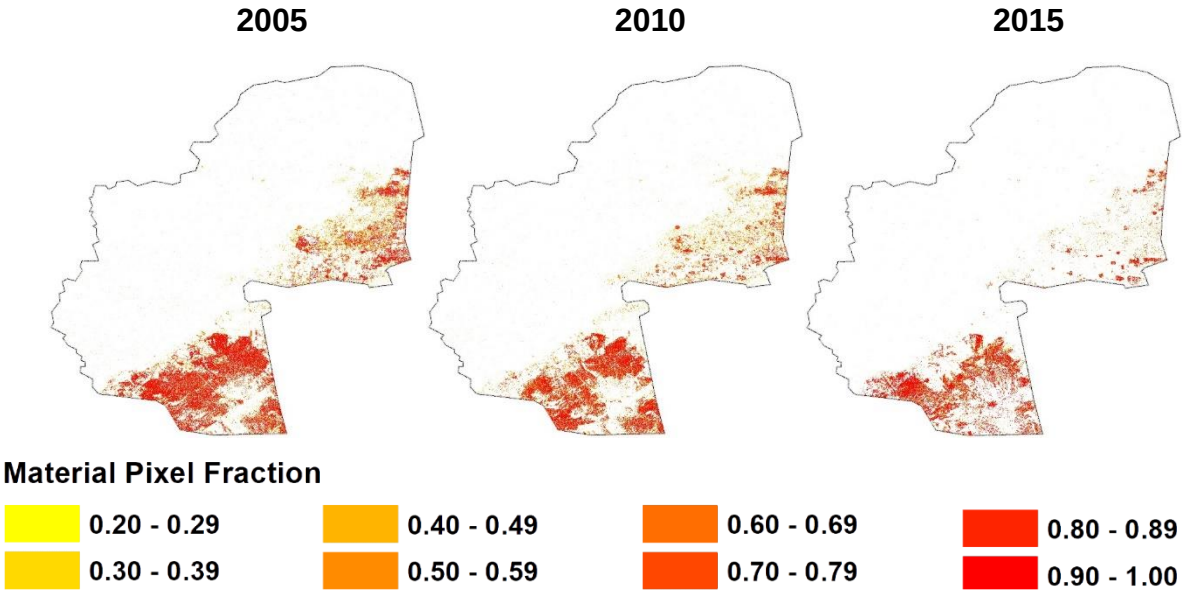

Figure 4.5: Bare Land Using Subpixel Classification

Results detections statistics for bare land indicate that the eighth group (0.90-1.00) contains most of detections through the study period as shown in Table No. 4.3. this is group (0.90-1.00) accounted for more than 2 million detections in 2005, equivalent to 55.8% of total detection, while in 2010 it dropped to 963,556 representing 47.3% and in 2015 has also declined sharply, with the number of detections reaching 934,356, less than 50% of the total detection for the same year. While the rest of groups had a few detections, which were semi equal values but less than the eighth group (0.90-1.00) and represented a small percentage of the total detections of bare land in each year of the study period.

Material Pixel Fraction	2005		2010		2015	
	Detections	hectares	Detections	hectares	Detections	hectares
0.20 - 0.29	112,356	2,528	203,956	4,589	144,444	3,250
0.30 - 0.39	164,044	3,691	183,333	4,125	176,889	3,980
0.40 - 0.49	183,333	4,125	192,000	4,320	137,867	3,102
0.50 - 0.59	145,200	3,267	114,711	2,581	133,378	3,001
0.60 - 0.69	119,911	2,698	119,600	2,691	89,556	2,015
0.70 - 0.79	134,133	3,018	55,822	1,256	69,733	1,569
0.80 - 0.89	262,667	5,910	202,667	4,560	182,889	4,115
0.90 - 1.00	2,093,289	47,099	963,556	21,680	934,356	21,023
Total	3,214,933	72,336	2,035,644	45,802	1,869,111	42,055

Table 4.3: Statistics of Bare Land Using Subpixel Classification

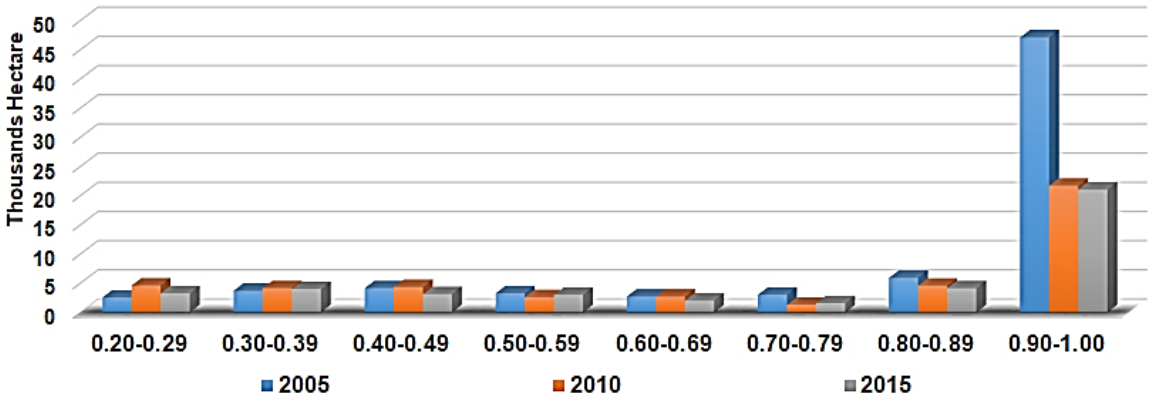

Figure 4.6: Areas Occupied of Bare Land between 2005 and 2015 Using Subpixel Classification

The eighth group represented most of the occupied area of the bare land during the study period, as shown in Figure No.4.6. The bare land in 2005 was about 47 thousand hectares, which accounted for 65.1% of the total land area in the same year. While a sharp decline was recorded, with an area of nearly 21 thousand hectares in 2010, which was slightly over 47%. In 2015 it decreased slightly as the area of bare land in the same group reached about 21 thousand hectares of the total area. While the rest of the groups did not represent any large areas of bare land in any of study period.

4.2.4 Water Bodies Class Results by Subpixel Classification

The water bodies are concentrated in the northeast, but there are some detections look like blood vessels in the human body are spread throughout the study area, which include both swamps, lakes, canals, and others. However, it seems at first glance that the water bodies were not affected during the study period as shown Figure No. 4.7.

As for the detection statistics, results as shown in Table No.4.4. The eighth group still contains most of the detections as in the rest of the classes by using Sub-pixel classification, but in a relatively few numbers of detections. Where the eighth group (0.90-1.00) have about 400 thousand of detections in 2005, it revealed 30.5% of the total detection in the same year, while in 2010 it was contained approximately 362 thousand by 39.8%, While in 2015 it contained about 317 thousand of the detection by 34%.

It is noted that the height of detections in the first group (0.20-0.29) during the study period, where the group contained in the detections of 27.6% in 2005 and 25.3% in 2010, while increased slightly in 2015 contained 22.7% of the total detections of water bodies in the same year.

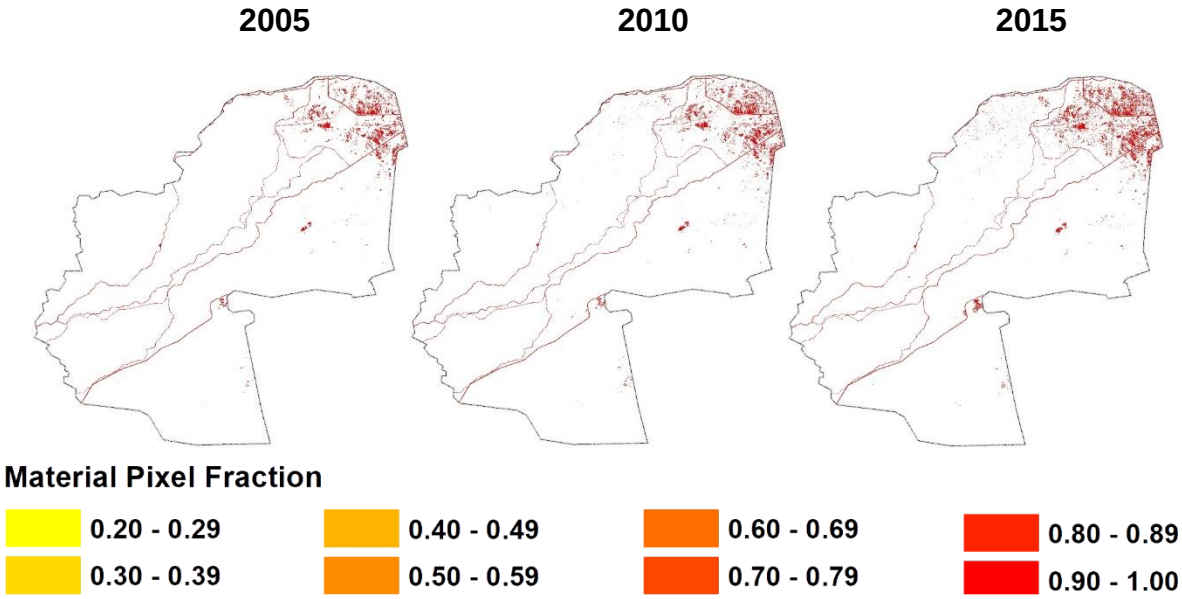

Figure 4.7: Water Bodies Using Subpixel Classification

Material Pixel Fraction	2005		2010		2015	
	Detections	hectares	Detections	hectares	Detections	hectares
0.20 - 0.29	296,397	6,450	303,669	6,241	320,444	5,218
0.30 - 0.39	132,223	1,025	125,060	1,586	112,498	1,562
0.40 - 0.49	101,293	892	126,335	2,843	126,356	3,692
0.50 - 0.59	51,433	782	76,621	215	72,444	2,354
0.60 - 0.69	22,057	321	35,152	810	23,156	711
0.70 - 0.79	5,715	201	28,083	541	19,200	369
0.80 - 0.89	26,802	6,510	35,980	2,587	32,089	1,200
0.90 - 1.00	393,510	7,125	362,982	9,812	317,867	7,810
Total	1,029,430	23,306	1,093,884	24,635	1,024,053	22,916

Table 4.4: Statistics of Water Bodies Using Subpixel Classification

The detections affected on the area occupied of each group, as shown in Figure 4.8, where the eighth group (0.90-1.00) contains the largest area of water bodies. In 2005, the water bodies area in the same group was 7,125 hectares, In the same year, the total area of the water bodies was 23,306 hectares. In 2010, the area occupied of the same group decreased to 9,812 of the total 24.635 hectares by 39.8%, while in 2015 it decreased to 7.810 by 34% of the total 22.916 hectares of water bodies in the same year.

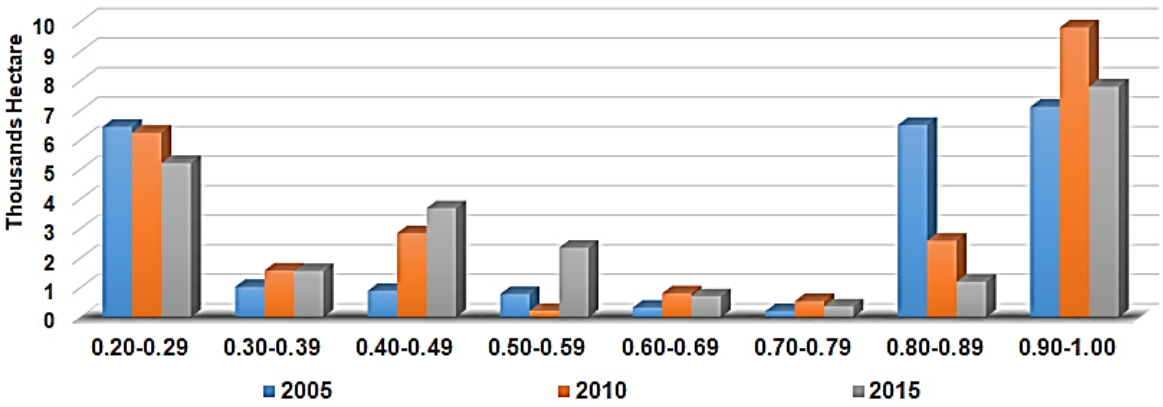

Figure 4.8: Areas Occupied of Water Bodies between 2005 and 2015 Using Subpixel Classification

While the increase in the first group (0.20-0.29) in 2005 amounted to approximately 6,450 hectares by 27.6% of the total, in 2010 it decreased as contained 6.241 hectares by 25.33%, while in 2015 increased to 5.218 hectares with 22.7% of the total area occupied by water bodies in same year.

4.2.5 Compilation of LULC Results using Subpixel Classification

The results of LULC by using Subpixel classification were collected for each year in the study period. All the groups of martial pixel fraction were collected together to represent the final classes of LULC for study area. Table 4.5 and Figure No.4.9 refer to the results of the Subpixel classification for the years of study period. The results of the LULC classification indicate that the study area was felled into four classes (Agriculture land, Built-up area, Bare land and Water bodies) as well as small areas of unclassified.

Land use / Land cover Class	2005		2010		2015	
	Area (hectares)	%	Area (hectares)	%	Area (hectares)	%
Agriculture Land	356,325	66.9%	376,859	70.7%	346,711	65.1%
Built-up Area	70,286	13.2%	76,915	14.4%	111,159	20.9%
Bare Land	72,336	13.6%	45,802	8.6%	42,055	7.9%
Water Bodies	23,306	4.4%	24,635	4.6%	22,916	4.3%
Unclassified	10,569	2.0%	8,611	1.6%	9,981	1.9%
Total Area (hectares)	532,822	100.00%	532,822	100%	532,822	100%

Table 4.5: Results LULC classes Using Subpixel Classification

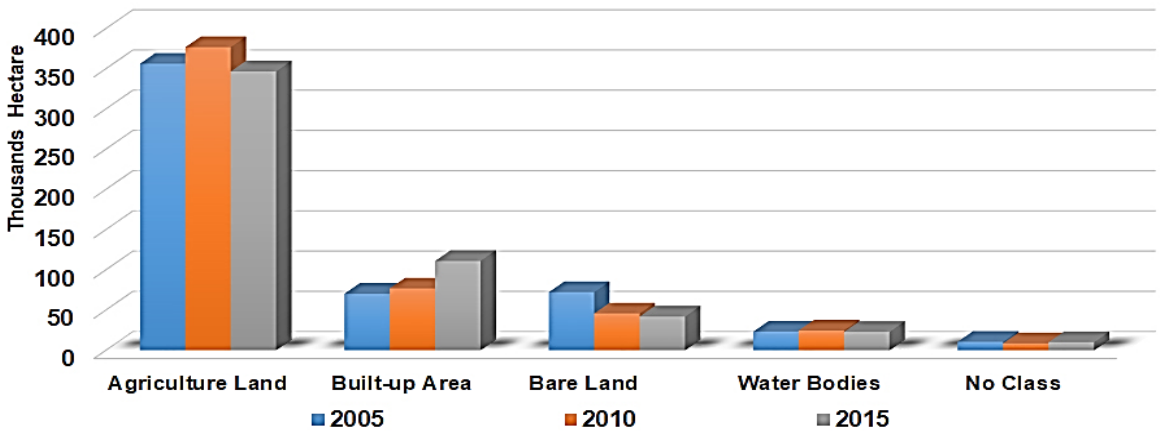

Figure 4.9: Areas Occupied of LULC classes between 2005 and 2015 Using Subpixel Classification

The results of the classification for 2005 indicate that agriculture is the predominant class in terms of occupied area and spread. The agricultural land area is estimated at 356,325 hectares by 66.9% of the total area, which is spread in all the Ash-Sharqia governorate except the south and southeast as shown Map No 4.1 and Table No.4.5.

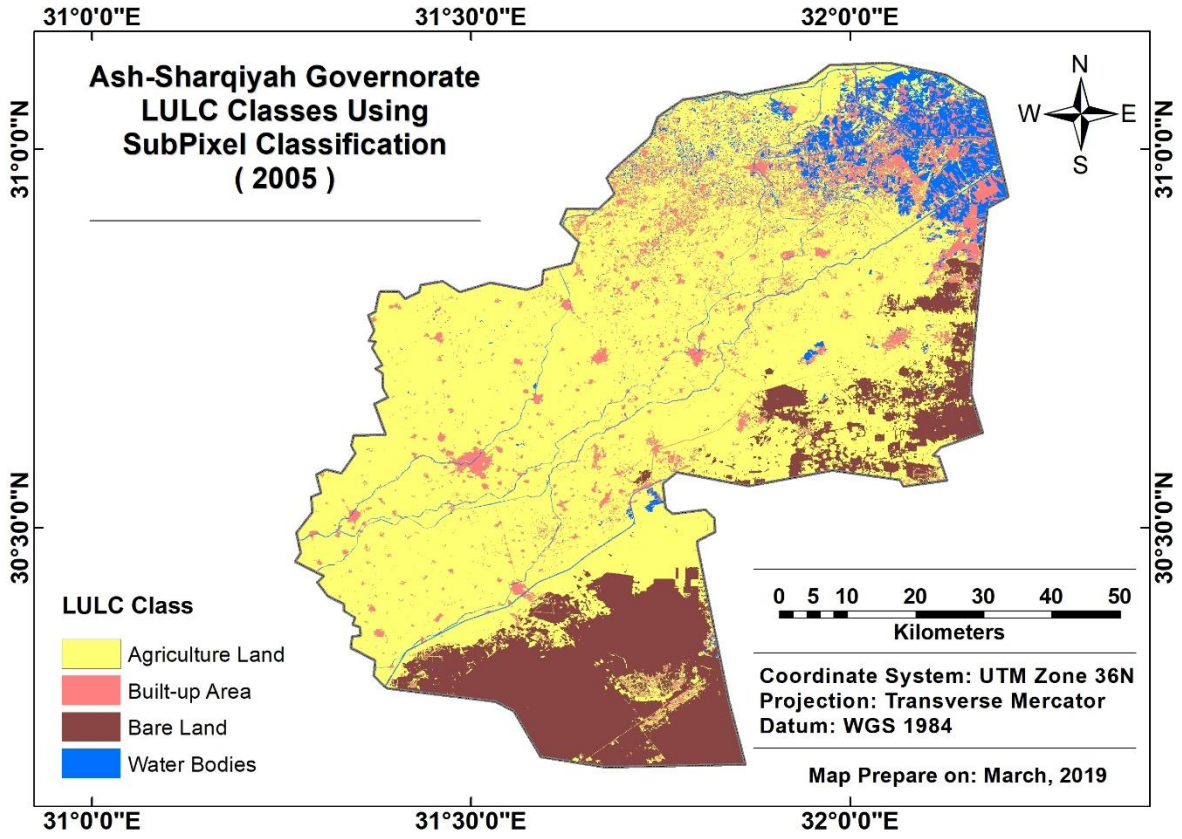

Map 4.1: LULC Classes Using Subpixel Classification For 2005

While the built-up areas in third place in terms of the occupied areas of the LULC classifications in 2005 with an area of 70.286 hectares by 13.2% of the total area and randomly distributed in the study area in the form of small concentrations pervade in the

agricultural lands. In the second place, Bare land class in terms of area occupied where the 72,336 hectares in 2005 by 13.6% of the total area of classification results, which is concentrated in the south and east of the study area where these areas are the future of the governorate in future urban development. Water bodies are in the fourth and final place in terms of the occupied area of the results of land use classification with an area of 23,306 hectares by 4.4%. It contains channels, agricultural drain systems, lakes, swamps, etc., distributed throughout the study area. There is also a large pool of water bodies class in the northeast of the governorate. This is explained by the dependence of the people of the area on the cultivation of rice by drowning, ponds for fish farming and salt production.

Results of 2010 indicate that agriculture land continues to first place as the largest in LULC classification in terms of occupied area as shown Map No. 4.2 and Table No 4.5 with an area of 376,859 hectares, an increase of 4% over 2005. The area occupied of built-up area increased by 76,915 hectares by 14.4%, while the bare land area decreased to 45,802 hectares by 4% compared to 2005, while water bodies occupied for 24,635 hectares by 4.6% of the total LULC classification results in same year.

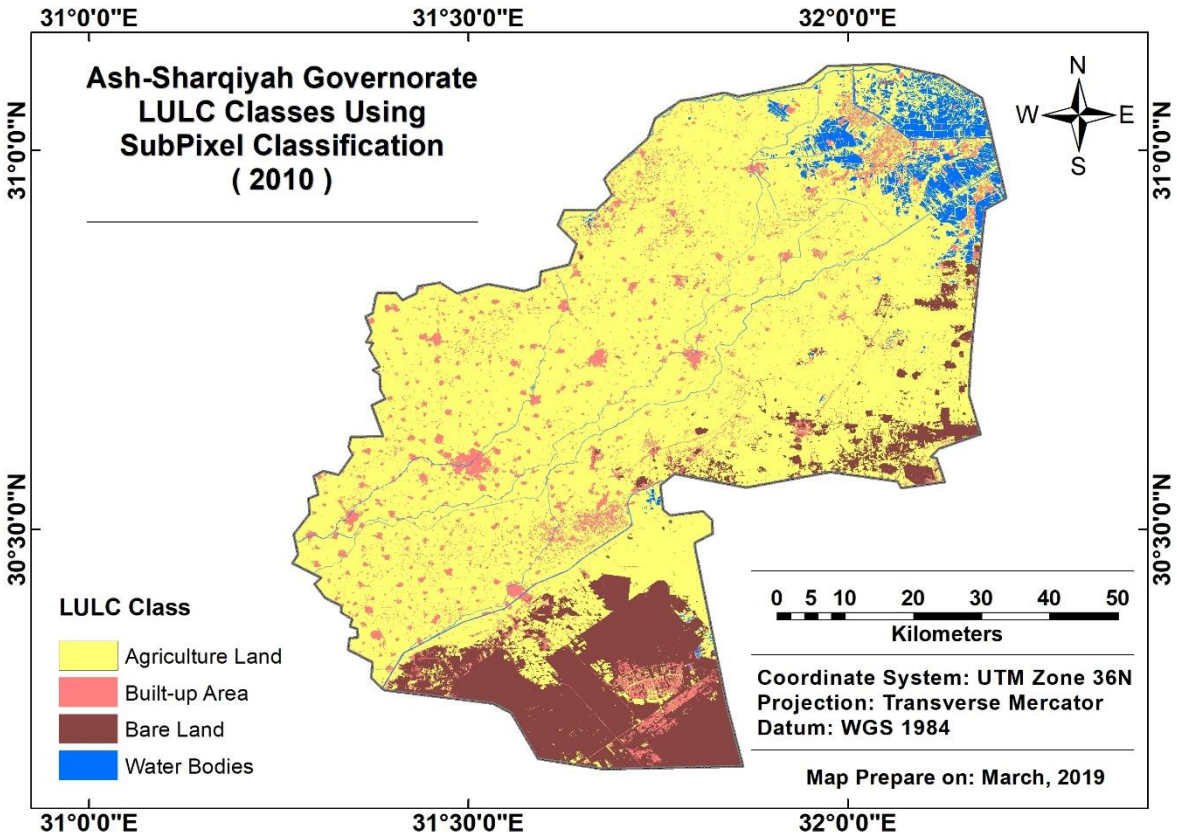

Map 4.2: LULC Classes Using Subpixel Classification For 2010

The results of Subpixel classification still indicate that agriculture land occupies the majority of LULC classification in the study area with an area of 346,711 hectares by 65.1% as shown in Map 4.3 and Table 4.5, While the built-up area was the second largest with an area of 111,159 hectares by 20.9%, then the bare land with an area of 42,055 hectares by 7.9%, followed by water bodies with an area of 22,916 hectares by 4.3% % of the total classification results.

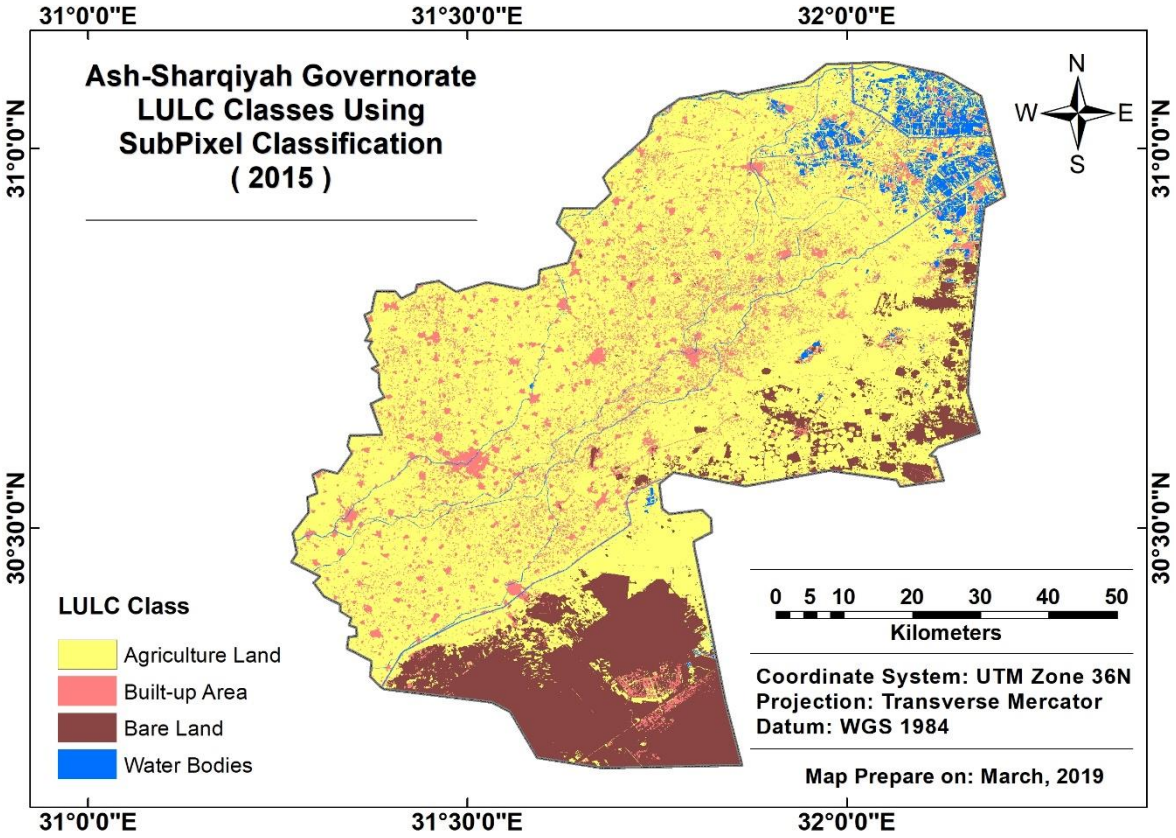

Map 4.3: LULC Classes Using Subpixel Classification For 2015

Table 4.6 and Figure 4.10 indicate the different occupied areas and percentages of each class of Subpixel classification result during the years of study period.

LULC	Differences of occupied areas between					
	2010 and 2005		2015 and 2010		2015 and 2005	
	hectare	%	hectare	%	hectare	%
Agriculture land	20,535 ▲	3.9%	-30,148 ▼	-5.7%	-9,614 ▼	-1.8%
Built-up Area	6,629 ▲	1.2%	34,244 ▲	6.4%	40,873 ▲	7.7%
Bare Land	-26,534 ▼	-5.0%	-3,747 ▼	-0.7%	-30,281 ▼	-5.7%
Water Bodies	1,329 ▲	0.2%	-1,719 ▼	-0.3%	-390 ▼	-0.1%
Study Area	532,822 hectares					

Table 4.6: Difference of occupied areas for LULC Using Subpixel classification

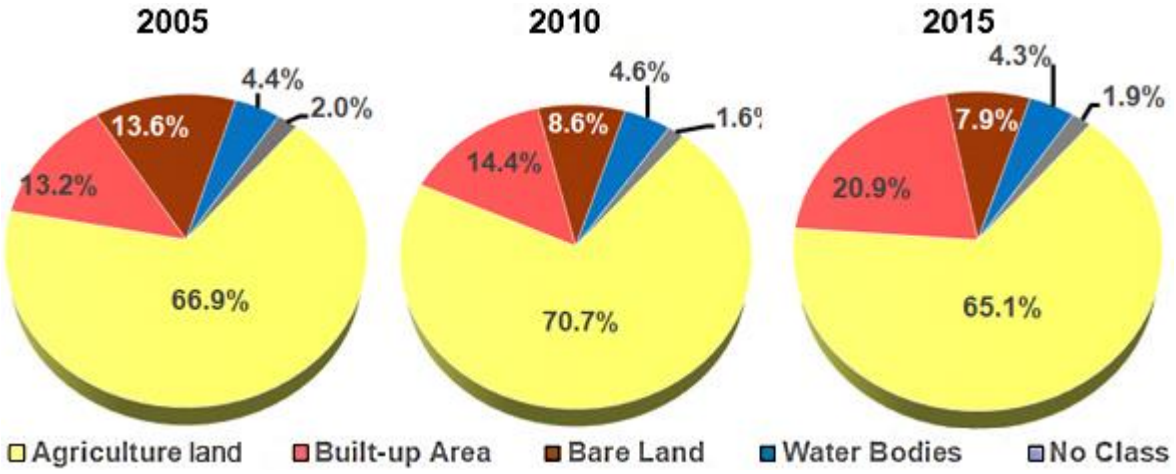

Figure 4.10: Percentage of area for LULC classes between 2005 and 2015 Using Subpixel Classification

The occupied area of Agriculture land was varied in the results of Subpixel classification. In 2010, the area increased 20.535 hectares about 3.9%, thus occupied 66.9% of the total area of classification categories in the study area. While compared to 2015 and 2010, the total area of agricultural land decreased by 30.148 hectares by 5.7%, to occupied agriculture land 70.7% and 65.1% in 2010 and 2015 respectively of the total area of classification categories.

In contrast to Agriculture land, Built-up areas continued to increase over the years of the study period, increasing in 2010 by 6.629 hectares by 1.2% compared with 2005 to occupied 14.4% of the total results of the classification in 2010 and increased significantly in 2015 about 34.244 hectares by 6.4% compared to 2010, to occupied 20.9% of the total results of the classification in the same year.

As for Bare land, there was a decline over the years of the study period. In 2010, it decreased 26,534 hectares by 5% in comparison to 2005, reaching 8.6% in 2010 compared with 13.6% in 2005 of the total area of LULC classification. And decreased in 2015 about 3,747 hectares by 0.7% compared to 2010 to record 7.9% of the total area of LULC classification in 2015.

As for water bodies, the percentage of occupied areas did not differ during the study period. In 2010, it increased by 1.450 hectares by 0.27%, while in 2015 it decreased by 1,329

hectares by 0.2% compared to 2010 where average area occupied by 4.4% at the level of the study period for LULC classification.

4.3 Object-Based Classification

After performing the LULC classification according process (rule set) for object-based classification, statistics were calculated for the resulting LULC map, such as total area and relative area of each class, in order to illustrate the result quantitatively and see the portion of each class on the whole area. Table No. 4.7 and Figure No. 4.11 illustrate the results of this area calculation.

LULC Class	2005		2010		2015	
	Area (hectares)	%	Area (hectares)	%	Area (hectares)	%
Agriculture Land	362,152	68.0%	376,053	70.6%	342,461	64.3%
Built-up Area	95,982	18.0%	101,256	19.0%	139,280	26.1%
Bare Land	55,022	10.3%	35,620	6.7%	34,250	6.4%
Water Bodies	18,301	3.4%	18,003	3.4%	16,025	3.0%
Unclassified	1,365	0.3%	1,890	0.4%	806	0.2%
Total Area (hectares)	532,822	100%	532,822	100%	532,822	100%

Table 4.7: Statistics of LULC classes Using OBIA Classification

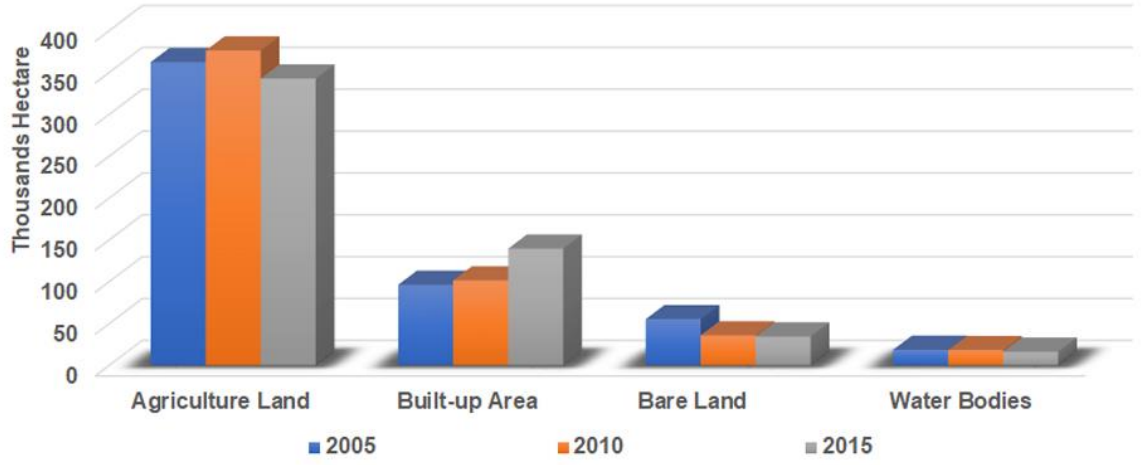

Figure 4.11: Areas Occupied of LULC classes between 2005 and 2015 Using OBIA Classification

In Ash-Sharqiyah governorate 2005, Agriculture land was the dominant class except the south and southeast as shown Map No.4.4 which occupied with over 362 thousands

hectares by 68% share. This LULC class included all kinds of vegetation, such as trees, shrubs, grasslands, or crops in agricultural fields. Also, agricultural land with low sparse vegetation was classified into the agricultural class.

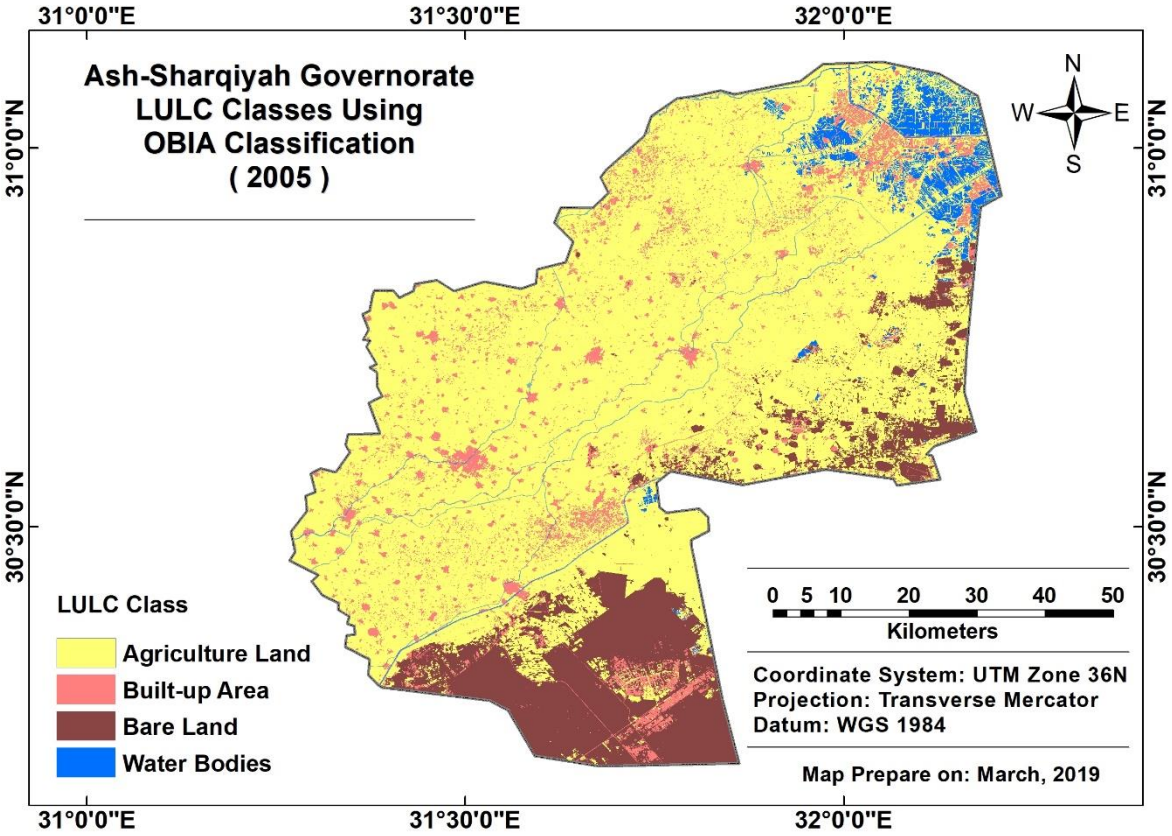

Map 4.4: LULC Classes Using OBIA Classification For 2005

Built-up area was another dominant class, made up with 95,982 hectares by 18% of the total area, where there are in scattered locations throughout the study area around agriculture land. The aim was to classify the built-up area as accurate as possible, so the focus in the classification process and rule set development was on this class.

Bare land was third occupied LULC class with 55,022 hectares by about 10% share, mostly in the southern, more rural part of the study area. Where it is concentrated in the far south and south east of the study area, which are considered areas to accommodate the population growth and future development of the governorate.

Water bodies, mostly canals and small swamps, occupied with 18,301 hectares by about 3.4% of the total area. The previous map shows many blue-colored areas in the far north east that indicate water bodies. Perhaps the explanation for this phenomenon is that these

areas are dedicated to the cultivation of rice and fish farming, so the spectral reflection of them indicates of water bodies. The unclassified class occupied less than 0.3% of the whole study area.

In 2010, agriculture land remained predominant class in the study area, as illustrated in Map No. 4.5, where it area occupied of 376,053 hectares by 70.6% share or the total study area. There was no significant difference in the built-up area, which occupied 101,256 hectares by 19% of the total area.

Bare land occupied 35,620 hectares by 6.7%, while the water bodies occupied 18,003 hectares by 3.4%. The unclassified in 2010 area increased to 0.4% of the total area.

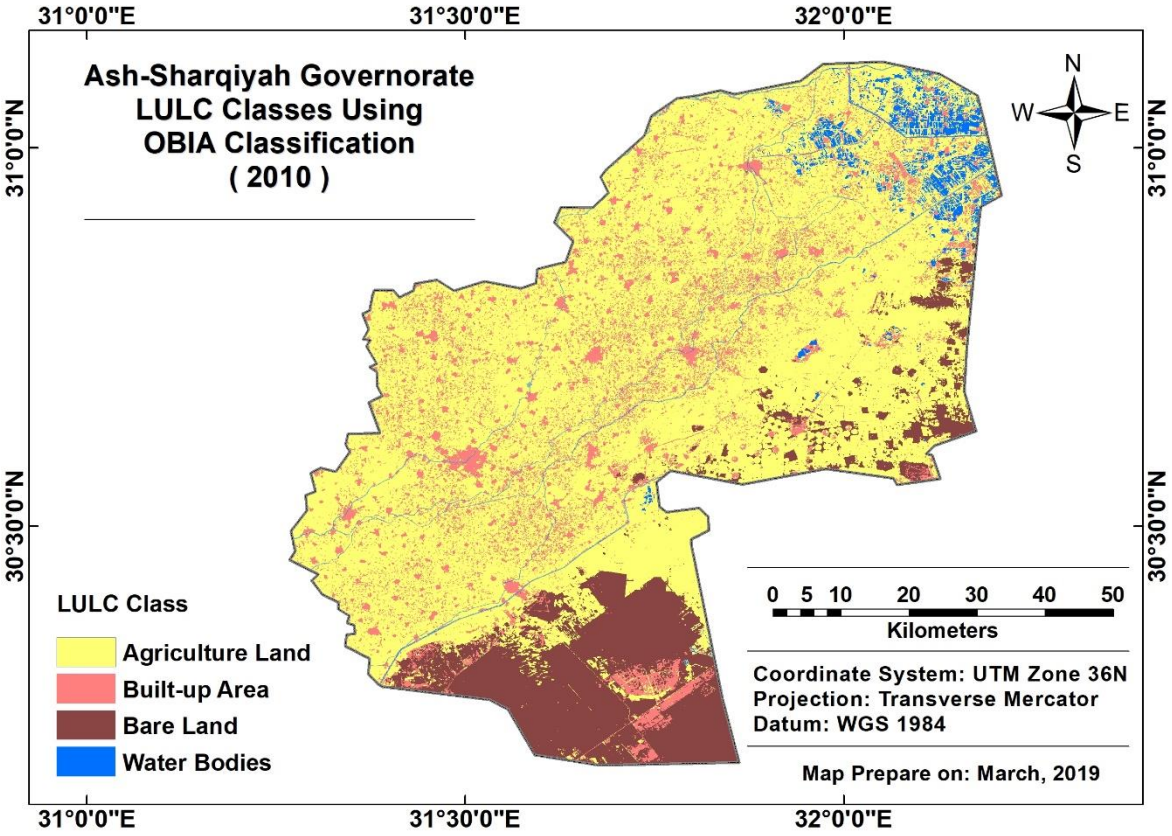

Map 4.5: LULC Classes Using OBIA Classification For 2010

The distribution of LULC classification classes in 2015 did not differ in terms of ranking of classes based on the area occupied for each of them. However, some locations appeared on the map that changed from class to another one as shown on Map No. 4.6.

In terms of agriculture land, it occupied 342,461 hectares by 64.3% of the total area. The built-up area occupied 139.280 hectares by nearly 26%. Bare land occupied area of 34.250 hectares by 6.4%, while the water bodies occupied area 16.025 hectares by 3% that is

nearly percentage of 2010. A little number of image objects were left unclassified for almost 2% of the whole image area, because it did not fulfill the criteria of any of the classes.

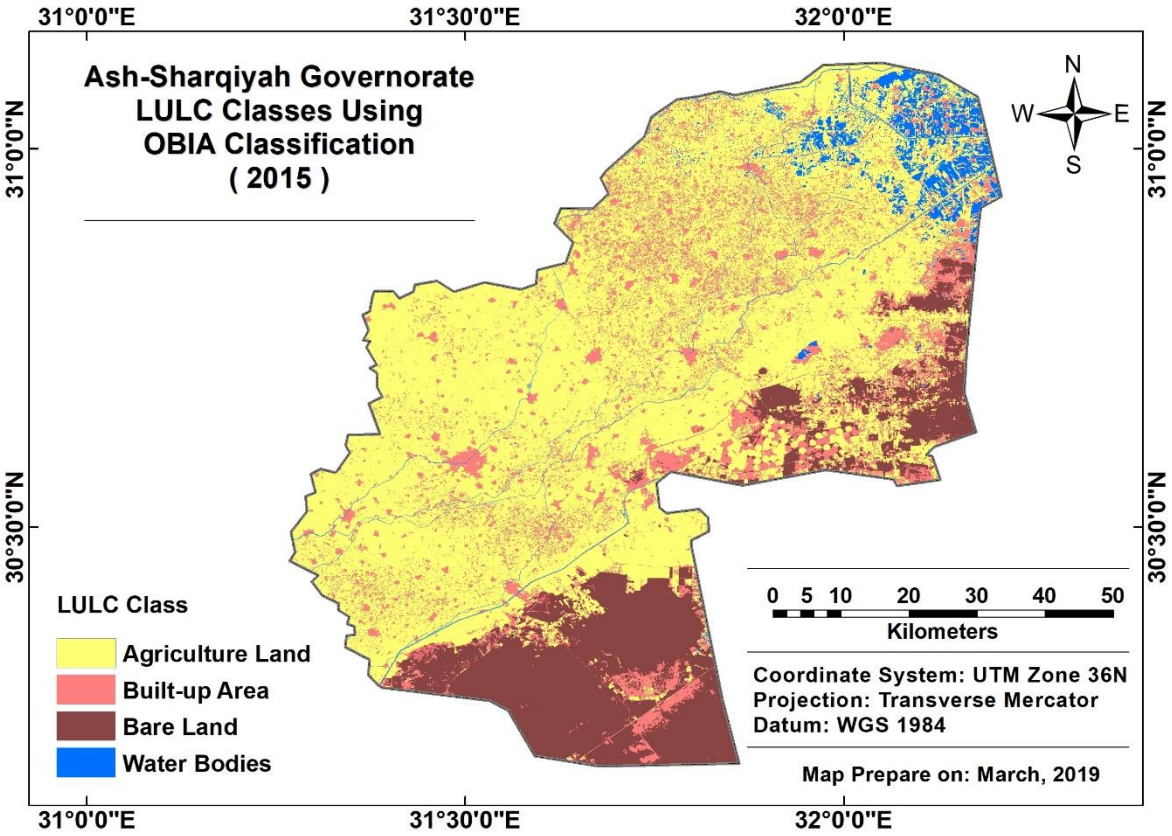

Map 4.6: LULC Classes Using OBIA Classification For 2015

Table No. 4.8 and Figure No. 4.12 indicate the different occupied areas and percentages of each class using OBIA classification result during the years of study period.

LULC	Differences of occupied areas between					
	2010 and 2005		2015 and 2010		2015 and 2005	
	hectare	%	hectare	%	hectare	%
Agriculture	13,901 ▲	2.61%	-33,592 ▼	6.30%	-19,691 ▼	3.70%
Built-up Area	5,274 ▲	0.99%	38,024 ▲	7.14%	43,298 ▲	8.13%
Bare Land	-19,402 ▼	3.64%	-1,370 ▼	0.26%	-20,772 ▼	3.90%
Water Bodies	-298 ▼	0.06%	-1,978 ▼	0.37%	-2,276 ▼	0.43%
Study Area	532,822 hectares					

Table 4.8: Difference of occupied areas for LULC Using OBIA classification

Occupied area of Agriculture land was varied in the results of Subpixel classification. In 2010, the area increased by 13,901 hectares by about 2.6%, thus accounted for 68% of the total area of classification categories in the study area. While the differences were significant between 2015 and 2010, where the area of agriculture land decreased 33,592

hectares by 6.3%, so that in 2015, agriculture occupied area 64.3% of the total area of study. The total differences between 2015 and 2005 indicate a decrease in the area of agriculture land 19.691 hectares by 3.7% of total study area.

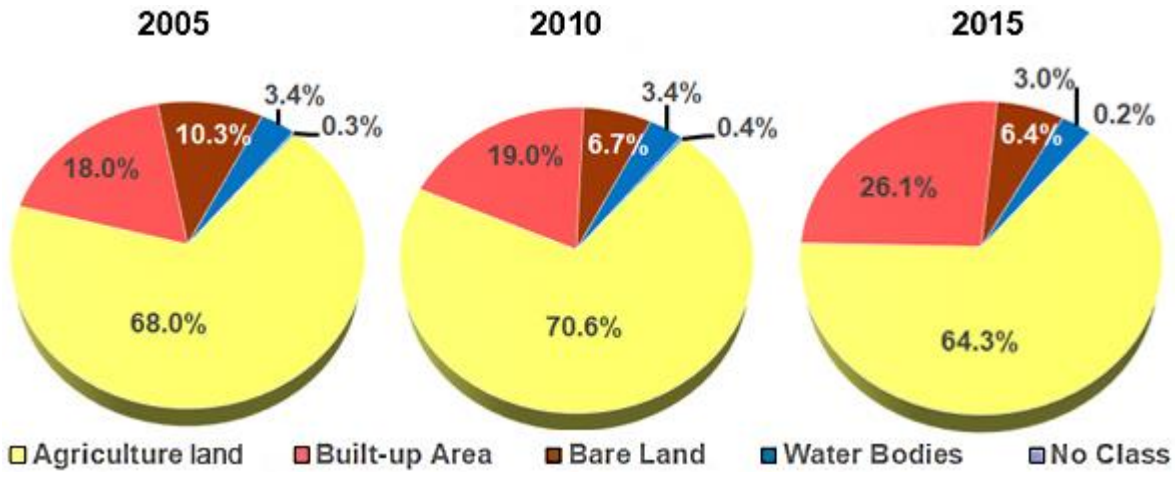

Figure 4.12: Percentage area of LULC classes between 2005 and 2015 Using OBIA Classification

The built-up area increased by 5.274 hectares in 2010 from 2005 by 0.99% where it occupied 19% in 2010, while in 2015 it increased by 38.024 hectares by 7.14% compared with 2010, where it occupied 26.1% in 2015. While the total period between 2015 and 2005 increased by 43.298 hectares by 8.13%, amounting to 18% in 2005 in the study area.

The bare land is the largest classes in the continuous decrease in occupancy area during the years of the study period, which decreased by 19.402 hectares between 2010 and 2005 by 3.64%, which in 2005 occupied area for 10.3% of the total area of study. While it decreased by 1.370 hectares between 2015 and 2010 by 0.26% where it occupied 6.7% in 2010. While the total study period between 2015 and 2005 decreased by 20.772 hectares by 3.9%, amounting to 6.4% in 2015.

The water bodies also continued to decrease the occupied areas, but very few percentages. The difference between 2010 and 2005 is estimated at 298 hectares at 0.06%, accounting in 2010 by 3.4% of the total area. In the study period between 2015 and 2010, the occupied area decreased by 1.978 hectares by 0.37% with the area of water bodies accounted for 3% in 2015. While in the total study period between 2015 and 2005, the area decreased by 2.276 hectares by 0.43%. This can be explained by the encroachment of citizens on

channels and lakes by throwing industrial and agricultural waste, which is reflected in the classification of water bodies in the study area.

4.4 Accuracy Assessment

After finish of land use / land cover classification and create a land cover map using two different classification approaches (Pixel based & Object based). An accuracy assessment was performed to check the quality of LULC classification result for each approach over the three-year period (study period). where allow evaluate how closely the classified image is to reference data "ground truth". Were collect reference data to determination of land use / land cover classes types at specific locations using visual assessment by interpreting imagery. Reference points were collected for each class, distributed throughout the entire scene based on the proportion of the area covered by each class, where the minimum number of points for each class was set to 10, this is the minimum that has been set to ensure the smallest class has enough points for accurate measurement of accuracy.

100 reference points were collected for each class according to the area occupied for each of them, where Agriculture land class collected 49 reference points, Built-up area collected 19 points, Bare land collected 22 points and Water bodies collected 10 points.

Figure No. 4.13 show the overall classification accuracy statistics, while Table No. 4.9 show details of classification accuracy statistics for each class.

The results of Pixel-based classification accuracy assessment in 2005 indicate get Built-up area was 68.42%, this is the lowest of user accuracy among the classification classes in the same year, while agriculture land obtained the highest user accuracy of 77.55%. According to the results of the user accuracy of other classification classes, Overall classification accuracy of that year was 73%. In 2010, Agriculture land obtained highest value in the user accuracy of 81.63%, while Water bodies obtained 70%, the lowest value among the other classes of classification in the same year. While the overall classification accuracy rating for the same year increased to 79% compared to 73% in 2005. In 2015, Built-up area obtained the highest value of user accuracy of 89.47% and Water bodies continued to be

the lowest class in the user accuracy at 60.00%, while the overall classification accuracy continued to rise to 80% compared to the previous year of study period.

When comparing the previous results of the pixel-based classification with the object-based classification, we observe the following**:**

	Study period	Class Name	Reference Totals	Classified Totals	Number Correct	Producers Accuracy	Users Accuracy
Pixel-based Classification	2005	Agriculture	49	49	38	77.55%	77.55%
		Built-up Area	20	19	13	65.00%	68.42%
		Bare Land	25	22	16	64.00%	72.73%
		Water Bodies	6	10	6	100.00%	60.00%
		Total	100	100	73		
		Overall Classification Accuracy					73.00%
	2010	Agriculture	45	49	40	88.89%	81.63%
		Built-up Area	23	19	15	65.22%	78.95%
		Bare Land	25	22	17	68.00%	77.27%
		Water Bodies	7	10	7	100.00%	70.00%
		Total	100	100	79		
		Overall Classification Accuracy					79.00%
	2015	Agriculture	45	49	40	88.89%	81.63%
		Built-up Area	28	19	17	60.71%	89.47%
		Bare Land	21	22	17	80.95%	77.27%
		Water Bodies	6	10	6	100.00%	60.00%
		Total	100	100	80		
		Overall Classification Accuracy					80.00%
Object-based Classification	2005	Agriculture	47	49	47	100.00%	95.92%
		Built-up Area	21	19	19	90.48%	100.00%
		Bare Land	22	22	20	90.91%	90.91%
		Water Bodies	10	10	10	100.00%	100.00%
		Total	100	100	96		
		Overall Classification Accuracy					96.00%
	2010	Agriculture	45	49	45	100.00%	91.84%
		Built-up Area	20	19	18	90.00%	94.74%
		Bare Land	26	22	21	80.77%	95.45%
		Water Bodies	9	10	9	100.00%	90.00%
		Total	100	100	93		
		Overall Classification Accuracy					93.00%
	2015	Agriculture	46	49	46	100.00%	93.88%
		Built-up Area	21	19	19	90.48%	100.00%
		Bare Land	24	22	21	87.50%	95.45%
		Water Bodies	9	10	9	100.00%	90.00%
		Total	100	100	95		
		Overall Classification Accuracy					95.00%

Table 4.9: Comparison of classification accuracy statistics

There is an improvement in the user accuracy of the object-based classification at the level of all classes and thus in the overall classification accuracy. The previous table indicates that in 2005 both Built-up area and Water bodies obtained the full mark 100% in the user

accuracy, while Bare land obtained 90.91%. While the overall classification accuracy in the same year was 96%, which is higher than the pixel-based classification of the same year. In 2010, the superiority of object-based classification continued to be higher than the pixel-based classification. Bare land class obtained the highest user accuracy value of 95.45% and Water bodies of 90%, while the overall classification accuracy in the same year was 93%. In 2015, Object-based classification was higher than of the pixel-based classification, where Built-up area obtained a full mark 100% of user accuracy rate, Water bodies class obtained 90%, while the overall classification accuracy in the same year 95%.

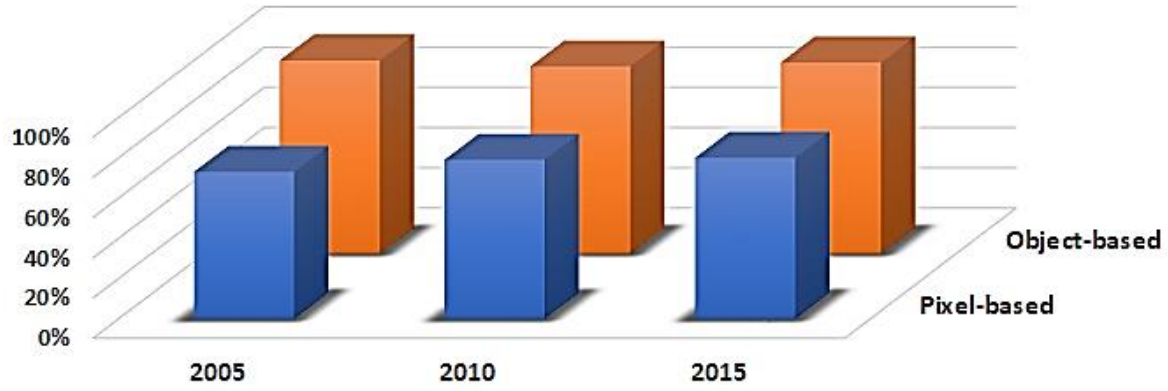

Figure 4.13: Overall classification accuracy statistics

Table No. 4.10 and Figure No. 4.14 show a kappa coefficient for each class of classification in the study area. Since the study was conducted for three years 2005, 2010 and 2015, the average Kappa coefficient results were chosen for the accuracy assessment to determine the best classification approach and closer to reality to move to the last step of analysis stage that is the detection of changes LULC.

Conditional	Pixel-based				Object-based			
	2005	2010	2015	Avg.	2005	2010	2015	Avg.
Agriculture land	0.560	0.677	0.666	0.634	0.923	0.852	0.887	0.887
Built-up Area	0.605	0.697	0.854	0.719	1.000	0.934	1.000	0.978
Bare Land	0.636	0.666	0.712	0.672	0.883	0.939	0.940	0.921
Water Bodies	0.575	0.947	0.575	0.699	1.000	0.890	0.890	0.927
Overall Kappa Statistics	**0.592**	**0.688**	**0.703**	0.661	0.940	**0.896**	**0.926**	0.921

Table 4.10: Kappa coefficient statistics

The results of Kappa coefficient indicate the superiority of the object-based classification significantly on the pixel-based classification during the three years specified in the study period. The average of Kappa coefficient for the pixel-based classification for Agriculture class was 0.634 compared to 0.887 in the object-based classification. In Built-up area class, the average of Kappa coefficient was 0.719 for the pixel-based classification while object-based classification was 0.978, the highest average for the Kappa coefficient between all classes. For Bare land class, it averaged of Kappa coefficient 0.672 for pixel-based classification while 0.921 for object-based classification. Finally, Water bodies class of the pixel-based classification was 0.699, while the object-based classification of the same class obtained 0.927 as the average of the Kappa coefficient for the study period.

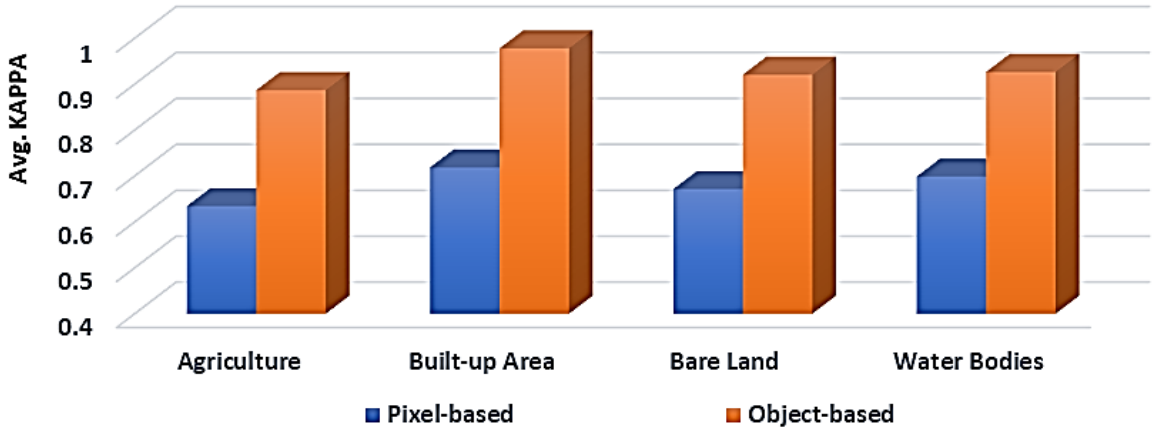

Figure 4.14: Average Kappa coefficient statistics

Based on these results, the object-based classification is the closest to reality by the results of the accuracy assessment using average of the Kappa coefficient for the years of the study period. Object-based classification maps will therefore be used to detect change LULC over the years of the study period.

4.5 Change Detection

After accuracy assessment of LULC classification by using two different approaches in this study. The results showed the superiority of Object-based classification approach.

Therefore was relied upon in the detection of changes of it in Ash-Sharqiyah governorate between 2005 and 2015.

Table No. 4.11 indicates results of change detection classes of LULC classification in the study area, where the matrix indicates direction of changes where the results split into two groups. The first one includes Agricultural land, Bare land and Built-up areas, which have significant changes of LULC throughout the study period. While the second group includes water bodies class only, this class did not changes LULC significantly throughout the study period, the changes in LULC in this category can be explained to the dumping of waste on the sides of canals and swamps.

		Initial (From) – per Hectare			
	LULC Class	Agricultural Land	Built-up Area	Bare Land	Water Bodies
Final (To) – per Hectare	**2005 - 2010**				
	Agricultural Land		770.32	1209.91	18.17
	Built-up Area	121.51		796.28	0.95
	Bare Land	110.14	25.24		0.17
	Water Bodies	8.60	7.23	1.27	
	2010 – 2015				
	Agricultural Land		16.27	55.2	12.63
	Built-up Area	2130.92		552.0	25.72
	Bare Land	119.21	57.80		0.24
	Water Bodies	3.24	4.13	1.12	
	2005 – 2015				
	Agricultural land		163.16	893.20	13.81
	Built-up Area	1990.19		1189.12	15.26
	Bare Land	115.53	33.10		0.17
	Water Bodies	5.90	5.57	1.04	

Table 4.11: Object-based classification change detection matrix indicating direction of change

Between 2005 and 2010, a large area of the study area changed from Bare land to agriculture land, amounting to 1209 hectares. This is due to the efforts of the state in reclamation of many areas of agricultural land. The development and construction of many bare lands to be converted to built-up area in that period, which amounted to 796 hectares, indicating the government's attempt to establish many new urban communities to meet the need for housing coupled with the increase in population in that country. The results show

that about 121 hectares were converted to urban purposes from agriculture land during the period 2005-2010. This may be due to some citizens violation of laws that stipulate not to build on agricultural land and convert it to urban activities. While in the same period, there were concrete efforts by the municipalities to change the built-up area to agricultural land with a total area of 770 hectares, mostly in accordance with the laws that provides restoration of agricultural land to original land use, which was built-up on it later.

Between 2010 and 2015, the magnitude of LULC changes varied as shown in Figure No. 4.15. Which compare between two different study periods. Where the second period of 2010 to 2015 indicates a significant increase in the convert of agricultural land into urban purposes by about 2130 hectares, possibly due to the political events that passed through the country at that time (January 2011 and June 2013 revolutions), which affected the weakness security force in imposing control over violating citizens the law that prevents the convert of agricultural land to urban activities. These political events also affected the retrieval of agricultural land from the violators in that period, as the areas converted from built-up areas to agricultural land significantly reduced about 16 hectares only. It did not

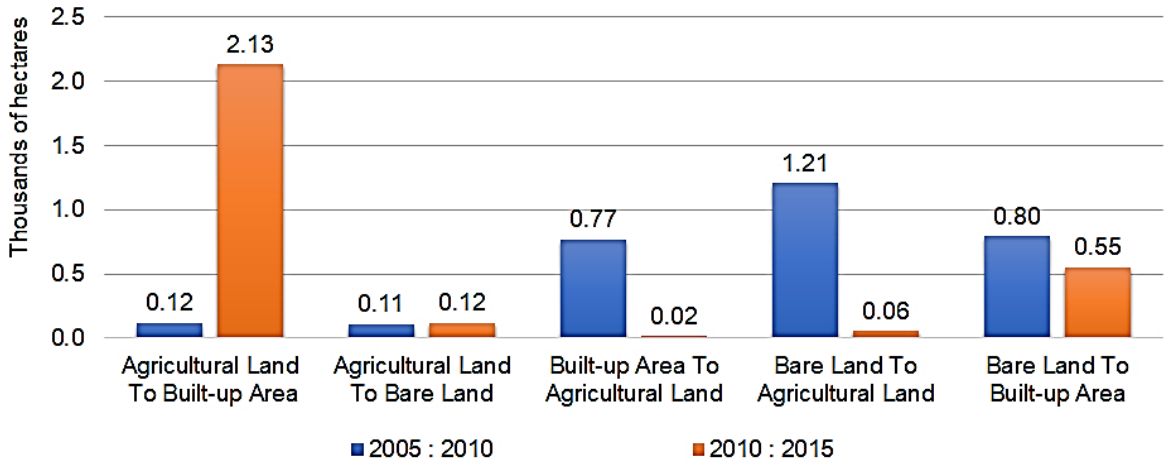

Figure 4.15: Magnitude of LULC changes for the most changed classes

differ much in relation to the changes of bare land, whether it was converted into Built-up area or reclaimed to become agricultural land, where the area decreased in that period to about 552 and 55 hectares respectively.

As for the changes of water bodies to built-up area, the area of land converted between

2010 and 2015 increased significantly by about 26 hectares compared with only one hectare between 2005 and 2010. This may be due to the violation of some citizens by building on the edges of water bodies or throw agricultural land and industrial waste in it.

The statistical results of change indicate that there are five categories of land use whose area has been significantly changed in the study area between the two study periods as follows: from Agriculture land to Built-up area, from Built-up area to Agricultural land, from Bare Land to Agricultural land, Agricultural land to Bare land and from Bare Land to Built-up area.

Municipality	Period	Agricultural To Built-up	Built-up To Agricultural	Bare Land To Agricultural	Agricultural to Bare land	Bare Land To Built-up
10 Ramadan	2005-2010	2.6	5.5	180.2	15.9	245.3
	2010-2015	38.5	2.4	8.0	17.3	149.9
Abu Hammad	2005-2010	6.1	58.6	60.6	5.5	39.9
	2010-2015	116.7	0.8	2.8	6.0	27.6
Abu Kabir	2005-2010	4.4	37.8	43.6	4.0	28.7
	2010-2015	76.8	0.6	2.0	4.3	19.9
Al-Husayniyah	2005-2010	50.6	250.6	398.1	35.0	122.8
	2010-2015	799.5	5.2	17.5	37.8	105.2
Al-Ibrahimiyah	2005-2010	1.7	10.8	17.0	1.5	11.2
	2010-2015	29.9	0.2	0.8	1.7	7.8
Awlad Saqr	2005-2010	6.1	44.8	70.4	6.4	46.3
	2010-2015	147.0	0.9	3.2	6.9	32.1
Bilbays	2005-2010	6.8	59.7	78.1	7.1	51.4
	2010-2015	157.5	1.0	3.6	7.7	35.6
Diyarb Najm	2005-2010	5.0	41.4	49.3	4.5	32.5
	2010-2015	96.9	0.7	2.2	4.9	22.5
Faqus	2005-2010	13.0	73.5	80.7	9.1	65.6
	2010-2015	199.6	1.3	4.5	9.8	45.5
Hihya	2005-2010	2.9	28.3	28.8	2.6	18.9
	2010-2015	50.6	0.4	1.3	2.8	13.1
Kafr Saqr	2005-2010	4.3	37.4	43.0	3.9	28.3
	2010-2015	85.7	0.6	2.0	4.2	19.6
Mashtul as-Suq	2005-2010	1.7	10.5	16.5	1.5	10.8
	2010-2015	29.0	0.2	0.8	1.6	7.5
Minya al-Qamh	2005-2010	5.5	51.2	64.6	5.9	42.5
	2010-2015	123.9	0.9	2.9	6.4	29.5
Zaqaziq	2005-2010	10.9	60.3	79.1	7.2	52.0
	2010-2015	179.2	1.1	3.6	7.8	36.1

Table 4.12: Magnitude of LULC Changes by hectare in Municipalities of Ash-Sharqiyah Governorate

Table No. 4.12 compares the areas of the most important LULC changes at the level of Municipalities of Ash-Sharqiyah governorate in the two study periods (2005 to 2010) and (2010 to 2015).

Maps No. 4.7 and 4.8 show a comparison between the top five categories of LULC changes in terms of the magnitude of each LULC changes in the municipalities of Ash-Sharqiyah Governorate. Where the results indicate that some municipalities are affected by the other. This is explained by the municipality's area or the prevailing LULC within the municipal boundaries. In general, the municipalities of the study area were affected by the policy of development and construction between 2005 and 2010. This is evident in the change of Bare land, whether in Built-up area or agriculture land. While In the period between 2010 and 2015, the study area was affected by exceptional political events (Jan 2011 & June 2013 revolutions), which weakened the state's ability to impose its control by preserving the agricultural land from violations by citizens.The results show that between 2005 and 2010,

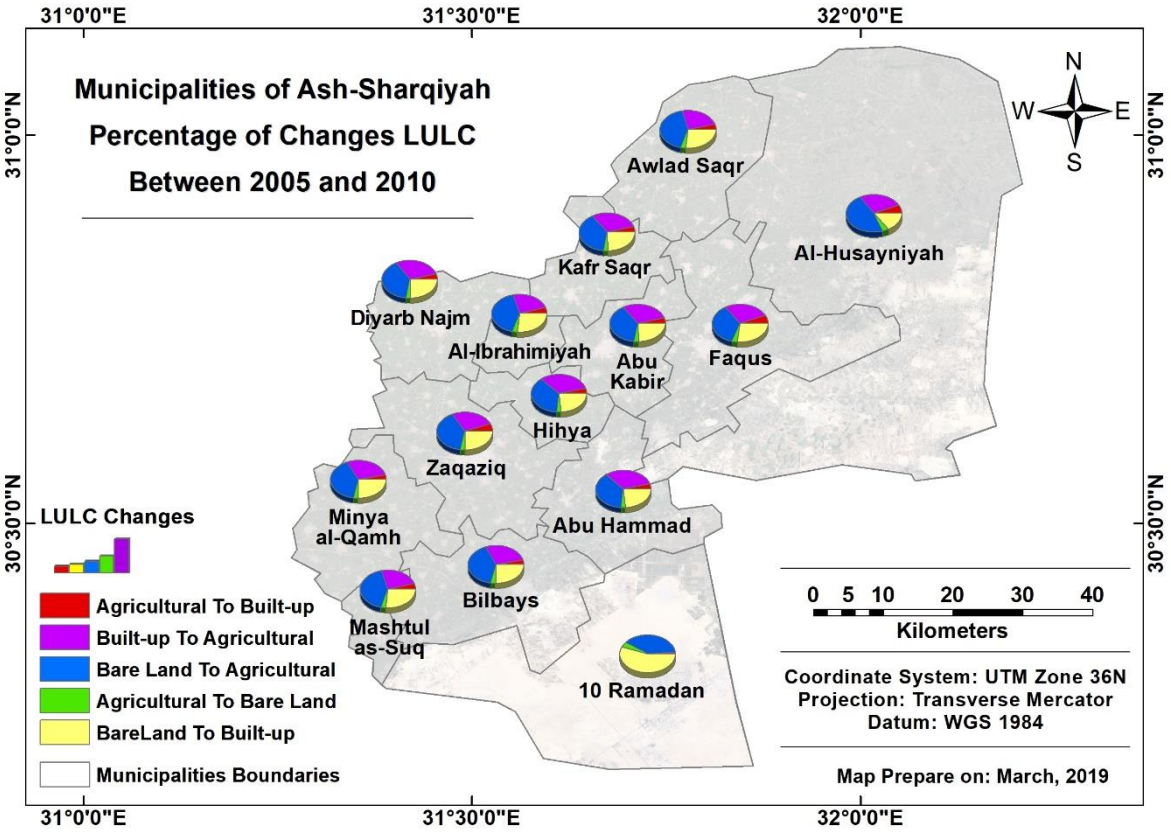

Map 4.7: Percentage of Changes LULC in Municipalities between 2005 and 2010

Al-Husayniyah municipality lost the largest area of agricultural land to Built-up area at the

level of Ash-Sharqiyah governorate by 50.6 hectares, while Mashtul as-Suq and Al-Ibrahimiyah municipalities are the least changed by 1.7 hectares in the same period. While the period result between 2010 to 2015 showed a significant increase in the convert of Agricultural to Built-up area in Al-Husayniyah municipality by about 800 hectares, nearly 1580% increase over the period 2005 to 2010.

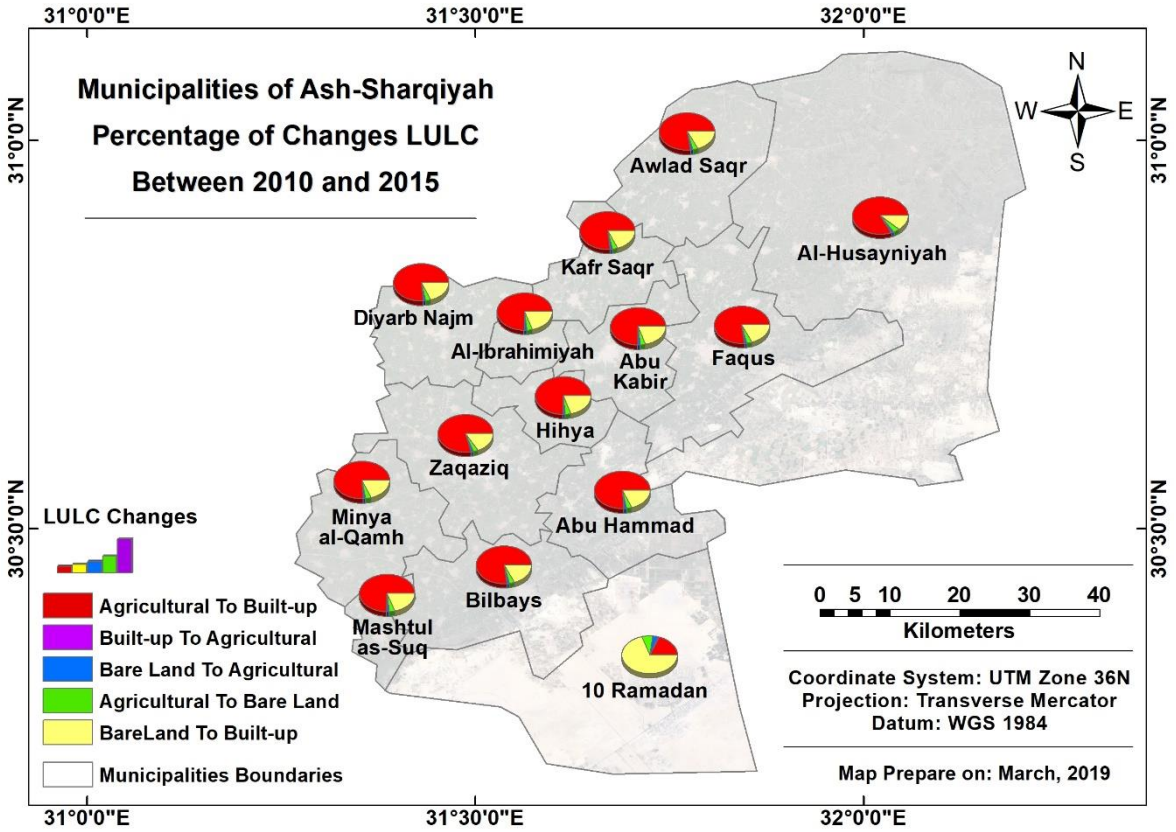

Map 4.8: Percentage of Changes LULC in Municipalities between 2010 and 2015

As for the restoration of agricultural land from the violation of the building regulations, which is the change of Built-up area to Agriculture land in the period from 2005 to 2010, 10-Ramadan municipality is the least area of about 5.5 hectares, Al-Husayniyah municipality has the largest area of change in that category by 250.6 hectares, compared to the period 2010 to 2015, we notice a very low in this category, where all municipalities range from 0.2 to 5.2 hectares, this indicates the weak role of municipalities in imposing the restoration of agricultural land from those who violated construction during that period.

In the category of changes from Bare land to Agriculture land or so-called reclamation of new desert lands, we note that in the period 2005-2010, Mashtul as-Suq municipality acquired the least area of change by only 16.5 hectares, while Al-Husayniyah municipality

has the largest area of reclamation desert land by 398.1 hectares. By comparing these statistics with the period 2010-2015, expect a decrease in the role of municipalities in reclaiming new lands in that period, where it was noted that Al-Husayniyah municipality acquired the largest area of change in that category by 17.5 hectares with a decrease of 2271% compared with the period 2005-2010.

The fourth category, which is the change of agricultural land to bare land or called the desertification phenomenon. It is caused by a variety of factors, such as through the overexploitation of soil through human activity and through climate change particularly the global warming. Desertification is a significant global ecological and environmental problem with far reaching consequences on socio-economic and political conditions. During the period 2005-2010 we note that Al-Husayniyah municipality is the largest in terms of changing agricultural land to bare land followed by 10-Ramadan municipality, because of the large area in addition to the part of them within the territory of desert, therefore, desertification is increasing in these municipalities. The situation is not very different in the period 2010-2015 where we notice a similarity in the areas of change of agriculture land to bare land, ranging from 1.6 hectares in Mashtul as-Suq municipality to 37.8 hectares in Al-Husayniyah municipality in the same period.

The fifth category is the change of Bare land to Built-up area, which reflects the development and construction of new settlements. The period 2005-2010 shows that 10-Ramadan municipality ranked first in the area of change by 245.3 hectares, while Mashtul as-Suq municipality acquired about 11 hectares only. In comparison with the period 2010-2015, there is a decrease in the convert from bare land to urban purposes. 10-Ramadan municipality acquired approximately 150 hectares of land that changed from Bare land to Built-up area while Mashtul as-Suq municipality remained in the last ranked by 7.5 hectares. Due to the importance of the loss of agricultural land for Egypt and its impact on increasing the deficit of food gap for a country of more than 100 million and population growth rate at 2.2% annually, in a region mostly covered by desert with extremely low rainfall (United Nations Environment Programme 2010). Since Ash-Sharqiyah Governorate is the largest

wheat producer in Egypt, which is currently the largest wheat-importing country in the world (FAO 2016). Therefore, we will focus more on detecting changes from Agricultural land to Built-up area.

Distribution Map No. 4.3 refers to the area (by hectares) for Agricultural land changes to Built-up area for the municipalities of Ash-Sharqiyah Governorate between 2005 and 2010. Where the values of the distribution areas of change for agricultural land in that period between less than 2 hectares to more than 8 hectares and is divided into five categories, where the map indicates that the largest affected municipalities in Ash-Sharqiyah governorate by the loss of Agricultural land and converted it to human activities are Al-Husayniyah, Faqus and Zagazig municipality.

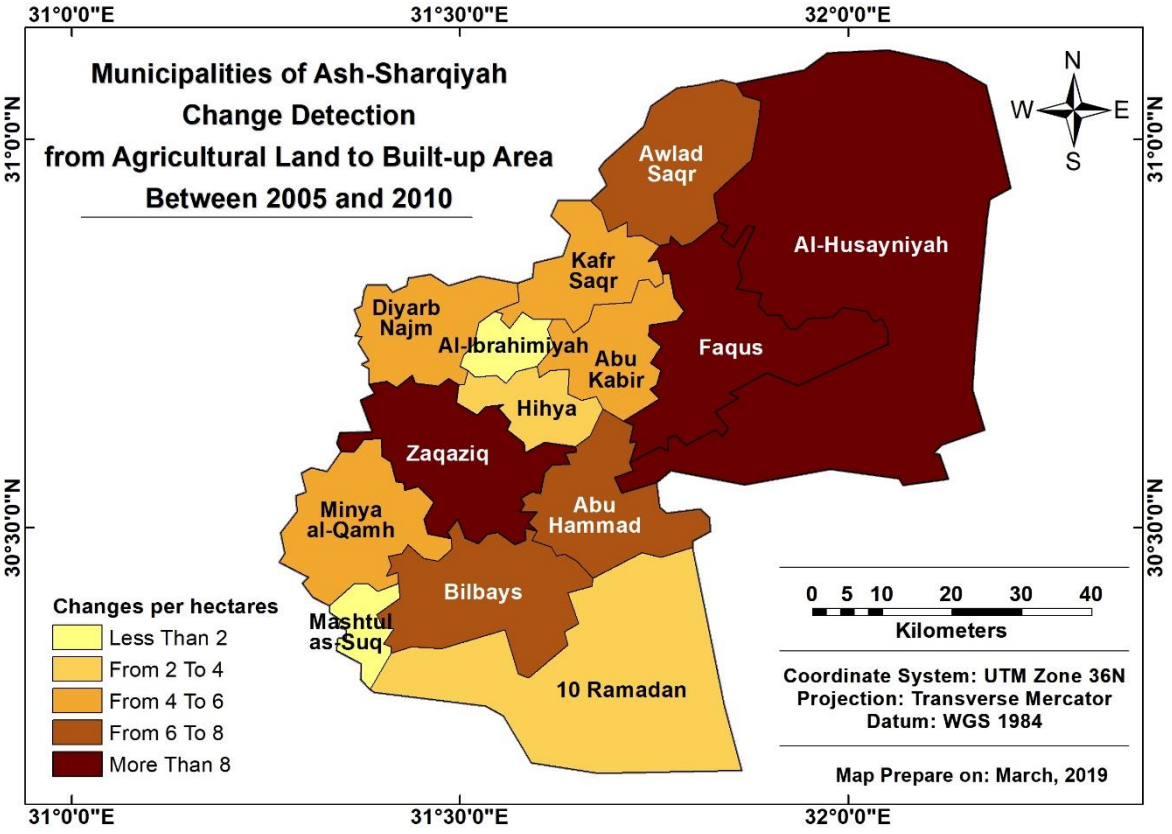

Map 4.3: Detection change of Agricultural land to Built-up in municipalities of study area 2005-2010

This is due to several reasons, for example: size area, spread of human settlements within Agricultural areas and high number of population with the absence of expansion Built-up areas within the boundaries of those municipalities, while Al-Ibrahimiyah and Mashtul as-Suq municipality are the least in terms of change of Agricultural land to Built-up by less than

2 hectares for each, which may be due to the percentage of loss of Agricultural land to the total area of the municipality.

Between 2010 and 2015, distribution map No. 4.4 shows that the values of Agricultural land change categories ranging from less than 60 hectares to more than 120 hectares are divided into five categories. Where the majority of Ash-Sharqiyah Governorate area of dark color and to indicate that the high rate of change of Agricultural land to urban activities, where the category contained more than 120 hectares on six municipalities (Awlad Saqr, Faqus, Al-Husayniyah, Zaqaziq, Minya al-Qamh and Bilbays) and may be due to several reasons, including the impact of exceptional political events on the weakness power of the municipalities to control the violators of the building systems on Agricultural land.

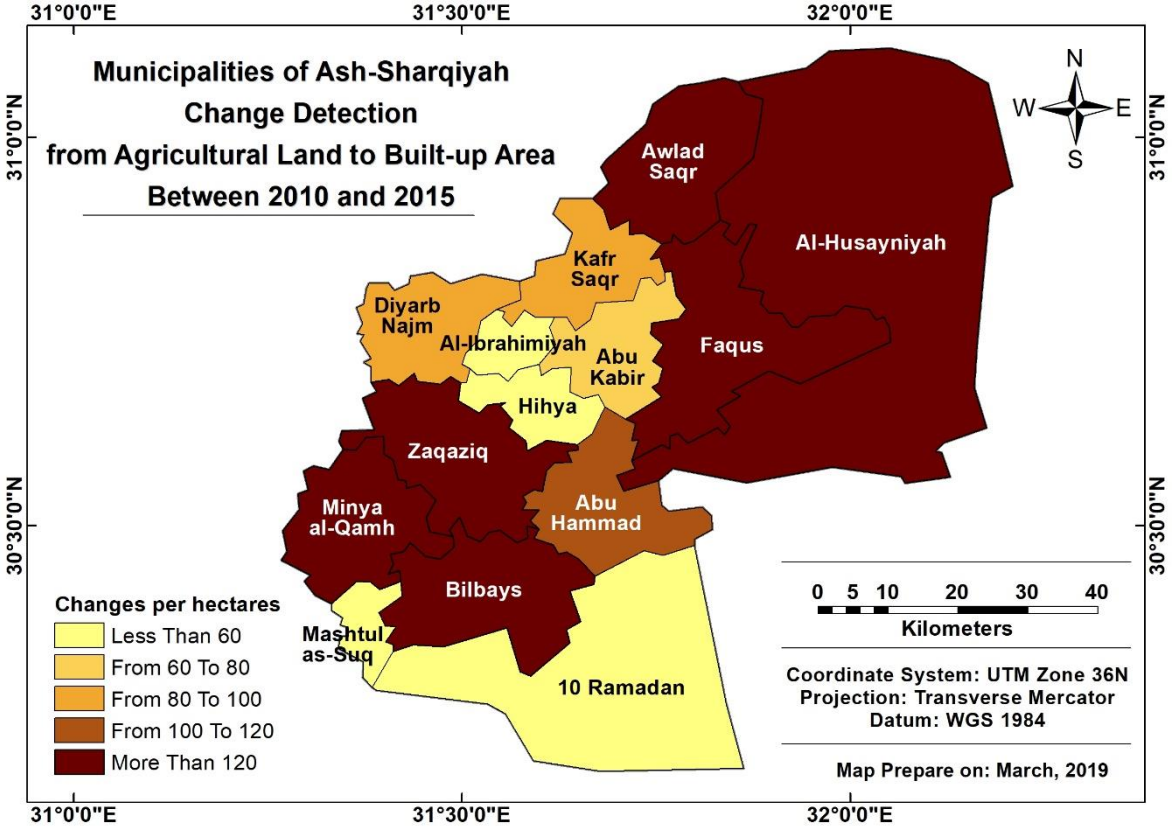

Map 4.4: Detection change of Agricultural land to Built-up in municipalities of study area 2010-2015

On the contrary, Al-Ibrahimiyah, Hihya, Mashtul as-Suq and 10-Ramadan municipalities are in the category of least converting from Agricultural land to Built-up area in the same period. This may be due to the decrease in the area of Agricultural land relative to the total area of the municipality or prevailing land use is non-agricultural, such as 10-Ramadan municipality is an industrial city in the first place with a few areas of Agriculture land.

A summary of this chapter: This chapter discussed the results of the classification of the study area into four categories (Agriculture land, Built-up Area, Bare land and Water bodies) by using two classification approaches used (pixel-based and object-based). Subsequently, the accuracy assessment of LULC classification results of both approaches was assessed and the results showed superior to object-based classification and closer proximity to reality in the study area. Where used results in the detection of change in LULC between the years 2005 to 2010 and 2010 to 2015.

Chapter-5: Conclusions

This study addressed detect land use / land cover changes in Ash-Sharqiyah Governorate of Egypt. Where Ash-Sharqiyah Governorate is largest producer of wheat, which is the basic staple of the Egyptian food. Egypt suffers from a food gap for several reasons, including the high rate of population increase and the lack of area of agricultural land, so recently increased demand for detecting changes of land use/ Land cover, which helps solve this issue.

The study period was chosen for the ten years between 2005 and 2015 and divided into two parts. The first period from 2005 to 2010 and the second from 2010 to 2015 due to political and economic events, that coincided with that period and affected LULC. In the first period (2005-2010), the Egyptian state followed the policy of expansion of the agricultural patch and reclamation of desert lands to try to solve the problem of the food gap and achieve self-sufficiency or food security. The second period (2010-2015) there were exceptional political events (January 2011 and June 2013 revolutions) coincided with the weakness of the municipal power to control the violators of the building systems on agricultural land and stopped many projects of reclamation of desert lands. Which added important factors to choose that period to study the detection of changes land use / land cover.

Two different classification approach was used (pixel-based and object-based) specifically, was chosen a technique Subpixel classification, which is one of the most important (pixel-based) classification approach to choose the most accurate and closest approach to reality.

Four categories have been identified which classification of LULC (Agriculture land, Built-up area, Bare land and Water bodies).

The average Kappa coefficient and statistics on Overall Classification Accuracy for the study period was used to determine which classification approaches were closer to reality. The results showed the superiority of the object-based approach where it obtained 0.921 as the mean value of the Kappa coefficient for all land uses, while the pixel-based approach obtained 0.661. The object-based approach to LULC classification proved to be the approach that shows promise with its ability to manage the attributes of modern VHR sensor data in the study area.

The results of the detection of changes LULC showed a significant difference between the two periods of study in some LULC classes. The results showed that the area of agricultural land was reduced by change to built-up area between 2005 and 2010 by 121.5 hectares, while change in the period (2010-2015) by 2130.9 hectares. This may be due to the excessive increase in the number of violators of built-up on agricultural land through violation of municipal building regulations. In contrast, about 770 hectares of Built-up area were changed to Agriculture in 2005-2010, but less in 2010-2015, where the results showed a change of approximately 16 hectares only. This reflects the deterioration of the agricultural land in that governorate. The shrinking of the agricultural area continued through the change of Agriculture land to Bare land or as called "Desertification". Between 2005 and 2010, approximately 110 hectares were changed. In 2010-2015, the change increased by approximately 120 hectares. In contrast, the government was able to reclaim many of the desert land, which was reflected in the change of Bare land to Agriculture land by about 1210 hectares in the period 2005-2010, while the change in the period 2010-2015 was reduced by nearly 55 hectares only. As for the change of Bare land to Built-up area or as called "Develop a new settlements" in the period 2005-2010 was changed to approximately 796 hectares while in the period 2010-2015 reduced the area to 552 hectares.

While on the level of the municipalities of Ash-Sharqiyah governorate. It turned out that Al-Husayniyah municipality is the most municipalities in terms of LULC changes. Where more

than 799 hectares of Agricultural land has been changed to Built-up in 2010-2015. Vice versa. The land was changed from Built-up to Agriculture land in 2005-2010 by approximately 250 hectares. In contrast, the same municipality lost nearly 35 and 37 hectares for both 2005-2010 and 2010-2015 respectively from Agriculture land to Bare land, so-called ''Desertification''. The municipality of 10-Ramadan was ranked first in land change from Bare land to Agriculture land by 254 hectares and 150 hectares in 2005-2010 and 2010-2015 respectively.

References

Al Tarawneh, W. (2014). Urban sprawl on agricultural land (literature survey of causes, effects, relationship with land use planning and environment). A case study from Jordan (Shihan municipality areas). Journal of Environment and Earth Science Vol.4(20), PP. 97-124. <http://citeseerx.ist.psu.edu/viewdoc/download?doi=10.1.1.854.4601&rep=rep1&type=pdf>. Access Date: 08-OCT-2018.

Anderson, J.R. (1976). *A land use and land cover classification system for use with remote sensor data* (Vol. 964): US Government Printing Office.<https://pubs.usgs.gov/pp/0964/report.pdf>.

Aplin, P.,Atkinson, P.M. (2001). Sub-pixel land cover mapping for per-field classification. International Journal of Remote Sensing Vol.22(14), PP. 2853-2858. <https://www.tandfonline.com/doi/abs/10.1080/01431160110053176>. Access Date: 28-SEP-2018.

Arif, M., Suresh, M. et al. (2015). Sub Pixel Classification of High Resolution Satellite Imagery. International Journal of Computer Applications Vol.129(1), PP. 9-15. <https://www.researchgate.net/profile/Kamal_Jain5/publication/284197043_Sub_Pixel_Classification_of_High_Resolution_Satellite_Imagery/links/57d6365c08ae5f03b4932c8d.pdf>. Access Date: 17-SEP-2018.

Atkinson, P. (1997). *Innovations in GIS 4* (Kemp, Z. Ed.). London: Taylor & Francis.<https://www.scribd.com/document/221898071/Innovation-in-GIS-Zarine-Kemp-Ed>.

Benz, U.C., Hofmann, P. et al. (2004). Multi-resolution, object-oriented fuzzy analysis of remote sensing data for GIS-ready information. ISPRS Journal of Photogrammetry and Remote Sensing Vol.58(3-4), PP. 239-258. <https://www.sciencedirect.com/science/article/abs/pii/S0924271603000601>. Access Date: 31-Jan-2019.

Bishop, Y.M., Fienberg, S.E. et al. (1977). Book review: Discrete multivariate analysis: Theory and practice. Applied Psychological Measurement Vol.1(2), PP. 297-306. <http://journals.sagepub.com/doi/abs/10.1177/014662167700100218?journalCode=apma>. Access Date: 06-April-2018.

Castilla, G.,Hay, G. (2008). Image objects and geographic objects *Object-based image analysis* (pp. 91-110): Springer.

Celik, T. (2009). Multiscale change detection in multitemporal satellite images. IEEE Geoscience and Remote Sensing Letters Vol.6(4), PP. 820-824. <https://ieeexplore.ieee.org/abstract/document/5196725/>. Access Date: 23-SEP-2018.

Chen, G., Weng, Q. et al. (2018). Geographic object-based image analysis (GEOBIA): emerging trends and future opportunities. GIScience & Remote Sensing Vol.55(2), PP. 159-182. <https://www.tandfonline.com/doi/abs/10.1080/15481603.2018.1426092>. Access Date: 01-OCT-2018.

Congalton, R.G. (1991). A review of assessing the accuracy of classifications of remotely sensed data. Remote Sensing of Environment Vol.37(1), PP. 35-46. <https://www.sciencedirect.com/science/article/pii/003442579190048B>. Access Date: 22-Feb-2018.

Congalton, R.G.,Green, K. (2008). *Assessing the accuracy of remotely sensed data: principles and practices*: CRC press

Congalton, R.G.,Mead, R.A. (1983). A quantitative method to test for consistency and correctness in photointerpretation. Photogrammetric Engineering and Remote Sensing Vol.49(1), PP. 69-74. <https://www.asprs.org/wp-content/uploads/pers/1983journal/jan/1983_jan_69-74.pdf>. Access Date: 06-April-2018.

Dissanska, M., Bernier, M. et al. (2009). Object-based classification of very high resolution panchromatic images for evaluating recent change in the structure of patterned peatlands. Canadian Journal of Remote Sensing Vol.35(2), PP. 189-215. <https://www.tandfonline.com/doi/abs/10.5589/m09-002>. Access Date: 29-OCT-2018.

Doygun, H. (2009). Effects of urban sprawl on agricultural land: a case study of Kahramanmaraş, Turkey. Environmental monitoring and assessment Vol.158(1-4), PP. 471. <https://link.springer.com/article/10.1007/s10661-008-0597-7>. Access Date: 09-OCT-2018.

El-Aziz, A.O.A. (2013). Monitoring and Change Detection along the Eastern Side of Qena Bend, Nile Valley, Egypt Using GIS and Remote Sensing. Advances in Remote Sensing Vol.2(03), PP. 276. <http://www.scirp.org/journal/PaperInformation.aspx?paperID=36887>. Access Date: 26-SEP-2018.

Felde, G., Anderson, G. et al. (2003). *Analysis of Hyperion data with the FLAASH atmospheric correction algorithm.* Paper presented at the Geoscience and Remote Sensing Symposium, 2003. IGARSS'03. Proceedings. 2003 IEEE International.PP:90-92. <http://ieeexplore.ieee.org/abstract/document/1293688/>. Access Date: 20-Jan-2018.

Gao, B.-C. (1996). NDWI—A normalized difference water index for remote sensing of vegetation liquid water from space. Remote Sensing of Environment Vol.58(3), PP. 257-266. <https://www.sciencedirect.com/science/article/pii/S0034425796000673>. Access Date: 05-Feb-019.

Hay, G.,Castilla, G. (2006). *Object-based image analysis: strengths, weaknesses, opportunities and threats (SWOT).* Paper presented at the Proc. 1st Int. Conf. OBIA.PP:4-5. <http://www.isprs.org/proceedings/xxxvi/4-c42/Papers/OBIA2006_Hay_Castilla.pdf>. Access Date: 25-SEP-2018.

Im, J., Jensen, J. et al. (2008). Object-based change detection using correlation image analysis and image segmentation. International Journal of Remote Sensing Vol.29(2), PP. 399-423. <https://www.tandfonline.com/doi/abs/10.1080/01431160601075582>. Access Date: 09-OCT-2018.

Jensen, J.R. (2015). *Introductory Digital Image Processing: A Remote Sensing Perspective* (4th ed.): Pearson Education, Incorporated.<https://books.google.com.sa/books?id=IWvDrQEACAAJ>.

Johannsen, C.J.,Daughtry, C.S. (2009). Surface reference data collection *The SAGE handbook of remote sensing* (pp. 244-256): Sage Publications.

López, E., Bocco, G. et al. (2001). Predicting land-cover and land-use change in the urban fringe: a case in Morelia city, Mexico. Landscape and urban planning Vol.55(4), PP. 271-285. <https://www.sciencedirect.com/science/article/pii/S0169204601001608>. Access Date: 08-OCT-2018.

Lu, D., Mausel, P. et al. (2004). Change detection techniques. International Journal of Remote Sensing Vol.25(12), PP. 2365-2401. <https://www.tandfonline.com/doi/abs/10.1080/0143116031000139863>. Access Date: 20-SEP-2018.

Ma, L., Li, M. et al. (2017). A review of supervised object-based land-cover image classification. ISPRS Journal of Photogrammetry and Remote Sensing Vol.130, PP. 277-293. <https://www.sciencedirect.com/science/article/pii/S092427161630661X>. Access Date: 14-Feb-2019.

Mather, P.M.,Koch, M. (1999). *Computer processing of remotely-sensed images: an introduction 2nd*: John Wiley & Sons

McFeeters, S.K. (1996). The use of the Normalized Difference Water Index (NDWI) in the delineation of open water features. International Journal of Remote Sensing Vol.17(7), PP. 1425-1432. <https://www.tandfonline.com/doi/abs/10.1080/01431169608948714>. Access Date: 05-Feb-2019.

Murcko, J. (2017). *Object-based classification for estimation of built-up density within urban environment.* (Environmental Sciences), Technische Universität Dresden. Retrieved from http://cartographymaster.eu/wp-content/theses/2017_Murcko_Thesis.pdf

Pathak, S. (2014). New Change Detection Techniques to monitor land cover dynamics in mine environment. The International Archives of Photogrammetry, Remote Sensing and Spatial Information Sciences Vol.40(8), PP. 875. <https://pdfs.semanticscholar.org/969f/f4bb0825dc86c9c3d3df267796ffbfcff9bb.pdf>. Access Date: 20-SEP-2018.

Radke, R.J., Andra, S. et al. (2005). Image change detection algorithms: a systematic survey. IEEE transactions on image processing Vol.14(3), PP. 294-307. <https://ieeexplore.ieee.org/abstract/document/1395984/>. Access Date: 20-SEP-2018.

Rahman, M.R.,Saha, S. (2008). Multi-resolution segmentation for object-based classification and accuracy assessment of land use/land cover classification using remotely sensed data. Journal of the Indian Society of Remote Sensing Vol.36(2), PP. 189-201. <https://link.springer.com/article/10.1007%2Fs12524-008-0020-4>. Access Date: 06-April-2018.

Richards, J.A.,Richards, J. (1999). *Remote sensing digital image analysis* (Vol. 3): Springer.<https://link.springer.com/content/pdf/10.1007/978-3-642-30062-2.pdf>.

Rosenfield, G.H.,Fitzpatrick-Lins, K. (1986). A coefficient of agreement as a measure of thematic classification accuracy. Photogrammetric Engineering and Remote Sensing Vol.52(2), PP. 223-227. <https://www.asprs.org/wp-content/uploads/pers/1986journal/feb/1986_feb_223-227.pdf>. Access Date: 07-April-2018.

Sagardia, R. (2005). *Use of subpixel classifier for wetland mapping: a case study of the Cuitzeo Lake, Mexico.* INTERNATIONAL INSTITUTE FOR GEO-INFORMATION SCIENCE AND EARTH OBSERVATION ENSCHEDE, THE NETHERLANDS. Retrieved from https://webapps.itc.utwente.nl/librarywww/papers_2005/msc/nrm/sagardia.pdf

Schiewe, J. (2002). Segmentation of high-resolution remotely sensed data-concepts, applications and problems. International Archives of Photogrammetry Remote Sensing and Spatial Information Sciences Vol.34(4), PP. 380-385. <http://test.ecognition.com/sites/default/files/383_358.pdf>. Access Date: 02-Feb-2019.

Shalaby, A.A., Ali, R. et al. (2012). Urban sprawl impact assessment on the agricultural land in Egypt using remote sensing and GIS: a case study, Qalubiya Governorate. Journal of Land Use Science Vol.7(3), PP. 261-273. <https://www.tandfonline.com/doi/abs/10.1080/1747423X.2011.562928>. Access Date: 08-OCT-2018.

Singh, A. (1989). Review article digital change detection techniques using remotely-sensed data. International Journal of Remote Sensing Vol.10(6), PP. 989-1003. <https://www.tandfonline.com/doi/abs/10.1080/01431168908903939>. Access Date: 01-Mar-2018.

Stehman, S.V. (2009). Sampling designs for accuracy assessment of land cover. International Journal of Remote Sensing Vol.30(20), PP. 5243-5272. <http://www.tandfonline.com/doi/abs/10.1080/01431160903131000>. Access Date: 20-Feb-2018.

Strobl, J., Blaschke, T. and Griesbner, G. (2000). Multiresolution segmentation: an optimization approach for high quality multi-scale image segmentation. In Blaschke, T. (Ed.), *Angewandte Geographische Informations-Verarbeitung* (Vol. XII, pp. 542): Herbert Wichmann Verlag.

Tian, J.,Chen, D.M. (2007). Optimization in multi-scale segmentation of high-resolution satellite images for artificial feature recognition. International Journal of Remote Sensing Vol.28(20), PP. 4625-4644.

<https://www.tandfonline.com/doi/abs/10.1080/01431160701241746>. Access Date: 31-Jan-2019.

Verhoeye, J.,De Wulf, R. (2002). Land cover mapping at sub-pixel scales using linear optimization techniques. Remote Sensing of Environment Vol.79(1), PP. 96-104. <https://www.sciencedirect.com/science/article/pii/S0034425701002425>. Access Date: 30-SEP-2018.

Vermote, E.F.,Kotchenova, S. (2008). Atmospheric correction for the monitoring of land surfaces. Journal of Geophysical Research: Atmospheres Vol.113(D23), PP. 1-12. <http://onlinelibrary.wiley.com/doi/10.1029/2007JD009662/full>. Access Date: 12-Jan-2018.

Walter, V. (2004). Object-based classification of remote sensing data for change detection. ISPRS Journal of Photogrammetry and Remote Sensing Vol.58(3-4), PP. 225-238. <https://www.sciencedirect.com/science/article/pii/S0924271603000595>. Access Date: 23-SEP-2018.

Zhang, Y.,Maxwell, T. (2006). *A fuzzy logic approach to supervised segmentation for object-oriented classification.* Paper presented at the ASPRS 2006 Annual Conference Reno, Nevada May.PP:1-5. <https://pdfs.semanticscholar.org/db5c/96f52370e72109fce5be34c7263ffe07501c.pdf>. Access Date: 29-OCT-2018.

Appendix : Rule-Set OBIA Documentation

Define ruleset of Object-Based classification Land use / Land cover by using eCognations developer 9.2 software

Layers:

- QuickBird II: Band 1 (Blue), Band 2 (Green), Band 3 (Red), Band 4 (NIR)
- WorldView-2: Band 1 (Blue), Band 2 (Green), Band 3 (Red), Band 4 (NIR)
- DubaiSat-2: Band 1 (Blue), Band 2 (Green), Band 3 (Red), Band 4 (NIR)

Classes:

- Agricultural Land
- Built-up Area
- Bare Land
- Water Bodies

Customized Features:

- NDVI: ([Mean Layer 4]-[Mean Layer 3])/([Mean Layer 4]+[Mean Layer 3]
- NDWI: [Mean Layer 2]-[Mean Layer 4])/([Mean Layer 2]+[Mean Layer 4]

Main Process:

- Segmentation:
    - Multiresolution segmentation: 5 [shape:0.2 compct:0.5] creating ‘level 1’

- Classify Agriculture Land:
    - Assign class: unclassified with NDVI < 1 and NDVI ≥ 0.1 and Layer 4 > 4 at level 1

- Classify Bare Land:
    - Assign class: unclassified with NDVI < -0.05 and NDVI > -0.2 and Area > 5000 Pxl and Standard deviation Layer 4 < 0.5 at level 1

- Classify Water Bodies:
    - Assign class: unclassified with Layer 4 < 4 and NDWI > 0.2 and NDWI < 1 and NDVI > -1 and NDVI < 0

- Classify Built-up Area:
    - Assign class: unclassified with NDVI < 0 and Layer 3 > 5 and Layer 1 > 7 and Area > 50 Pxl at level 1
    - Multiresolution segmentation: 5 [shape:0.5 compct:0.6] creating ‘level 2’
    - Assign class: unclassified with Texture Rang > 15.5 and Texture Variance < 168 at level 2

- Extract:
    - At level 1: export object shapes ‘vector level1’
    - At level 2: export object shapes to ‘vector level2’